NUREG/CR-3941
AAEC/C40
Vol. 1

Radionuclide Migration Around Uranium Ore Bodies -- Analogue of Radioactive Waste Repositories

Annual Report
July 1982 - June 1983

Prepared by P. L. Airey

Australian Atomic Energy Commission
Lucas Heights Research Laboratories

Prepared for
U.S. Nuclear Regulatory Commission

8411060506 841031
PDR NUREG
CR-3941 R PDR

NOTICE

This report was prepared as an account of work sponsored by an agency of the United States Government. Neither the United States Government nor any agency thereof, or any of their employees, makes any warranty, expressed or implied, or assumes any legal liability of responsibility for any third party's use, or the results of such use, of any information, apparatus, product or process disclosed in this report, or represents that its use by such third party would not infringe privately owned rights.

NOTICE

Availability of Reference Materials Cited in NRC Publications

Most documents cited in NRC publications will be available from one of the following sources:

1. The NRC Public Document Room, 1717 H Street, N.W.
   Washington, DC 20555
2. The NRC/GPO Sales Program, U.S. Nuclear Regulatory Commission,
   Washington, DC 20555
3. The National Technical Information Service, Springfield, VA 22161

Although the listing that follows represents the majority of documents cited in NRC publications, it is not intended to be exhaustive.

Referenced documents available for inspection and copying for a fee from the NRC Public Document Room include NRC correspondence and internal NRC memoranda; NRC Office of Inspection and Enforcement bulletins, circulars, information notices, inspection and investigation notices; Licensee Event Reports; vendor reports and correspondence; Commission papers; and applicant and licensee documents and correspondence.

The following documents in the NUREG series are available for purchase from the NRC/GPO Sales Program: formal NRC staff and contractor reports, NRC-sponsored conference proceedings, and NRC booklets and brochures. Also available are Regulatory Guides, NRC regulations in the *Code of Federal Regulations*, and *Nuclear Regulatory Commission Issuances*.

Documents available from the National Technical Information Service include NUREG series reports and technical reports prepared by other federal agencies and reports prepared by the Atomic Energy Commission, forerunner agency to the Nuclear Regulatory Commission.

Documents available from public and special technical libraries include all open literature items, such as books, journal and periodical articles, and transactions. *Federal Register* notices, federal and state legislation, and congressional reports can usually be obtained from these libraries.

Documents such as theses, dissertations, foreign reports and translations, and non-NRC conference proceedings are available for purchase from the organization sponsoring the publication cited.

Single copies of NRC draft reports are available free, to the extent of supply, upon written request to the Division of Technical Information and Document Control, U.S. Nuclear Regulatory Commission, Washington, DC 20555.

Copies of industry codes and standards used in a substantive manner in the NRC regulatory process are maintained at the NRC Library, 7920 Norfolk Avenue, Bethesda, Maryland, and are available there for reference use by the public. Codes and standards are usually copyrighted and may be purchased from the originating organization or, if they are American National Standards, from the American National Standards Institute, 1430 Broadway, New York, NY 10018.

GPO Printed copy price: $5.50

NUREG/CR-3941
AAEC/C40
Vol. 1

Radionuclide Migration Around Uranium Ore Bodies -- Analogue of Radioactive Waste Repositories

Annual Report
July 1982 - June 1983

Manuscript Completed: June 1984
Date Published: October 1984

Prepared by
P. L. Airey

Australian Atomic Energy Commission
Lucas Heights Research Laboratories
Sutherland, 2232 NSW
Australia

Prepared for
Division of Radiation Programs and Earth Sciences
Office of Nuclear Regulatory Research
U.S. Nuclear Regulatory Commission
Washington, D.C. 20555
NRC FIN B6661

RADIONUCLIDE MIGRATION AROUND URANIUM ORE BODIES - ANALOGUE OF RADIOACTIVE WASTE REPOSITORIES

CONTRACTOR : Australian Atomic Energy Commission

Project Officer	: P.L. Airey
Scientific Staff	: D. Roman C. Golian * S. Short * T. Nightingale * R.T. Lowson (part time) G.E. Calf (part time)
Administrative Assistant	: R. Lowerson * (part time)
University of Sydney	: B.G. Davey + (part time) D. Gray *
University of Wollongong	: J. Ellis (part time)
Consultant	: P.J. Shirvington

* Supported by USNRC Grant.

+ Project officer, Sub-contract 'Uranium Series Disequilibria and Ore Zone Mineralogy'.

With a contribution from B.L. Dickson and R. Meakins,
Division of Mineral Physics, CSIRO

ABSTRACT

A number of uranium ore bodies in the Northern Territory of Australia have been evaluated as geochemical analogues of high-level radioactive waste repositories. The aim of the study is to contribute to the understanding of the scientific basis for the long-term prediction of the transport of radionuclides. Particular attention is being paid to investigations of (i) mechanisms of mobilization and subsequent retardation of uranium series nuclides following the weathering of metamorphic host rocks, (ii) the role of iron minerals in the retardation of uranium and thorium, (iii) the role of groundwater colloids in the transport of radionuclides, (iv) experimental methods for studying the time dependence of adsorption coefficients, and (v) conceptual methods for studying the effect of transport of uranium series nuclides through crystalline host rocks over geological time. The possibility of incorporating certain transuranic and fission product elements into the analogue is discussed.

SUMMARY AND CONCLUSIONS

The aim of the investigation is to contribute to an understanding of the scientific basis for the long-term prediction of the migration of designated radionuclides from proposed high-level radioactive waste repository (HLWR) sites. A geochemical analogue approach is being used. Detailed studies are being made of the groundwater induced redistribution of uranium series nuclides within and down-gradient of uranium ore bodies in the Alligator Rivers region of the Northern Territory of Australia. A unique feature of uranium deposits is the presence of potentially measurable levels of the transuranics ^{237}Np, and ^{239}Pu and the fission products ^{99}Tc and ^{129}I which have developed over geological time.

Current Status

(i) *Mobilization of radionuclides over geological time.* Many of the ore bodies intersect the surface, and comprise weathered profiles overlying crystalline rock sequences. The radionuclides are mobilized by weathering and are redistributed throughout the resulting iron-bearing clays and quartz. A detailed mineralogical investigation of the weathering processes has been undertaken. An open system uranium model has been developed to describe the gross features of the analogue. It has been correlated mathematically with other models, particularly with the USGS Uranium Trend Model.

(ii) *Groundwater induced transport of radionuclides - the role of colloids.* Systematic studies have been made of the levels of uranium, thorium and radium isotopes in groundwater intersecting the deposits. Attempts are being made to include the fission products ^{129}I and ^{99}Tc and ^{36}Cl. Down-gradient of the Ranger One deposit, it has been possible to show that the uranium retardation factor is about 250. Reference is made to an independent estimate of the parameter from the Carizzo aquifer, Texas.

Unlike uranium, a very substantial proportion of thorium is transported by colloids. The thorium isotopes do not appear to be in equilibrium with the solution. The implications to the prediction of the long-term migration rate are being evaluated.

(iii) *The role of iron mineralogy in uranium, thorium and radium transport.* Chemical techniques have been used to study the distribution of uranium, thorium and radium isotopes throughout the amorphous iron, the crystalline iron and the clay/quartz fractions of the weathered profile. Uranium and thorium concentrate in the iron phases; radium tends to associate with the clay/quartz. Since the crystalline iron, which is formed from the amorphous phase, is not readily accessible to groundwater, an additional mechanism for the retardation of uranium and thorium has been identified.

(iv) *Time dependence of radionuclide sorption coefficients.* Crucial to the attempt to assess the validity of laboratory data in predicting the long-term fate of radionuclides is the question of the variation with time of empirical adsorption coefficients. Two approaches are being used to address this question:

(a) Systematic studies are being made of the sorption and leaching properties of uranium, thorium and radium isotopes on ore samples where the geological history, the mineralogy and the radionuclide distribution have been thoroughly characterized.

(b) Measurements have been made of the relative ratios of the parent-daughter couples $^{232}Th/^{228}Ra$, $^{230}Th/^{226}Ra$, $^{228}Th/^{224}Ra$ and $^{227}Th/^{223}Ra$. Because of the very low levels of dissolved thorium, the data set is not complete. Nevertheless, attempts are being made to interpret systematic differences in terms of the time dependence of distribution coefficients.

Complementary laboratory experiments are being undertaken to study the effect of α-recoil on adsorption coefficients.

(v) *Migration through crystalline rocks.* Work is under way to assess the validity over geological time of the matrix-diffusion mechanism of the migration of radionuclides through crystalline rocks.

Recommendations

Recommendation 1. *Further investigations of the long-term transport of uranium series nuclides.* Special attention should be paid to increasing the understanding of phenomena relevant both to the uranium deposits and to proposed HLWR sites. These include:

- the roles of colloids and of organic complexing agents in the transport of actinides,
- the role of specific minerals within the host rock in causing radionuclide retardation,
- the effect of time, and recoil processes on sorption properties, and
- the matrix-diffusion mechanism of migration of radionuclides through crystalline rock.

Recommendation 2. *Incorporation of transuranic and fission product elements into the analogue.* The value of the uranium deposits as HLWR analogues will be greatly enhanced if it is found possible to measure levels of ^{237}Np, ^{239}Pu, ^{99}Tc and ^{129}I.

Recommendation 3. *Application of the analogue to the transport of radionuclides down-gradient of the repository site.* Uranium series nuclides are ubiquitous; their distributions can be studied in host rocks and groundwater associated either with the deposits or with the proposed repository sites. Clearly, the more analogous the geologies, the more direct the comparisons. If ^{237}Np, ^{239}Pu, ^{99}Tc and ^{129}I can be studied in the deposits, and correlated with aspects of uranium series transport, relevant information may be transferred to the repository site. *Should this prove possible, the ultimate aim of the investigation will have been achieved as a basis will have been developed for predicting the long-term migration of critical radionuclides away from HLWR sites.*

CONTENTS

FIGURES

TABLES

1. INTRODUCTION

The United States Nuclear Regulatory Commission (NRC) has the responsibility of determining whether the disposal of high-level radioactive wastes (HLW) at selected geologic sites can be achieved without undue risk to public health and safety, and has proposed a rule (10 CFR 60[1]) which specifies criteria for the disposal of these wastes. Further, geological repositories in the United States will have to comply with standards set by the Environmental Protection Agency (EPA). The criteria under which performance conditions set out in 10 CFR 60 are consistent with the Draft EPA Standard No. 19 have recently been discussed[2]; this standard applies to integrated releases over a period of 10,000 years.

Birchard and Alexander[3] pointed out that assessment of repository sites over these time-scales poses three critical questions :

"(1) Can the performance of a system be predicted for thousands of years or more without a record of equal or greater length?

(2) How can the interactions of man-made elements such as neptunium, plutonium and technetium be predicted in the repository?

(3) How can laboratory experiments on complex processes be scaled from the laboratory to repository dimensions?"

A partial answer to these questions may be obtained by studying carefully selected geochemical analogues. No single analogue will completely model a repository site. The complexity of the problem is illustrated by a recently published discussion of geological factors to be considered when locating a repository.[4] Increasing confidence in the long-term prediction of radionuclide transport will develop with insights obtained from a range of investigations.

The natural reactor system at the Oklo mines in the Franceville Basin, Gabon, is the most extensively studied analogue of a nuclear waste repository.[5] Uranium mineralization occurred about 2.05×10^9 years ago and it seems likely that conditions for criticality were established soon after and were maintained for a period between 10^5 and 5×10^5 years. During this time, the average thermal loading within the reactor zones was about 50 W m^{-2} or two to five times greater than that determined for reference waste repositories.[6] Aqueous solutions circulating through the critical zone were heated to temperatures between 450 and 600°C. Significant fractions of technetium (15 to 40%), ruthenium (10 to 25%) and neodymium (0 to 15%) were leached from the reactor core but retained within a few tens of metres of the source. There is no evidence for the migration and redistribution of ^{239}Pu. Distribution coefficients for ruthenium and technetium deduced from Oklo data are 10^2 to 10^4 times greater than those found from sorption studies on granite, argillite and tuff.[5]

In general, geochemical analogues need not be as comprehensive as Oklo to be useful. However, they should all exhibit certain common features:

(a) They should contain a well defined boundary across which transport may be measured, i.e. a spatial discontinuity.

(b) There should be a method for establishing a time frame. This may involve knowledge of the time of development of the feature. If radioactive nuclides are being studied, there may be independent methods for dating key processes.

There are several classes of analogues :

(i) *Intrusives.*[7-9] The penetration of intrusives at known geological times can provide useful analogues. Brookins and co-workers[7-8] recently described two examples. In one instance they studied the Alamosa River intrusive which penetrates tuffaceous rocks and andesites of the Platoro Caldera in the San Juan Mountains of southern Colorado. The intrusive was emplaced about 29.1 million years before present (MYBP), and initiated extensive hydrothermal circulation. Detailed studies were made of the variation of Th, U, Co, Sr, Ba, Cs, Rb, Sc, V and Fe with distance from the contact zone. The distribution of U, Th, rare earth elements, V, and Ti in each rock is apparently unaffected by the intrusion despite the hydrothermal activity which, on the basis of evidence from similar areas, may have lasted from 0.5 to 2 million years. The absence of migration between tuffs and monzonites supports continued assessment of such rock formations as radwaste repositories. An earlier study of the Eldore-Bryan stock intruding into the Idaho Springs Formation, Colorado, showed the suitability of some crystalline rocks for elemental retention in the intrusion zone.

(ii) *Existing disposal sites.* Detailed studies of existing disposal sites can provide information on the migration of radionuclides over many years in different geological settings and various climatic regimes (for example, current investigations carried out at Maxey Flats, Kentucky; West Valley, New York; Sheffield, Illinois; and Barnwell, South Carolina[3]).

(iii) *Host rock/groundwater systems.* Host rock/groundwater systems are geochemical analogues of aspects of the radionuclide transport process, if criteria (a) and (b) are accepted. Although the applicability of the analogue is limited, some very important questions may be addressed. Krishnaswami et al.[10] recently investigated virtually every long-lived (half-life > 1 day) member of the ^{238}U and ^{232}Th series in groundwater samples from different hydrogeologic settings in Connecticut. They concluded that sorption removes radium and thorium from these groundwaters on a time-scale of 3 minutes

or less; that desorption occurs within a timescale of 1 week or less; that there is equilibrium between solution and solid phases; and that uranium, thorium and lead retardation factors may be calculated from isotopic data. Retardation factors for radium under these conditions varied from 4800 in a sample from arkosic rocks of Triassic-Jurassic age, to 123,000 in groundwater from crystalline bedrock. In an analogous investigation, Laul and co-workers[11], studied the ^{228}Ra-^{228}Th-^{224}Ra series in brines from the Wolfcamp and Granite Wash aquifers. The data were interpreted as indicating little retardation of radium in brines, but retardation factors of about 80 for thorium.

(iv) *Uranium deposits.* Uranium deposits comprise a range of isotopes belonging to the ^{238}U, ^{235}U and ^{232}Th series. In addition, sufficient quantities of the transuranic elements ^{237}Np and ^{239}Pu, and the fission products ^{99}Tc and ^{129}I, are probably present to allow quantitative measurement and the mobility of such radionuclides in natural systems. Carefully chosen deposits are therefore useful analogues of nuclear waste repositories.

In 1981, the Australian Atomic Energy Commission (AAEC) contracted with the NRC to undertake a systematic investigation of the radiunuclide migration around ore bodies in the Alligator Rivers Uranium Province in the Northern Territory of Australia (Figure 1). The deposits have been chosen for study for the following reasons :

(i) There are a number of accessible deposits which may be compared to establish general features of radionuclide redistribution within and down-gradient of the deposit.

(ii) At least four of the deposits intersect the ground surface. The uranium series nuclides are therefore distributed between the main metamorphosed sequences and the overlying weathered profile. It is therefore possible, in principle, to compare the radionuclide transport within the crystalline schists, gneisses and silicified carbonates, and the iron-bearing clays and quartz into which they weather.

(iii) Weathering leads to mobilization of uranium and provides a rational basis for the definition of zero time, which is essential for the mathematical modelling of transport.

(iv) Groundwater intersects all deposits and not only induces redistribution of radionuclides within the ore zone but also leads to down-gradient transport. In some cases, retardation factors related to migration through the late Quaternary may be studied.

(v) Low levels of the transuranics ^{237}Np and ^{239}Pu and the fission products ^{129}I and ^{99}Tc, which are relevant to the calculation of the total dose commitment to the public, may be incorporated into the analogue.

Three specific research-oriented tasks were defined :

Task C. Determine whether short-time sorption/leaching behaviour is like long-time behaviour by conducting laboratory leaching experiments on weathered zone material.

Task D. Conduct experiments to compare migration in zones where uranium is in the 4+ valence state.

Task E. Conduct experiments to compare migration distances and rates of transport away from the Jabiluka Two ore body.

This investigation is an extension of previous studies of uranium series disequilibria at the Nabarlek deposit[12] and the Austatom prospect[13]. Analogous studies in the Koongarra deposit have also been reported[14].

An account is given of progress since the presentation of the first Annual Report[16]; in essence, it is a synthesis of much of the material contained in the fifth, sixth and seventh Quarterly Reports[17,18]. Summary accounts were presented at three recent conferences[19,21].

References

1. U.S. Nuclear Regulatory Commission, "10 CFR Part 60 - Disposal of High-level Radioactive Wastes in Geologic Repositories", Federal Register, 46 (130) 35280, 8 July, 1981.

2. M.S. Chu, N.R. Ortiz, K.K. Wahi, R.E. Pepping and J.E. Campbell, "An Assessment of the Proposed Rule (10 CFR 60) for Disposal of High-level Radioactive Wastes in Geologic Repositories", Vol. 1, USNRC Report NUREG/CR-3111, SAND 82-2969, prepared for NRC by Sundia National Laboratories, June, 1983.

3. G.F. Birchard and D.H. Alexander, "Natural Analogues - A Way to Increase Confidence in Predictions of Long-term Performance of Radioactive Waste Disposal", in Scientific Basis for Nuclear Waste Management VI, Ed D.G. Brookins, pp.323-329 in Proceedings of Materials Research Society Symposia, Vol. 15, 1983.

4. W.S. Fyfe, "Suitability of Natural Geomedia for Radwaste Storage", pp.281-289, ibid.

5. D.B. Curtis, T.M. Benjamin, A.J. Gancarz, "The Oklo Reactors : Natural Analogues to Nuclear Waste Repositories", Los Alamos National Laboratory Report LA-UR-81-3783.

6. G.E. Raines, L.D. Rickerston, H.D. Claiborne, J.L. McElroy and R.W. Lynch, "Development of Reference Conditions for Geologic Repositories for Nuclear Waste in the USA" , pp.1-10 in Scientific Basis for Nuclear Waste Management (Plenum Press, NY), 1981.

7. D.G. Brookins, M.S. Abashian, L.H. Cohen, A.E. Williams, H.A. Wollenberg, and S. Flesser, "Natural Analogues : Alamosa River Monzonite Intrusive into Tuffaceous and Adesitic Rocks", in Scientific Basis for Nuclear Waste Management VI, Ed D.G. Brookins, pp.299-306 in Proceedings of Materials Research Society Symposia, Vol. 15, 1983.

8. D.G. Brookins, M.S. Abashian, L.H. Cohen and H.A. Wollenberg, "A Natural Analogue for the Storage of Radwaste in Crystalline Rocks", in Scientific Basis for Nuclear Waste Management VI, Ed D.G. Brookins, pp.231-238 in Proceedings of Materials Research Society Symposia, Vol. 15, 1983.

9. J.J. Papike, C.K. Shearer, S.B. Simon, J.C. Laul, R.J. Walker, "Pegmatite/Wallrock Interactions : Natural Analogues for Radionuclide Migration", EOS, 64(18), p.351 (1983).

10. S. Krishnaswami, W.C. Graustein, K.K. Turikian, and J.F. Dowd, "Radium, Thorium and Radioactive Lead Isotopes in Groundwater : Application to the in situ Determination of Adsorption-Desorption Rate Constants and Retardation Factors", Water Res. Res., 18, 1633-1675 (1982).

11. J.C. Laul, R.W. Perkins, and N. Hubbard, "An Aspect of Th and Ra Chemistry in the Wolfcamp and Granite Wash Aquifers, Palo Duro Basin, Texas", EOS, 64(18), p.227 (1983).

12. P.J. Shirvington, "$^{234}U/^{238}U$ Activity Ratios in Clay as a Function of Distance from Primary Ore" (1979) in Proceedings of IAEA International Symposium Uranium in the Pine Creek Geosyncline, Sydney, Ed J. Ferguson and A.B. Goleby (IAEA, Vienna, 1980), pp.509-520.

13. P.J. Shirvington, "Fixation of Radionuclides in the ^{238}U Decay Series in the Vicinity of Mineralized Zones : 1 The Austatom Uranium Prospect, NT, Australia", Geochim. Cosmochim. Acta, 47, pp.403-412 (1983).

14. B.L. Dickson, and A.A. Snelling, "Movements of Uranium and Daughter Isotopes in the Koongarra Uranium Deposit (1979), in Proceedings of IAEA International Symposium Uranium in the Pine Creek Geosyncline, Sydney, Ed J. Ferguson and A.B. Goleby (IAEA, Vienna, 1980), pp.499-507.

15. Ranger Uranium Environmental Inquiry, Second Report (Presiding Commissioner Mr Justice R.W. Fox), (Australian Government Publishing Service, Canberra), Chap. 5, p.51, 1977.

16. P.L. Airey, D. Roman, C. Golian, S. Short, T. Nightingale, R.T. Lowson and G.E. Calf, "Radionuclide Migration around Uranium Ore Bodies - Analogues of Radioactive Waste Repositories", USNRC Contract NRC-04-81-172, Annual Report 1981-82, AAEC Report C29, 1982.

17. P.L. Airey, D. Roman, C. Golian, S. Short, T. Nightingale, R.T. Lowson and G.E. Calf, "Radionuclide Migration around Uranium Ore Bodies - Analogues of Radioactive Waste Repositories", USNRC Contract NRC-04-81-172, (a) Quarterly Report No. 5, AAEC Report C34, 1983, (b) Quarterly Report No. 6, AAEC Report C37, 1983.

18. P.L. Airey, D. Roman, C. Golian, S. Short, T. Nightingale, R.T. Lowson, G.E. Calf, B.G. Davey, D. Gray and J. Ellis, "Radionuclide Migration around Uranium Ore Bodies - Analogues of Radioactive Waste Repositories", USNRC Contract NRC-04-81-172, Quarterly Report No. 7, AAEC Report C38, 1983.

19. P.L. Airey, "The Transport of Uranium Series Nuclides Down-gradient of Ore Bodies in the Alligator Rivers Uranium Province", pp.19-1 to 19-7 in Proceedings of Scientific Workshop on Environmental Protection in the Alligator Rivers Region, Vol. 1, 1983.

20. P.L. Airey, C. Golian, T. Nightingale, D. Roman and S. Short, "Groundwater Induced Migration of Uranium and its Daughter Products in the Vicinity of the Ranger No. 1 Ore Body", in Proceedings of Aust. Water and Wastewater Association International Specialist Conference on Water Regime in Relation to Milling, Mining and Waste Treatment including Rehabilitation with Emphasis on Uranium Mining, Darwin, Paper 18, 1983.

21. P.L. Airey. D. Roman, C. Golian, S. Short, T. Nightingale, R.T. Lowson, B.G. Davey, D. Gray, "Radionuclide Migration around Uranium Ore Bodies in The Alligator Rivers Region of the Northern Territory, Australia - Analogue of Radioactive Waste Repositories", in Proceedings of USNRC Contractors' Meeting, August, 1983 (in press).

2. METHODOLOGY

2.1 General

The broad aims of the project, discussed in detail in the first Annual Report[1], are

- to establish the scientific principles whereby laboratory and field observations made over a timescale of days, months or a few years may be used to predict transport over thousands to hundreds of thousands of years, and

- to demonstrate the application of these principles to the prediction of radionuclide transport in geologic settings being considered for HLW repositories.

Broadly speaking, the program is implemented in three stages :

Stage (1) The validity of the Alligator Rivers ore deposits as analogues of radioactive waste repositories is investigated. A detailed understanding is sought of the redistribution of radionuclides within, and their migration from the deposits.

Stage (2) Correlations are established between the results of sorption/leaching studies and those properties of the ore which reflect the cumulative effect of transport over geologic time.

Stage (3) A basis is sought for applying the correlations which were developed for the geochemical analogue, to a wide range of geologic settings.

A schematic representation of the geochemical analogue approach is shown in Figure 2. The ore samples are represented by a matrix hosting a suite of radionuclides M, and associated either with natural or 'synthetic' groundwater. The correlations between the laboratory and field work can be seen by comparing the right- and left-hand portions of the diagram. Three important relationships are illustrated:

1. The relationship between the groundwater chemistry and the distribution of radionuclides through the ore sample. This is fundamental to the understanding of the mechanism of mobilization of radionuclides and sub-surface transport.
2. The relationship between leaching experiments and the distribution of radionuclides through the ore sample. These experiments may contribute to the interpretation of laboratory observations in terms of the sample geochemistry which has evolved over geological time.
3. The relationship between the sorption experiments and the matrix composition.

2.2 Stage 1 - Development of the Geochemical Analogue

2.2.1 Geochemical modelling

A mathematical model has been developed to describe the gross features of the redistribution of uranium and radium within the upper sequences of the uranium deposits. It is useful

- for defining a time frame associated with leaching, deposition and erosion,
- for relating parameters between one deposit and another,
- for providing a basis for correlating laboratory sorption/desorption experiments with the rate of redistribution of uranium series nuclides throughout the ore body, and
- for providing a quantitative basis for assessment of possible extensions to the analogue.

2.2.2 Investigation of ore samples

The geochemical model describes only the gross features of the near surface zones of the uranium deposits. Model output needs to be interpreted in terms of detailed studies of the ore samples.

Mineralogy

X-ray diffraction and optical techniques are used to study the mineralogy. Special attention is paid to iron minerals on which a substantial proportion of uranium and thorium is adsorbed, and which comprise a significant fraction of groundwater particulates.

Selective Phase Separation

Sequential leaching techniques have been applied to the separation of identifiable phases from the weathered ore. If the coextracted uranium series nuclides are uniquely associated with the separated phase, this provides a powerful technique for studying their distribution throughout the ore samples. Observed disequilibria may reflect the time which has elapsed since weathering and provide a basis of correlating a class of laboratory observations with the output of the geochemical model.

2.2.3 Groundwater studies

Groundwater is the principal means of sub-surface transport of uranium series nuclides. Studies are therefore being undertaken of groundwater migration and solute transport mechanisms. Isotope hydrology techniques have been used, since the data may be interpreted in terms of the cumulative effect of migration of water over thousands of years. Attempts are being made to quantify the relative roles of solute and colloidal transport.

2.2.4 Extension of the analogue

Preliminary studies are being made of uranium series transport within the crystalline rock of the Jabiluka Two ore body. Interpretation of the disequilibria in terms of the matrix diffusion theory of solute transport will be attempted. Since the timescales accessible to $^{230}Th/^{234}U$ and $^{234}U/^{238}U$ investigations (<500,000 y) may be too short, measurements of lead/uranium ratios are being undertaken. The analogue could be extended further to include such nuclides as ^{129}I, ^{99}Tc and possibly ^{237}Np and ^{239}Pu.

2.3 Stage 2 - Laboratory Sorption/Leaching Studies

A systematic set of laboratory sorption/leaching experiments is being undertaken to establish correlations (2) and (3) (Figure 2). As indicated in Section 2.1, sorption/leaching experiments are conceptually different. There are clear advantages for running both classes of experiment simultaneously on the same sample. Uranium-236, an isotope not found in nature, is added to the aqueous phase and the $^{234}U:^{236}U:^{238}U$ ratios measured in solution and on the substrate. The ^{236}U distribution coefficient is used to monitor sorption; the corresponding ^{234}U and ^{238}U parameters reflect leaching.

2.4 Stage 3 - Application to Other Geologic Settings

As indicated in Section 2.1, the insights obtained from the geochemical analogue need to be validated and applied to geologic sites being considered for HLW repositories. Sorption/leaching studies could be made on host rock, based on either ambient levels of uranium, thorium and radium, or appropriate non-radioactive elements. The data could be used to predict the migration of transuranic and fission product nuclides on the basis of correlations established from the uranium deposits (Section 2.2.4).

References

1. P.L. Airey, D. Roman, C. Golian, S. Short, T. Nightingale, R.T. Lowson and G.E. Calf, "Radionuclide Migration around Uranium Ore Bodies - Analogues of Radioactive Waste Repositories", USNRC Contract NRC-04-81-172, Annual Report 1981-82, AAEC Report C29, 1982.

3. OPEN SYSTEM MODEL

3.1 Review of Open System Models

The application of uranium series disequilibria to geochronology has recently been extensively reviewed.[1] A few salient points only need to be made. Materials such as speleothems, corals, shells and travertines behave as closed systems under the following conditions : the samples are impermeable to groundwater, show no evidence of weathering or secondary mineralization, and have no detrital material. Virtually none of these conditions apply to the weathered sequences of uranium ore bodies; therefore open system modelling techniques must be applied.

An early attempt to develop an open system model of aragonitic mollusc shells was made by Rosholt.[2] The development was made necessary by the observation of an excess of ^{231}Pa in some samples. It is assumed (a) that the uranium is slowly assimilated by the shells over a relatively long period after deposition in marine sediments, and (b) that all of the ^{231}Pa and ^{230}Th are authigenic and none are leached from the shell. Analytical expressions for the ^{231}Pa, ^{230}Th, ^{234}U and ^{238}U in the shell sample are developed and rationalized with experimental values by adjusting the $^{234}U/^{238}U$ ratios associated with the uranium flux R_F and the uranium leached from the sample R_L. In a later development of the model, Szabo and Rosholt[3] allowed for an initial assimilation of uranium and subsequent weathering, leading to the uptake of ^{230}Th and ^{231}Pa as well as ^{234}U.

Hille[4] proposed another approach in which the daughter products remain chemically stable but the uranium, which migrates into the shell shortly after the death of the organism, can change with time according to a first order law.

Of more direct relevance to the current work is the uranium trend dating model developed recently by Rosholt[5]. The aim of this model is to date the deposition of alluvial, eolian, lacustrine and other deposits. The principle depends on the fact that water, with a small amount of uranium and its daughter products, permeates the deposit. The flux of the mobile phase uranium is defined in terms of an empirical factor F(0) which is associated with an exponential decay constant λ_o. Time t is measured from the commencement of the movement of water through the system. The model is empirical in the sense that rigorous mathematical equations based on established physical parameters are not generated. However, a relationship is developed between $(^{234}U-^{238}U)/^{238}U$ and $(^{238}U-^{230}Th)/^{238}U$ which defines the 'uranium trend line', the product $\lambda_o t$, and related parameters involving the isotopic decay constants. A calibration from known deposits is required to separate λ_o from t and hence to determine the age of the deposit.

3.2 Description of Model*

The principal features of the present open system model were outlined in the first Annual Report.[6] The upper sequences of the ore body were classified into four zones (Table 1). These zones correlate broadly with the mineralogical description of the area. Additional evidence for the classification comes from the systematic variation in the $^{230}Th/^{234}U$ ratios (Figure 3). Data from Ranger One, Jabiluka One and Nabarlek show similar trends. Zone I exhibits large $^{230}Th/^{234}U$ ratios due to the systematic leaching of uranium. Zone II generally shows a ^{230}Th deficit which is evidence for deposition. The transition zone III gives evidence for some loss of uranium associated with the mobilization of the element during the weathering process.

A schematic representation of the model is shown in Figure 4. The dynamics of the system is determined not only by the groundwater flow characteristics, but also by the rate of advance of the weathering front W, which is assumed to balance approximately the rate of surface erosion E and the time-averaged position of the water table over a very long period. If E and W were not in balance, the thickness of the weathered zone, which has been developing since the Tertiary, would be either very small (E>W) or very large (W>E).

The aim of the model is to calculate the following parameters :

- the residence time t of the sample within its particular zone,
- the net rate of leaching (or accumulation) of uranium,
- the activity ratio $^{234}U/^{238}U$ associated with leaching or deposition.

If t and the heights h_I, h_{II}, h_{III} above the boundaries of the respective zones I/II, II/III and III/IV are known, the rate of advance of the weathering W (= rate of erosion E) may be calculated from the average values of the quotients h_I/t, h_{II}/t or h_{III}/t.

In the calculation, it is necessary to define two independent sets of initial conditions :

- $(^{234}U/^{238}U)_0$, $(^{230}Th/^{234}U)_0$ and $(^{231}Pa/^{235}U)_0$. The values of the activity ratios for zone I, say, are assumed to be equal to those found in the upper region of zone II. The initial values for zones II and III are defined similarly.
- t_0. The initial time t_0 is defined as the time of the passage of the zone boundary. Thus for zone I, t_0 refers to the time at which the boundary between zone I and II coincides with the sample.

* Mathematical symbols are listed in Appendix C.

3.3 Generalization of the Model

In the published version of the model[6] it was assumed that leaching or deposition were linear functions of time. This arbitary restriction has been removed in the development discussed below. Following Hille[4], it is now assumed that the leaching and deposition are first order processes, i.e. they are proportional to the concentration of accessible uranium in the ore.

This is a satisfactory description for leaching; however, it means that the rate of deposition is related to a property of the substrate and is only valid if there is good correlation between the level of uranium in the ore and in the groundwater. It is argued in Section 6.5 that, in the weathered region, the relevant property is the number of accessible sites on the amorphous component of the iron or aluminium. It is important to note that the formulation presented below, is identical to that given in the first Annual Report for low leaching rates.

The generating equations can be written as follows :

$$U_8 = U_8(t_o) \exp - (\lambda_8 + \xi)\, t \qquad (1)$$

$$U_5 = U_5(t_o) \exp - (\lambda_5 + \xi)\, t \qquad (2)$$

Hence

$$-dU_4/dt = (\lambda_4 + R\xi)U_4 - \lambda_8 U_8 \qquad (3)$$

$$-dI/dt = \lambda_i I - \lambda_4 U_4 \qquad (4)$$

$$-dPa/dt = \lambda_p Pa\ \lambda_5 U_5 \qquad (5)$$

where $\lambda_8 U_8$, $\lambda_5 U_5$, $\lambda_4 U_4$, $\lambda_i I$ and $\lambda_p Pa$ are activities of ^{238}U, ^{235}U, ^{234}U, ^{230}Th and ^{231}Pa respectively; ξ is the rate of leaching (+ve) or deposition (-ve); R is the $^{234}U/^{238}U$ ratio of the leachate (or of the depositing material); t is the elapsed time; and $U_8(to)$, $U_5(to)$ are the levels of ^{238}U, ^{235}U at the initial time, t (Section 3.2).

The following expressions are developed in Appendix A:

(a) Uranium-234

$$Su = Su(t_o) \exp (b-a)t + \frac{\lambda_4}{(b-a)} (\exp(b-a)t - 1) \qquad (6)$$

(b) Thorium-230

$$Si \times D = Si(t_o) \exp(a - \lambda_i)t + \lambda_i(1 - \exp(a - \lambda_i)t)/(\lambda_i - a)$$

$$+ \lambda_i\lambda_4((b - a) \exp((a - \lambda_i)t + (a - \lambda_i) \exp-(b - a)t + \lambda_i - b)/$$

$$[(b - a)(a - \lambda_i)(b - \lambda_i)\, S(t_o)] \qquad (7)$$

where $D = 1 + \lambda_4(1 - \exp -(b-a)t)/(b-a)\, Su(t_o)$.

(c) Protactinium-231

$$Sp = Sp(to) \exp (c-\lambda_p t) + \frac{\lambda_p}{c-\lambda_p} (\exp (c-\lambda_p)t - 1) \quad (8)$$

where $Su = {}^{234}U/{}^{238}U$ (9)

$$Si = {}^{230}Th/{}^{234}U \quad (10)$$

$$Sp = {}^{231}Pa/{}^{235}U \quad (11)$$

$Su(t_0)$, $Si(t_0)$ and $Sp(t_0)$ are the values at the defined zero time t_0

$$a = \lambda_4 + R\xi \quad (12)$$

$$b = \lambda_8 + \xi \quad (13)$$

$$c = \lambda_5 + \xi \quad (14)$$

3.4 Computational Methods

The computational techniques which were outlined in the first Annual Report[6], require the following steps :

(1) Select an appropriate range of values for the variable parameters ξ and R, and the activity ratios $Su(t_0)$, $Si(t_0)$ and $Sp(t_0)$ at zero time.

(2) Calculate the values ${}^{234}U/{}^{238}U$, ${}^{230}Th/{}^{234}U$ and ${}^{231}Pa/{}^{235}U$ and compare them with the measured values.

(3) List those sets of parameters in which all observed and calculated activity ratios agree to within 10 per cent.

(4) Select those sets of parameters which are internally self-consistent. The criteria used are :

   (a) mass balance: the total leaching rate should approximately balance the total deposition;

   (b) the assumed constancy of the rate of erosion E and the rate of advance of the weathering front W, i.e. $W = t/h_{III}$ (Figure 4), should be approximately constant.

Data from Jabiluka One, Ranger One and Nabarlek have been recomputed and the values listed in Tables 2 to 6a.

Sensitivity Analysis

One of the advantages of developing full analytical expressions for the activity ratios is that the sensitivity of the computer values to the

variable parameters can be readily assessed. An extreme example of the importance of a sensitivity analysis is shown in Figure 5. In this instance, the activity ratios $^{230}Th/^{234}U$, $^{231}Pa/^{235}U$ and $^{234}U/^{238}U$ are plotted as a function of the leaching (deposition) rate ξ when R is 0.50 and the elapsed time is 75,000 years. A discontinuity in $^{230}Th/^{234}U$ is observed at moderate values of ξ. The uncertainties in the estimates of the parameters are listed in Tables 2 to 6. They represent the range of values corresponding to a 10 per cent change in $^{230}Th/^{234}U$.

3.5 Comments on the Validity of the Model

Independent confirmation of the validity of general features of the model is obtained from field observations.

3.5.1 Four-zone classification

The sub-division of the upper sequences of the ore bodies into four zones is generally consistent with the description of the soil profile description for core S1/146 (Table 7).

3.5.2 Dominance of the uranium flux in the vertical profile

A common feature of all the uranium deposits studied is the large excess of ^{230}Th. Values of $^{230}Th/^{234}U$ greater than 2 are frequently observed. Appreciable amounts of uranium must be leached to maintain this disequilibrium. Estimates of the leaching rates are given in Tables 2 to 6. An example was provided in Section 6.5.1 of the first Annual Report, where it was shown that if all the leached uranium from Ranger One were transported laterally with the horizontal component of groundwater flow, either it would remain dissolved in the groundwater, in which case the concentrations would reach values up to twenty times those observed, or the uranium would be precipitated down-gradient of the deposits, in which case there would be secondary accumulation with a significant excess of ^{234}U.

Secondary surface accumulations have in fact been observed down-gradient of the Nabarlek ore body. However, since the samples show a substantial excess of thorium, it is assumed that the redistribution has been caused by surface erosion. Of greater relevance is the sub-surface secondary mineralization associated with Koongarra. Further work is under way to evaluate the model on the basis of the data from this deposit.

3.5.3 Separation of zones of leaching and zones of deposition

General evidence for the separation of zones of leaching and deposition has been obtained from the consistent trend of $^{230}Th/^{234}U$ activity ratios from three deposits (Figure 3). Confirmation has recently been obtained from studies of the $^{230}Th/^{234}U$ and $^{234}U/^{238}U$ activity ratios

in phases extracted sequentially from S1/146 core samples from Ranger One. Of particular interest are the data from the amorphous iron phase as the secondary crystalline minerals from which they are derived are less accessible to leaching and deposition processes. In the upper zone I, there is an excess of ^{230}Th; $^{230}Th/^{234}U$ ratios vary from 1.4 to 4.7. In the zone of deposition, zone II, ^{230}Th is deficient (activity ratios vary from 0.75 to 0.37). Full details are discussed in Section 6.5.2.

3.5.4 Erosion

Estimates of the erosion rates at Ranger One and Jabiluka One vary between 0.02 and 0.96 mm/y, with a mean value of about 0.02 mm/y. There are problems in relating the calculated erosion rates to the assumed stability of the landscape since the Tertiary period. However, it is pointed out that erosion is a local phenomenon, and that observations at a specific site over a relatively restricted period (<500,000 y) cannot necessarily be generalized over geological time. Attempts to estimate erosion and deposition rates gave values that were consistent with those found from the model.

3.6 Correlation with the Uranium Trend Dating Model[5]

The general features of the uranium trend dating model have been outlined in Section 3.1. Attempts have been made to interpret perturbations in the levels of uranium series nuclides produced by the flux of uranium in the mobile aqueous phase. To apply the model to specific soil horizons, a uranium trend line is obtained by plotting $(^{234}U-^{234}U)/^{238}U$ against $(^{238}U-^{230}Th)/^{238}U$. Specific expressions have been obtained for these ratios in terms of

- the decay constants of ^{238}U, ^{234}U and ^{230}Th,
- the elapsed time t, and
- the decay constant λo,

where the parameter λo is the decay constant associated with the uranium flux F(0). In the words of Rosholt, "The actual physical significance of F(0) is not well understood. It is related to the flux of mobile phase uranium through a deposit; isotopic data for deposits of known age indicate that this flux decreases exponentially with time."[5]

The open system model (Section 3.2) has many features in common with the uranium trend model and may be correlated with it.

(a) The parameters $(^{234}U-^{238}U)/^{238}U$ and $(^{238}U-^{230}Th)/^{238}U$ which define the trend line are equivalent to (Su(1) and (1-Si) (equations (9) and (10)) respectively.

(b) The uranium trend dating model is defined in terms of two variable parameters, t and λo (the empirical decay constant associated with F(0); the relationship between (Su-1) and (1-Si) is determined by t, a first order leaching (or desorption) term ξ, and the ratio R of the ^{234}U to ^{238}U leaching rates.

To establish a relationship between the grouped parameter λo and the terms ξ and R, attempts are made to obtain a suite of calibration curves analogous to the curve 3 of reference [5]. If successful, new insights into the significance of λo on the one hand and ξ and R on the other may be obtained. Work is currently proceeding along these lines.

References

1. M. Ivanovich, "Uranium Series Disequilibria Applications in Geochronology", Chap. 3, pp.56-78, in Uranium Series Disequilibrium. Applications to Environmental Problems, Ed M. Ivanovich and R.S. Harmon, Clarendon Press, Oxford, 1982.

2. J.N. Rosholt, "Open System Model for Uranium Series Dating of Pleistocene Samples", pp.299-311 in Proceedings of Symposium on Radioactive Dating Methods and Low-level Counting, Monaco 1967, (IAEA Vienna).

3. B. Szabo and J.N. Rosholt, "Uranium Series Dating of Pleistocene Malloscan Shells from Southern California - An Open System Model", J. Geophys. Res., 74, 3253-60 (1969).

4. P. Hille, "An Open System Model for Uranium Series Dating". Earth Planet. Sci. Lett., 42, 138-143 (1979).

5. J.N. Rosholt, "Uranium Trend Dating of Quaternary Sediments", U.S. Geological Survey Open File Report 80-1087, 1980.

6. P.L. Airey, D. Roman, C. Golian, S. Short, T. Nightingale, R.T. Lowson and G.E. Calf, "Radionuclide Migration around Uranium Ore Bodies - Analogues of Radioactive Waste Repositories", USNRC Contract NRC-04-81-172, Annual Report 1981-82, AAEC Report C29, 1982.

4. APPLICATION OF THE OPEN SYSTEM MODEL TO THE NABARLEK DEPOSIT

4.1 Geology - Brief Description

Hegge et al.[1] have provided a brief description of the geology of the Nabarlek region (Figure 1) : uranium mineralization consists of massive and disseminated pitchblende associated with a halo of secondary minerals; the ore body occurs within chloritic schists and is best developed where the adjacent country rocks are chloritic; hematite is a major constitent near the centre of the zone of mineralization; the ore body is underlain by the Oenpelli dolerite sill which locally is about 200 m thick. A generalized geological cross section[1] is shown in the insert of Figure 6.

The principal aquifers are within the fracture zones of the relatively impermeable crystalline rock mass. The groundwater generally occurs over a 20 m interval between 55 and 35 m. The top of the aquifer zone ranges from 10 to 25 m below the surface. The aquifer is overlain by weathered material which, within the mine area, is often clayey and extends to depths of about 10 to 20 m. This is overlain by less than 1 m of lateritic soil and sand. During the wet season, the groundwater flow is generally towards the east and is controlled largely by the topography. The direction changes towards the south-west during the wet season, and is possibly determined by the bed-rock fracture patterns.

4.2 Uranium Series Disequilibria Within the Ore Body

4.2.1 Four-zone model

A series of drill core samples was collected from the Nabarlek ore body (Figures 7-10) and assayed for $^{234}U/^{238}U$, $^{230}Th/^{234}U$ and $^{226}Ra/^{230}Th$ ratios. The data are listed in Table 8. Figure 3 indicates the variation of $^{230}Th/^{234}U$ ratio with depth; the analogous relationship for Ranger One and Jabiluka One deposits is shown as an insert (see Figure 22 of Ref. 2). A large surface excess of thorium overlays a zone of depletion. The activity ratio rises in the transition region between the weathered and unoxidized host rock. From this, it is clear that the four-zone model developed for Ranger One and Jabiluka One can be applied to the Nabarlek ore body.

BOUNDARY CONDITIONS FOR THE FOUR-ZONE MODEL (NABARLEK)

Zone	Depth to Zone Interface (m)	$(^{234}U/^{238}U)_0^+$	$(^{230}Th/^{234}U)_0^+$	Comment
I	1.7±0.1	1.0	0.7	Zone of leaching; correlates with unsaturated zone.
II	10±1	1.0	1.0	Zone of deposition; correlates with saturated zone in weathered zone.
III	*	1.0	1.0	Transition zone between weathered and unweathered host rock.
IV				Unweathered (crystalline) zone.

+ Values of the isotope ratio at the zero time point t_o.[2]

* The zone interface cannot be located from the $^{230}Th/^{234}U$ ratios.

A schematic representation of the four-zone model is shown in Figure 4. The interpretation of the zero time t_o, the method for calculating E, the rate of surface erosion, W, the rate of advance of the weathering front, and L(D), the rate of leaching (deposition) are set out in Reference (2).

Computed values for the model parameters are listed in Table 8. The calculations cannot be extended to zone III because the isotope data are not sufficiently different from those in zone IV.

From Table 8 it can be seen that there is significant uranium leaching in the upper zone and deposition in zone II. The upper zone is interpreted as the unsaturated region, averaged throughout the late Quaternary. Its thickness (1.7 m) is substantially less than that observed at Ranger One and Jabiluka One (8 ± 1 m). It is also deduced from the model that

(i) the average rate of surface erosion (0.05 m/1000 y) is comparable to that observed at Ranger One and Jabiluka One (0.02 - 0.9 m/1000 y (see Tables 2-6)), and

(ii) in general, the leaching rate is somewhat greater.

Zone I corresponds to the surface layer of sandy lateritic soil, which is generally unsaturated; zone II corresponds to a saturated weathered region; and zone III is a transition region between the fully weathered schists and the underlying fractured rock (zone IV).

4.2.2 Uranium migration, vertical component

As with the Ranger and Jabiluka ore bodies, the vertical uranium flux far exceeds the horizontal component induced by regional groundwater flow. Quantitative estimates are inevitably crude but important in assessing the ore body of the geochemical analogue of a waste repository. Data were used from drill holes 52, 71 and 91 which intersect the deposit (Figures 7-10). The results are listed in Table 9.

Averaged over available profiles, the annual leaching rate per cubic metre of core in zone I is about 2.7 mg. The corresponding deposition rate in zone II is 124 mg. Although the leaching rate, expressed as a percentage of total uranium, is greater in zone I, the calculated deposition rate in zone II is greater by more than an order of magnitude. There are two possible causes for this discrepancy:

(i) At low proportional deposition/leaching rates, the calculation is extremely inaccurate and can serve only as a guide to quantitative behaviour.

(ii) In contrast to the Ranger One study[2], the contribution of zone III (a region of leaching) to the total flux cannot be calculated.

4.2.3 Uranium migration, horizontal component

4.2.3.1 Groundwater

Before the commencement of mining, it is highly likely that a component of the regional groundwater flow intersected the deposit.[3] The net horizontal flux of dissolved uranium out of the zone of mineralization can be estimated. It is necessary to assume that a representative concentration of uranium in groundwater immediately down-gradient of the deposit is that in OB 20 (Figure 6), i.e. 79 $\mu g\ L^{-1}$. If the distance across the zone of mineralization is assumed to be about 100 m, the gradient $dU/dx = 0.8\ \mu g\ L^{-1}\ m^{-1}$. Hence if the porosity ($\emptyset$) is 0.5, the depth of weathered host rock (H) is 10 m, and the groundwater velocity is V m y^{-1}, the net annual rate of transport of uranium per cubic metre of core (T) is

$$T = dU/dx \times \emptyset \times H \times V$$

$$= 4 \times V(mg\ m^{-1}\ y^{-1}) .$$

4.2.3.3 Erosion

The average rate of surface erosion is about 0.06 mm y^{-1}. If an average uranium level of 500 $\mu g\ g^{-1}$ and a bulk density of say, 1.3-1.4, is assumed, the annual rate of uranium loss is $0.06 \times 0.1 \times 10^4\ cm^2 \times 2.6\ g\ cm^{-2} \times 500 \times 10^{-3}\ mg\ g^{-1}$ or 39 mg m^{-2}. Thus, as with Ranger One, erosion

is probably the major mechanism of removal of uranium from the ore body. It would thus appear that the accumulation of uranium near the surface down-gradient of the ore-bearing zone is due principally to erosion.

References

1. M.R. Hegge, D.V. Mosher, G.S. Eupene and P.S. Anthony "The Role of Clay Adsorption in Genesis of Uranium Cores", in Proceedings of IAEA International Symposium Uranium in the Pine Creek Geosyncline, Sydney, Ed J. Ferguson and A.B. Goleby (IAEA, Vienna, 1980), pp.521-529.

2. P.L. Airey, D. Roman, C. Golian, S. Short, T. Nightingale, R.T. Lowson and G.E. Calf, "Radionuclide Migration around Uranium Ore Bodies - Analogues of Radioactive Waste Repositories", USNRC Contract NRC-04-81-172, Annual Report 1981-82, AAEC Report C29, 1982.

3. J.A. Grounds, "Groundwater Monitoring Procedures and Evaluation at Nabarlek, NT", in Proceedings of the AWWA International Specialist Conference on Water Regime in Relation to Milling, Mining and Waste Treatment, paper 16, Darwin (1983).

5. MINERALOGY OF DRILL CORE SAMPLES*

5.1 Introduction

There is a relationship between the release and redistribution of radionuclides, the mineralogy and the geochemical and hydrochemical processes occurring in the accessible time-scale. To investigate this relationship, the mineralogy of two drill holes at Jabiluka One (DH 3 and DH 16) and one at Ranger One (S1/146) is being studied and correlated with measured uranium series disequilibria. The aims of these investigations are:

(i) to correlate differences in mineralogy and geochemical history with the isotopic data;

(ii) to gain information on weathering processes which may be important for the transport and storage of radionuclides;

(iii) to gain an understanding of the processes and time-scale of schist weathering;

(iv) to identify the mineral components associated with the radionuclides under investigation (Section 6).

5.2 X-ray Diffraction Methods

For the initial investigations of the mineralogical composition, X-ray diffraction (XRD) was carried out on the <100 mesh B.S. powder prepared with a ring grinder. This technique enables identification of such components as iron oxides and oxyhydroxides which, although present in small concentrations, may have a major effect on radionuclide storage. Two types of samples were used:

(i) Random Powders. There is no preferred orientation, and all hkl reflections should be observed in the ratios recorded in the Powder Diffraction File.[1]

(ii) Sedimented Aggregates. In sedimented aggregates the plate-like clay minerals have a preferred orientation; particles tend to lie parallel to each other and the underlying surface. In a completely basal orientation, the identification of the minerals in a sample relies solely on the basal reflections. The sedimented aggregates are saturated with various cations at different relative humidities, heated, and treated with organic solvents to identify the reflections positively.

The theory and practice of XRD analysis has been described in detail by Klug and Alexander.[2] The interpretation of the reflections from random powders and sedimented aggregates has been discussed by several workers.[3-8] Unless otherwise stated, these references were used to interpret all XRD patterns.

* Drill locations are shown in Figure 1.

5.3 Experimental

The <100 mesh B.S. samples (used for isotope counting) were run as random powders without additional treatment. Samples run were:

Jabiluka One : DH 3 - 11.0 m, 11.3 m, 14.0 m, 20.1 m, 29.6 m, 70.5 m

DH 16 - 4.0 m, 8.2 m, 13.1 m, 19.5 m, 45.1 m, 54.6 m

Ranger One : S1/146 - 2.7 m, 4.0 m, 9.1 m, 13.1 m, 14.6 m, 21.0 m

The S1/146 2.7 m, 4.0 m, 9.1 m, 13.1 m samples were also separated into <2 μm and >2 μm sized fractions. Diffraction patterns of the >2 μm fraction were obtained for all four samples and the 2 <m fraction for the 2.7 m and the 13.1 m sample was also analysed. The samples were run from 2-75° 2θ, using CoK_{α} radiation.

The <2 μm fractions for the untreated samples were collected by sedimentation, according to Stokes' law, following ultrasonic dispersion which minimized alteration of the samples. Sedimented aggregates were prepared by filtering onto a ceramic tile or evaporating onto a glass slide. Magnesium (Mg) and potassium (K) saturated aggregates were prepared. The Mg saturated aggregates were run dry (Mg(air dry)) and wet (Mg(wet)), or glycerated to facilitate identification. The K saturated samples were also heated for two hours at 120°C (K(120°), 200°C, 300°C, 400°C and 550°C. All K samples were analysed by XRD between each heating sequence.

The samples from S1/146 were inspected for structure and fabric, and their colour was determined using a Munsell colour chart.

5.4 Results and Discussion

The diffraction patterns from all treatments for the sedimented aggregates of DH 16 - 4.0 m and DH 16 - 54.6 m are shown in Figure 11. The Mg(air dry) XRD pattern for the DH 16 - 4.0 m sample shows three reflections: the 1.00 nm reflection corresponds to the 001 reflection of mica; the 1.45 nm reflection corresponds to the 001 reflection of chlorite, smectite or vermiculite; and the 0.72 nm reflection corresponds to the 002 of 1.4 nm minerals, and have an intensity due to the 001 reflection of kaolinite (identified by XRD on the random powders).

Smectite can be distinguished from chlorite or vermiculite by its swelling property when wet or when treated with organic solvents. The swelling of part of the 1.4 nm peak to 1.87 nm in the Mg(wet) diffraction pattern and 1.78 nm in the Mg(glycerol) diffraction pattern of sample DH 16 - 4.0 m indicates the presence of smectite. Smectite will also collapse, giving a 1.0 nm spacing, when the K saturated aggregate is heated. The presence of smectite is also indicated by a large fall in intensity of the 1.4 nm reflection and an increase in intensity of the 1.00 nm reflection of the K(120°) diffraction pattern relative to the K(air dry) diffraction pattern.

When saturated with K and air dried, vermiculites are distinguished from the other 1.4 nm minerals by the fact that they collapse, giving a 1.0 nm spacing. Comparison of the K(air dry) with the Mg(air dry) diffraction pattern of sample DH 4 - 16.0 m shows a small amount of collapse which indicates the presence of some vermiculite.

Any remaining intensity of the 1.4 nm reflection after heating to 120°C or 200°C is due to chlorite. The constituents of the sedimented aggregates of DH 16 - 4.0 m are therefore chlorite, kaolinite, mica, smectite, and vermiculite.

In comparison, the 54.5 m sample shows no swelling or collapse, indicating the absence of smectite or vermiculite. Kaolinite was not observed in the random powder diffraction pattern. The constituents are therefore chlorite and mica.

The Mg(wet), Mg(air dry), K(wet), K(air dry) and K(120°C) diffraction patterns show changes in the mica peak position and width. This suggests that some of the mica is interstratified, the interstratification being either mica/smectite or mica/high charge smectite. The sample from DH 3 - 20.1 m shows a greater concentration of interstratified mica than other samples; its diffraction pattern was similar to that of regularly interstratified mica/smectite.[9]

Figure 12 shows the random powder diffraction patterns for three unweathered rock samples. Sample DH 3 - 29.6 m is representative of most of the Jabiluka One rock samples. As was previously observed by petrological techniques[10], the three major components are quartz, mica and chlorite. The hkl reflections enable the identification of the polytype. The 060 reflection occurs at 0.1500 nm (73.3°C 2θ), so the mica and chlorite are dioctahedral. (The cations in the octahedral sheets are 3+ ions, such as Al^{3+} or Fe^{3+}, so only two thirds of the octahedral cation sites are filled to achieve charge balance.) Sample DH 3 - 29.6 m can therefore be denoted as

quartz/chlorite IIb/muscovite $2M_1$
(dioctahedral)

Also shown in Figure 12 are the diffraction patterns for samples DH 3 - 70.5 m and DH 16 - 19.5 m. These samples differ from the others, they contain no mica and the 060 reflection is at 0.153 nm, indicating that the chlorite is trioctahedral. (The octahedral sheets contain 2+ ions, such as Mg^{2+} and Fe^{2+}, so all of the octahedral cation sites are filled.) The chlorite may be due to the alteration of biotite (a trioctahedral mica) or some other Mg^{2+} or Fe^{2+} rich mineral.

Figure 13 illustrates the technique used to identify goethite at low levels. The 110 reflection of goethite (0.417 nm) is observed in the <2 μm sedimented aggregate diffraction patterns. This is a much more sensitive technique than the use of whole sample random powder for several reasons:

- Interference from quartz and clay mineral reflections is reduced owing to the low levels of quartz in the <2 μm fraction and the reduced intensity of the hkl reflections of the clay minerals.

- The 110 reflection of goethite is intensified by the orientation effect.

- Goethite is decomposed at 200-300°C whereas other minerals in these samples are unaltered in that range of temperatures. This allows the reflection to be assigned unambiguously.

The mineralogical descriptions of DH 3, DH 16 and S1/146 obtained with these techniques are shown in Tables 10-12 which give the percentage quartz and the mineralogy of the <2 μm fraction. A quantitative description is not feasible due to the effects of orientation and isomorphous replacement on intensities. The values given for the clay mineralogy are percentages of the total intensity for each material. Although not necessarily the same as the actual percentages of materials in the sample, these values are a very useful illustration of mineralogical trends.

Tables 10 and 11 give the results for the Jabiluka One samples. The unweathered rock samples (below 15 m) contain approximately 50% quartz and amounts of chlorite and muscovite. Other minerals occasionally observed are pyrite and anatase. There is both lateral and vertical heterogeneity, however, samples within 10 m of each other (i.e. DH 3 - 20.1 m/29.6 m and DH 16 - 45.1 m/54.6 m) have similar concentrations of the three major minerals in their random powder diffraction patterns.

Chemical weathering is observed above the 15 m depth, but the weathering products (smectite, kaolinite, vermiculite) are major constituents of the <2 μm fraction only above 10 m. However, even for the shallowest sample (DH 16 - 4.0 m), well over 50% of the sample consists of quartz, chlorite and mica.

The mineralogy (Table 12) and weathering profile (Table 7) of the Ranger One sample S1/146 is substantially different from that of the Jabiluka profiles. The rock contains quartz, chlorite and 1M muscovite; in contrast with the Jabiluka samples, which contain $2M_1$ muscovite. The weathering is deeper and much more intense. Between 21.0 m (unweathered rock) and 14.6 m all the chlorite has been weathered. Mica is also highly reduced, going up the profile. The major clay minerals from 2.7 to 14.6 m are kaolinite and smectite.

The profile description can be correlated with the description of soils in this area given by Eupene et al.[11] It can be seen that the profile is lateritic, and that there is a fluctuating water table induced by the alternating wet and dry seasons. The Eh of much of the groundwater is less than 100 mV, so significant amounts of ferrous ion will be present in solution.[12] This ferrous ion is transported upwards to the ferruginous zone (2.7 m) where it oxidizes and is precipitated to form

ferric oxides. The existence of a pallid zone (9.1 m, 4.0 m) overlain by a mottled zone (2.7 m) is a normal lateritic phenomenon.

The presence of goethite (FeOOH) in both the 13.1 m and the 14.6 m samples below the pallid zone is unusual. This goethite contains 10-20% aluminium, and seems to have been precipitated after the release of iron during the weathering of the chlorite and mica[13] in the parent material. The precise conditions leading to this double iron zoning effect are not yet fully understood.

The presence of secondary uranium minerals such as saleeite [$Mg(UO_2)_2(PO_4)_2$ 8-$10H_2O$] and metatorbernite [$Cu(UO_2)_2(PO_4)_2$8-$10H_2O$] in the pallid zone, and sklodowskite [$Mg(UO_2)_2(SiO_2)_2(OH)_26H_2O$] in the mottled zone of some profiles in this region[11], suggests that these weathering and lateritic conditions have led to uranium transport within the profile. Other work has shown (Section 6) that uranium is associated with iron oxides and oxyhydroxides. Together, these phenomena are of importance in the investigation of the transport of uranium and the other radionuclides.

References

1. Joint Committee on Powder Diffraction Standards, "PDF Powder Diffraction File", 1601 Park Lane, Swarthmore, Pennsylvania, USA.

2. H.P. Klug and L.E. Alexander, X-ray Diffraction Procedures, (J. Wiley, NY, 1974).

3. S.W. Bailey, "Structures of Layer Silicates", in Crystal Structures of Clay Minerals and their X-ray Identification, Ed G.W. Brindley and G. Brown (Mineralogical Society, London, 1980), pp.1-124.

4. G.W. Brindley, "Order-Disorder in Clay Mineral Structures", in Crystal Structures of Clay Minerals and their X-ray Identification, Ed G.W. Brindley and G. Brown (Mineralogical Society, London, 1980), pp.125-195.

5. D.M.C. MacEwan and M.J. Wilson, "Interlayer and Intercalation Complexes of Clay Minerals", in Crystal Structures of Clay Minerals and their X-ray Identification, Ed G.W. Brindley and G. Brown (Mineralogical Society, London, 1980), pp.197-248.

6. R.C. Reynolds, "Interstratified Clay Minerals", in Crystal Structures of Clay Minerals and their X-ray Identification, Ed G.W. Brindley and G. Brown (Mineralogical Society, London, 1980), pp.249-304.

7. G. Brown and G.W. Brindley, "X-ray Diffraction Procedures for Clay Mineral Identification", in Crystal Structures of Clay Minerals and their X-ray Identification, Ed G.W. Brindley and G. Brown (Mineralogical Society, London, 1980), pp.305-360

8. G. Brown, "Associated Minerals", in Crystal Structures of Clay Minerals and their X-ray Identification, Ed G.W. Brindley and G. Brown (Mineralogical Society, London, 1980), pp.361-410.

9. R.C. Reynolds and J. Hower, "The Nature of Interlaying in Mixed layer Illite-Montmorillonite", Clays Clay Miner., 18, 25-36 (1970).

10. G.R. Ewers and J. Ferguson, "Mineralogy of the Jabiluka, Ranger, Koongarra, and Nabarlek Uranium Deposits", in Proceedings of IAEA International Symposium Uranium in the Pine Creek Geosyncline, Sydney, Ed J. Ferguson and A.B. Goleby (IAEA, Vienna, 1980), pp.363-374.

11. G.S. Eupene, P.F. Fee and R.G. Colville, "Ranger 1 Uranium Deposits", in Economic Geology of Australia and Papua New Guinea; Australas. Inst. Min. Metall., Monograph Series No. 5, 1 Metals (1975), pp.308-317.

12. A.P. Schwab and W.L. Lindsay, "Effect of Redox on the Solubility and Availability of Iron", Soil Sci. Soc. Am. J., 47, 201-205 (1983).

13. J.A. Veith and M.L. Jackson, "Iron Oxidation and Reduction Effects on Structural Hydroxyl and Layer Charge in Aqueous Suspensions of Micaceous Vermiculites", Clays Clay Miner., 22, 345-353 (1974).

6. SELECTIVE PHASE SEPARATION - WEATHERED ZONE

6.1 Introduction

As noted in Section 2, the principal aim of this project is to establish the validity of combining laboratory adsorption and hydrological data to predict the migration of radionuclides over tens to hundreds of thousands of years. Over this period, there has been time for the radionuclides to adsorb on accessible surfaces and subsequently redistribute through other phases. For instance, it has been shown that uranium and a range of other metals adsorb initially on the amorphous iron phase of alluvial sediments.[1] With the passage of time, there is a transition to secondary crystalline iron minerals in which the trace metals are far less accessible to the mobile phase (groundwater).

As a working hypothesis, it is assumed that laboratory leaching experiments reflect the distribution of radionuclides through the ore sample (relationship 2, Figure 2). If this can be established, by the use of geochemical analogue, progress will have been made towards understanding how sorption/leaching experiments can be used to predict long-term transport in the geological settings being considered for high-level waste repositories.

Chemical fractionation is one of the procedures which can be used to investigate the sites of radionuclide concentration. The power of uranium series studies is that, in addition, parent/daughter disequilibria can be measured in each phase. Isotope fractionation reflects the time dependent physicochemical processes associated with the radionuclide redistribution over very long periods.

6.2 Chemical Procedures

The method of chemical fractionation into the various mineralogical groups follows well established methods in soil science and geochemistry and is summarized below:

(a) Soluble salts and exchangeable ions. The sample is extracted with unbuffered 0.1 M NH_4Cl (2 g + 80 mL) at ambient temperature for 24 hours with continuous agitation.[2,3]

(b) Amorphous minerals and ferrihydrite. The residue from (a) is extracted with Tamm's acid oxalate[4,5] (2 g + 80 mL) at ambient temperature in the dark for four hours.

(c) Crystalline iron minerals. The residue from (b) is extracted twice, for half an hour in each case, at 80°C with citrate-dithionite-bicarbonate solution using continuous agitation.[6]

(d) Residual amorphous inorganic materials, aluminous interlayers, allophane and imogolite. The residue from (c) is shaken with 5% Na_2CO_3 (2 g + 80 mL) solution at ambient temperature for 16 hours.[7,8]

(e) Resistant minerals including clay minerals, quartz, anatase and zircon. The residue from (d) is digested with a mixture of nitric, hydrofluoric and perchloric acids. Residual insoluble material is fused with sodium peroxide.[9]

After each extraction, the solution is separated from the residue by centrifugation (3500 rev./min for 15 to 30 min) and the supernatant passed through a 0.45 μm membrane filter. The residue is washed with 15-20 mL of 0.1 M NH_4Cl, separated in the same manner and the washing combined with extract. Analytical yield tracers of ^{236}U or ^{232}U and ^{228}Th are added and solutions made up to 100 mL with NH_4Cl solution.

In the case of the Na_2CO_3 extraction, 20 mL of acetone is added before centrifugation to flocculate peptized clays; the supernatant is then filtered through a Whatman No. 542 paper filter. Tracers are added and the solution made up to volume.

The residue from the Na_2CO_3 extraction is dried at 105°C and counted for ^{226}Ra (by emanation of ^{222}Rn to isotopic equilibrium) after standing for 20 days. It is then digested in a sequence of nitric, hydrofluoric and perchloric acids and, upon evaporation to dryness, dissolved in 9 M HCl. This solution is centrifuged to separate any silicious residue, the residue washed thoroughly with more 9 M HCl and then made up to volume with added tracers.

The residue (if any) from centrifugation of the acid digestion is dried at 105°C, tracers added, and then fused with 1 g of Na_2O_2 in a platinum crucible. The cooled melt is dissolved in 9 M HCl and made up to volume.

6.3 Verification of the Sequential Extraction Procedure

The sequential extraction procedure (Section 5.2) is designed to distinguish various classes of soil and rock and to investigate the association of the ^{238}U decay series radionuclides with each of these classes. However, because mineralogical and chemical factors may cause ambiguities, they have been investigated as follows:

(a) Iron-rich chlorite and biotite are attacked by acid oxalate[10], and illite may also be susceptible to this reagent. None of these minerals were observed in the diffraction patterns of the four core samples. Tamm's acid oxalate (TAO) reagent also extracts organic complexes of Fe and Al.[11,12] The organic carbon contents, determined by the McLeod's method[13], were 2.7 m - 0.08%, 4.0 m - 0.03%, and 9.1 m - 0.03%.

(c) Magnetite (Fe_3O_4) and maghemite (F_2O_3) may be partially dissolved by TAO.[14,15] Chao and Zhou[16] recently determined that up to 20%

of the magnetite in a synthetic sample will be dissolved after four hours' treatment with TAO. The concentrations of these minerals were determined by collection on a magnetic stirrer. Extractions were repeated twice; the values given in Table 13 represent the upper limits only. Under these conditions some confidence can be placed on the interpretation that the iron removed by Tamm's acid oxalate is due principally to amorphous iron oxides and ferrihydrate.

It can be concluded that factors that could lead to ambiguities in the sequential extraction scheme are not present.

X-ray diffraction analysis was used to investigate the effect of the TAO and the citrate-dithionite-bicarbonate (CDB) extractions on the solids. The random powder diffraction patterns of samples treated by TAO and the CDB were compared with those of the untreated samples; the results are as follows:

(i) Little or no effect was observed on any reflection of the TAO treated samples.

(ii) In the CDB treated sample diffraction patterns, the iron oxide and oxyhydroxide reflections disappeared, whereas the quartz and clay mineral reflections were not affected. The 2.7 m and 4.0 m samples lost the hematite 100 reflection at 0.258 nm and the 13.1 m sample lost the goethite 110 reflection at 0.417 nm. The level of goethite in the 9.1 m sample was very low and no change could be observed by visual inspection due to the major overlap from the kaolinite reflections.

Figure 14 shows the effects of TAO and CDB extractions on the 22-26°2θ region of the 13.1 m diffraction pattern. It can be seen that the goethite, quartz and clay mineral reflections are not affected by the TAO extraction, whereas the CDB extraction, although it did not affect the quartz and clay minerals, resulted in the complete loss of the goethite reflection, as expected. This is confirmed by the colour of the samples. The 2.7 m sample is red owing to the presence of hematite, whereas the 13.1 m sample is yellow, indicating the presence of goethite. The 4.0 m and 9.1 m samples are white, being subsamples from the pallid zone. The TAO extraction did not affect the colour of the samples but with CDB extraction all the residues were completely colourless, indicating the dissolution of all iron.

6.4 Results

6.4.1 Mineralogy

A systematic study has been made of the mineralogical samples from the Ranger One drill core S1/146, taken at depths of 2.7, 4.0, 9.1 and 13.1 m. Details are presented in Section 4 and summarized in Table 7. Briefly,

the 2.7 m and 4.1 m samples come from the mottled zone which lies below the ferruginous or ferricrete layer; the 9.1 m sample is from the pallid zone; and the 13.1 m sample is from a zone of weathered rock (Cahill formation, Upper Mine Series).

6.4.2 The distribution of uranium and thorium in extracted phases

The distributions of ^{238}U, ^{234}U and ^{230}Th in the five extractants are listed in Tables 14-17. The variation of $^{234}U/^{238}U$ and $^{230}Th/^{234}U$ ratios with the percentage uranium extracted is illustrated in Figures 15 and 16 respectively. Tests of the reproducibility of the techniques are outlined in Table 18. The proportions of ^{238}U and the $^{234}U/^{238}U$ activity ratios in three duplicated extractions from two samples are in good agreement. Further, the total uranium obtained by summing the results of α-spectrometric assays of each of the extracts were in good agreement with those found by delayed neutron activation analysis on whole (solid) samples (Table 19).

6.5 Discussion

6.5.1 Uranium

Uranium and thorium appear to be associated more with iron minerals than with the clay/quartz phase. Only a small proportion of uranium is exchangeable (extracted with 0.1 M NH_4Cl). The $^{234}U/^{238}U$ activity ratios vary between 1.17 and 1.27, which is consistent with values for samples from wells immediately down-gradient of Ranger One and indicates that the most labile forms of uranium in water are in equilibrium with the exchangeable component.

The $^{234}U/^{238}U$ activity ratio varies substantially between different extracts. This is due to the net effect of a number of factors, including

- the initial activity ratio,
- recoil,
- decay, and
- leaching or deposition.

The greatest isotopic fractionation is found in the 13.1 m sample which may be described, in broad terms, as weathered rock. The process of weathering involves the decomposition of chlorite and muscovite which forms vermiculite as the first product and smectite and kaolinite as ultimate products. During the decomposition, iron is released and deposited as goethite. Accompanying these processes is the mobilization of uranium. The observed enrichment of ^{234}U in the clay/quartz may be

due to the recoil effects discussed below. By contrast, the $^{234}U/^{238}U$ activity ratios in the amorphous iron phase in the saturated zone at 9.1 and 13.1 m horizons are 0.80 and 0.67 respectively. This is consistent with the assumption of Zielinski and co-workers[1] that the uranium in the amorphous phase is in equilibrium with groundwater as the dissolved uranium close to the Ranger One deposit is generally depleted in ^{234}U. It should however be pointed out that the sample at 4.0 m is slightly enriched.

Recoil. Following a recoil event, the ^{234}U is ejected an average distance of about 20 nm.[17] The iron (manganese and amorphous alumina) phases represent between 1 and 4% of the weight of the ore samples, but contain between 50 and 98% of the uranium. On the other hand, the clay/quartz fraction is about 95% of the dry weight and more than 60% of the water saturated weight. Statistically then, the ^{234}U is likely to lodge in the clay/quartz phase following recoil. This would provide a reason for the observed activity ratios being greater than the average for the sample. Evidence for the recoil mechanism is supported by the decrease in $^{234}U/^{238}U$ ratio from 1.78 for the 2.7 m sample, through 1.32 at 4 m to 1.27 at 9 m. Thus the shallower the sample, the lower the time-averaged water content, the higher the averaged weight fraction of the clay/quartz phase, and hence the higher the probability of lodgement of a recoil ^{234}U. An explanation for the high activity ratios in the 13.1 m sample is still being sought.

6.5.2 Thorium

As with uranium, the thorium concentrates in the iron phases; the percentage of thorium varies from 75 to 96. Of particular interest are the $^{230}Th/^{234}U$ activity ratios in amorphous iron, which is considered to be the primary site for the adsorption of metal ions from groundwater. The activity ratios in the 2.7 and 4.1 m samples are high due to the leaching of uranium; in the 9.0 and 13.1 m samples, the values are less than unity as a consequence of net uranium deposition in the pallid zone (Figure 16). The $^{230}Th/^{234}U$ ratios vary by more than a factor of ten.

By contrast, the $^{230}Th/^{238}U$ activity ratios in the crystalline iron phase show little variability. The average value for the four samples is 2.45±0.7. The $^{230}Th/^{234}U$ activity ratios are slightly more constant (2.3±0.4). The standard deviations are of the population. It is tentatively assumed that the ratios are chemically controlled during the crystallization of the secondary iron phase. Since radiogenic decay processes would lead to secular equilibrium, the high activity ratio would only be maintained if chemical control were re-established at times commensurate with the half-life of ^{230}Th (75,200 y). Hence, at least over these time-scales, crystalline iron phases must be labile. It is generally accepted that ions from groundwater do not readily exchange with crystalline iron.[1]

6.5.3 Radium

The radium data for core S1/146 are listed in Table 20. A notably larger fraction of ^{226}Ra is in the clay/quartz phase than uranium. More significantly, the ^{226}Ra is in excess of the parent ^{230}Th. Apart from the 13.1 m sample, the excesses are not large and can readily be explained in terms of either recoil effects or preferential isomorphous substitution into the clay lattice. As with ^{234}U, recoil ^{226}Ra lodges in the clay/quartz phase.

6.6 Relevance of the Studies to the Long-term Prediction of Radionuclide Transport

Care must be taken when relating these findings to the prediction of the long-term migration of allogenic radionuclides. The uranium series elements measured in this study are essentially authigenic. They are generated *in situ* by radioactive decay or released by the weathering process. However, a number of factors are relevant:

(i) As previously reported[18], evidence is presented that the amorphous iron (manganese and aluminium) is the phase primarily involved in the sorption of metal ions from groundwater solution. However, a substantial proportion of uranium and thorium is associated with secondary crystalline iron phases. Since it appears that the amorphous and crystalline iron phases are exchangeable, at least over times commensurate with the half-life of ^{230}Th, there is a mechanism for the long-term retardation of radionuclide transport:

$$\text{M(solution)} \rightleftharpoons \text{M-Fe(amorphous)} \rightleftharpoons \text{M-Fe(crystalline largely inaccessible to groundwater)}$$

(ii) Some radionuclides of particular relevance to HLW repository siting (e.g. ^{226}Ra) are formed by radioactive decay over thousands to tens of thousands of years. Under the conditions being investigated, a significant fraction of the recoil radium would be ejected into the clay/quartz and hence be largely inaccessible to the groundwater. Evidence for groundwater inaccessibility is provided by the large differences between $^{234}U/^{238}U$ ratios in the solid and aqueous phases.

References

1. R.A. Zielinski, S. Bloch and T.R. Walker, "The Mobility and Distribution of Heavy Metals during the Formation of First Cycle Red beds", Econ. Geol. (in press).

2. B.M. Tucker, "Laboratory Procedures for Cation Exchange Measurements on Soils", CSIRO Division of Soils Tech. Paper No. 23 (Canberra, 1974).

3. G.P. Gillman, R.C. Bruce, B.G. Davey, J.M. Kimble, P.L. Searle and J.O. Skjemstad (1983), "An Inter-laboratory Comparison of Methods used for Determination of Cation Exchange Capacity", Comm. Soil Sci. Plant Nutr. (in press).

4. O. Tamm, "Über die Oxalatmethode in der Chemischen Bodenanalyse", Från Statens Skogsforsoeksans., Stockholm, 27:1-20, 1932.

5. U. Schwertmann, "Differenzierung der Eisenoxide des Bodens durch Extraktion mit Ammoniumoxalate-Lösung", Z. Pflanzen., Dgg., Bodenk., 105:194-202, 1964.

6. O.P. Mehra and Jackson, M.L., "Iron Oxide Removal from Soils and Clays by a Dithionite-Citrate System buffered with Sodium-Bicarbonate", 7th Nat. Conference, Clays Clay Miner., Monograph No. 5, pp.317-327, 1960.

7. E.A.C. Follett, W.J. McHardy, B.D. Mitchell and B.D.L. Smith, "Chemical Dissolution Techniques in the Study of Soil Clays: Part I", Clay Miner., 6:23-45, 1965.

8. B.D. Mitchell and V.C. Farmer, Clay Miner. Bull., 5:128-144, 1962.

9. L.A. White, "Environmental Monitoring - Methods Employed in the Soil Monitoring Program, Alligator Rivers Region 1979-1982", in Proceedings of Environmental Protection in the Alligator Rivers Region Scientific Workshop, Office of the Supervising Scientist, Darwin, NT, 1983.

10. M.A. Arshad, R.J. St Arnaud and P.M. Huang, "Dissolution of Trioctahedral Layer Silicates by Ammonium Oxalate, Sodium Dithionite-Citrate-Bicarbonate, and Potassium Pyrophosphate", Can. J. Soil Sci., 52, 19-26, 1972.

11. J.A. McKeague and J.H. Day, "Dithionite and Oxalate Extractable Fe and Al as aids in Differentiating Various Classes of Soils", Can. J. Soil Sci., 46:13-22, 1966.

12. E.A.C. Follett, W.J. McHardy, B.D. Mitchell and B.F.L. Smith, "Chemical Dissolution Techniques in the Study of Soil Clays: Part I", Clay Miner., 6:23-45, 1965.

13. S. McCleod, "Studies on Wet Oxidation Procedures for the Determination of 'Organic C' in Soil", in Notes on Soil Techniques, CSIRO Division of Soils (Canberra, 1975).

14. R. Baril, and G. Britton, "Anomalous Values of Free Iron in Some Quebec Soils Containing Magnetite", Can. J. Soil Sci., 47:261, 1967.

15. E.E. Gamble and R.B. Daniels, "Iron and Silica in Water, Acid Ammonium Oxalate and Dithionite Extracts of some North Carolina Coastal Plain Soils", Soil Sci. Soc. Am. Proc., 36, 930-943, 1972.

16. T.T. Chao and L. Zhou, "Extraction Techniques for Selective Dissolution of Amorphous Iron Oxides from Soils and Sediments", Soil Sci. Soc. Am. J., 47, pp.225-232 (1983).

17. R.L. Fleischer and O.G. Raabe, "Recoiling Alpha-emitting Nuclei - Mechanisms for Uranium Series Disequilibrium", Geochim. Cosmochim. Acta 42:973-978, 1978.

18. P.L. Airey, D. Roman, C. Golian, S. Short, T. Nightingale, R.T. Lowson and G.E. Calf, "Radionuclide Migration around Uranium Ore Bodies - Analogues of Radioactive Waste Repositories", USNRC Contract NRC-04-81-172, Quarterly Report No. 6, AAEC Report C37, 1983.

7. ADSORPTION-LEACHING EXPERIMENTS

7.1 Aims

The traditional method for predicting the long-term transport of radionuclides is to combine adsorption coefficient measurements with predictions of groundwater flow. Many of the complexities associated with long-term prediction are becoming apparent from studies of the distribution of uranium series nuclides over chemically separate mineral phases (Section 6.2).

One of the immediate aims of the experimental program is to establish

- the correlation between sorption and leaching behaviour (Correlation 3, Figure 2), and
- the correlation between leaching and the distribution of radionuclides throughout the mineral phases of the ore bodies (Correlation 2, Figure 2).

7.2 Methods

7.2.1 Aqueous phase

Only batch experiments have been attempted with ore from Ranger One. The aqueous phase was 'synthetic Ranger groundwater' spiked with a ^{236}U tracer The composition was obtained by a statistical analysis of more than 100 data points for each of the significant solute species K^+, Ca^{2+}, Mg^{2+}, HCO_3^-, SO_4^{2-} and SiO_2 from borewater in the vicinity of the Ranger One ore body. Early problems with solution stability were overcome by slightly adjusting the water composition to avoid the supersaturation predicted by the WATEQ water equilibrium program[1]; the components are listed in Table 21.

Four environmental extremes of pH and Eh were postulated:

(a) pH 5.5 oxidizing;

(b) pH 5.5 reducing;

(c) pH 8.5 oxidizing; and

(d) pH 8.5 reducing.

Oxidizing groundwater was prepared from aerated distilled water and 100 ppm H_2O_2. The hydrogen peroxide was added at the start of the experiment to ensure that all labile (solute, colloidal and surface) iron was in the Fe(III) state and that all accessible uranium was in the U(VI) state. Reducing groundwater was prepared by adding 100 ppm of hydroxylamine to

deaerated distilled water. The dominant uranium species in the Ranger synthetic groundwater were:

(a) pH 5.5 oxidizing UO_2^+, UO_2OH^+, $UO_2Si(OH)_3^+$ $UO_2CO_3^o$;

(b) pH 5.5 reducing $U(OH)_4^o$, $U(OH)_5^-$

(c) pH 8.5 oxidizing $(UO_2)_3(OH)_5^+$, $UO_2(CO_3)_3^{4-}$ $(UO_2)(CO_3)_2^{2-}$; and

(d) pH 8.5 reducing $U(OH)_5^-$.

Associated colloidal and pseudo-colloidal forms may also have been present.

7.2.2 Sorption-desorption experiments

Sorption and leaching experiments are conceptually different. The former reflect the short-term uptake of uranium, the latter, the net effect of the processes of redistribution of uranium throughout the ore over geological time. There are clear advantages of running both classes of analysis simultaneously on the same sample. As was indicated in Section 2.3, ^{236}U, an isotope not found in nature is added to the aqueous phase and the ^{234}U:^{236}U:^{238}U ratios measured both in solution and on the substrate. The ^{236}U distribution coefficient monitors sorption; the corresponding ^{234}U and ^{238}U parameters reflect desorption. Eventually the distribution of ^{236}U between the chemically separable phases of the ore will be studied and the results compared with those of ^{234}U and ^{238}U.

There have been some changes in technique over the past few months. Earlier difficulties with pH stability were described in the seventh Quarterly Report.[2] At present, 14-day batch experiments are run in which 1 to 2 g of ore are exposed to 100 mL of groundwater and oscillated gently but continuously on a table top shaker. At the end of the equilibration period, the solid and liquid are separated by centrifugation at 3500 rev./min for one hour; the supernatant is then passed through a 0.45 μm filter. Uranium-232 is added to the aqueous phase as an analytical yield tracer. After evaporating an aliquot to dryness, the residue is dissolved in 8 M HNO_3, passed through a strong anion resin in the NO_3^- form to remove thorium, evaporated to dryness, and electrodeposited onto a stainless steel planchette from an ammonium nitrate-formic acid solution. The uranium isotopes are assayed by α-spectrometry.

The adsorption coefficient K_d is defined as the ratio of the weight of uranium adsorbed per unit weight of adsorbate to the weight of dissolved uranium per unit volume of solution after adsorption equilibrium has been attained. Assuming a linear isotherm, the adsorption coefficient

for a particular system is constant. Since the mass of ^{236}U is negligible,

$$K_d = (A_o - A_f)V/A_f w \ (mLg^{-1})$$

where A_o is the initial total solution activity, A_f is the final total solution activity, V is the volume of solution (mL), and w is the weight of soil (g).

7.3 Preliminary Results

7.3.1 Long-term leaching experiments

The 4.0 and 13.1 m samples from the Ranger One S1/146 core were chosen for the initial leach tests. These samples were well characterized mineralogically, were from different zones of the weathered profile (see Section 4), and had been studied by the sequential extraction technique. Samples were prepared by grinding them with a tungsten carbide rotary grinder. Initially it was intended that each experiment would last 365 days with 10 samples collected in equal steps across the logaramithic scale 1 to 100.

The aqueous phase was made oxidizing and adjusted to pH 5.5. The ^{236}U spike was added (150 dpm) to each sample. Uranium-238 could not be detected in the day 1 sample, and there was only a trace at day 26. The experiment was then terminated owing to the loss of pH control, a problem which was solved by adjusting the groundwater composition as described above (Section 7.2.1). The results of the experiment are given in Table 22.

The most significant feature of this series of experiments is the lack of concordance between the ^{236}U and ^{234}U, ^{238}U data. This is illustrated by at least two results:

(1) The calculated distribution coefficient K_d varies by more than an order of magnitude.

(2) Even though ^{234}U and ^{38}U are leached into the solution from the ore sample, the levels in the aqueous phase are substantially greater than those of the added ^{236}U.

7.3.2 Fourteen-day experiments

Having solved the problem of the stability of the aqueous phase, a number of fourteen-day batch experiments were run on the S1/146, 4.0 m ground sample. The data are listed in Table 23. Two useful observations may be made :

(i) The linear coefficients of desorption of ^{238}U based on the total uranium content of the material are considerably greater than the corresponding adsorption coefficient of ^{236}U. If the adsorption and desorption coefficients were intrinsically equal, differences between the two uranium isotopes would reflect the fact that much of the ^{238}U is inaccessible to the groundwater. Under oxidizing conditions, the ratio of the adsorption coefficients (Table 23) is close to the sum of the fraction of ion-exchangeable uranium (0.008) and that extracted with acid oxalate, i.e. associated with amorphous iron oxide (24.4%, Table 15). This is further support for the hypothesis that only the uranium associated with the amorphous iron is in equilibrium with the groundwater.

(ii) Under reducing conditions, the K_d factors increase because of the formation of the less soluble U(IV) species. A corresponding decrease is observed in the K_d (^{236}U)/K_d (^{238}U) ratio, possibly indicating that, relative to ^{236}U, a greater proportion of the ^{238}U is inaccessible to the groundwater. This effect may be due to the partial dissolution of the more labile amorphous iron following reduction to the ferrous state.

It is useful to compare the data listed in Table 23 with those quoted in the literature. At pH 6, Borovec[3] found that with respect to UO_2^+, clay minerals have K_d values ranging from 50 for kaolinite to 10^3 for montmorillonite in the sequence kaolinite<illite<montmorillonite. The ratio of the amount of negative to positive charges on surfaces increases in the order kaolinite<illite<montmorillonite. Other values, such as humic acids ($K_d \sim 10^4$), Fe(III) oxyhydroxides (10^6) amorphous $Ti(OH)_4$ (10^5-10^6), peat (10^4-10^6), 'limonite' (10^4) and fine-grained natural goethite (10^3), have been measured, usually with respect to UO_2^+.[3-6] Giblin[4], however, found a K_d (max.) of 3.5×10^4 for a sample of kaolinite exposed to a synthetic groundwater containing extremely high levels of sulphate. The kaolinite had not been washed with tartaric acid or its equivalent to remove amorphous iron and alumina. The work of Muto[5] is open to similar criticism.

In comparing adsorption data from different laboratories, it must be remembered that the synthetic groundwater consists of the complex mixture of species listed in Section 7.2.1. The comparison is further complicated by the likely presence of colloidal or pseudo-colloidal forms. Nevertheless, our data agree broadly with literature results and provide evidence that Ranger One weathered zone material contains one or more constituents that are more adsorptive than pure clay minerals. The most obvious candidates are amorphous iron, manganese and aluminium hydroxides.

Clay minerals have more negative than positive surface charges over the typical groundwater pH ranges, whereas the hydrous oxide surface is positively charged to about pH 8.[5] Aqueous uranium species,

especially the U(IV) ions which are neutral or negatively charged in systems where pH is mediated by an HCO_3^-/CO_2 couple and the water is usually reducing (negative Eh), should therefore have a greater affinity for these surfaces than the pure clays.

Phosphate, arsenate/arsenite, selenate/selenite anions, which have been well studied in soil science and whose mobility is largely controlled by their affinity for surface Al-OH and Fe-OH groups,[7] may be suitable as simple analogues for solute uranium species.

Future adsorption work will include monitoring the anions as well as pH. It is possible that future model adsorption experiments will also be performed on lightly crushed unground samples using only the <2 μm fraction isolated by the standard water settling procedure which utilized the Stokes equation. It has been claimed that this fraction accounts for almost all the sorption capacity of weathered rocks and soils.

7.4 Effect of α-recoil on Adsorption Coefficients

7.4.1 Significance of the experiment

The effect of α-recoil on the adsorption coefficient is significant only for those nuclides generated at significant levels after the parent has leached into the geological strata. The most significant species, according to criterion of peak annual dose, are ^{237}Np and ^{226}Ra. The variation with decay time of the activities in irradiated fuel elements and high-level waste is shown in Figure 17. In both cases, ^{226}Ra grows to appreciable levels within 1000 years after discharge from the reactor. An analogous effect is noted for ^{237}Np from spent fuel, since the isotope is a product of α-decay from ^{245}Cu through ^{241}Pu and ^{241}Am. Since plutonium is removed during reprocessing, the level of ^{237}Np in high-level waste is constant. The curves in Figure 17 do not, of course, relate directly to the variation of ^{226}Ra and ^{237}Np down-gradient of a repository. They must be modified by factors pertaining to the relative leachability of the immobilized waste form and the relative retardation factors in the near and far field. Nevertheless, they provide a justification for attempting to quantify the effect of α-recoil on adsorption coefficients.

7.4.2 Effect of α-recoil on radium adsorption on clay

The experimental procedure was outlined in Section 7.1.1.1 of the first Annual Report.[1] Briefly, ^{228}Th is separated from its daughter products, particularly ^{224}Ra. Aliquots of ^{228}Th and the reference isotope ^{226}Ra are added to dilute suspensions of mineralogically pure illite, kaolinite and montmorillonite, and the pH is adjusted to approximately 7.5 by adding dilute sodium hydroxide. With montmorillonite and kaolinite, greater than 97% of the thorium is adsorbed on the clay; with illite, 86% is adsorbed.

By definition, the adsorption coefficient K_d^r of the reference isotope ^{226}Ra is given by :

$$K_d^r = {}^6R_a / {}^6R_{aq} \quad . \tag{15}$$

where ^6R_a and $^6R_{aq}$ are the levels of ^{226}Ra on 'accessible' surface sites and in aqueous solution respectively. The ^{228}Th daughter ^{224}Ra (^4R) grows in with a half-life of 3.24 days. Being formed by α-decay, a fraction D_i recoils into inacessible sites i of the clay lattice :

$$\underset{\text{(aqueous)}}{{}^4R_{aq}} \rightleftharpoons \underset{\text{(accessible)}}{{}^4R_a} \qquad \underset{\text{(inaccessible, i.e. not in equilibrium with } {}^4R_{aq})}{(+ {}^4R_i)} \quad . \tag{16}$$

By definition, the empirical adsorption coefficient

$$K_d = ({}^4R_a + {}^4R_i)/{}^4R_{aq} \tag{17}$$

The aim of the experiment is to determine the ratio ρ of the adsorption coefficients :

$$\rho = K_d / K_d^r \quad . \tag{18}$$

Experimental results are presented in Table 24. In each of the dilute clay suspensions, recoil increased adsorption factors by about a factor of two.

7.4.2.1 Recoil parameter $\emptyset_a$

As was pointed out in the first Annual Report quantitative interpreation of the leaching experiments requires an estimate of the probability $\emptyset_a$ that the α-recoil product from a parent species adsorbed on the surface will lodge in an inacessible region of the substrate. A simple relationship exists between $\emptyset_a$ and ρ (equation 18). This treatment is a slight extension of that set out in the first Annual Report.

$$\emptyset_a = {}^4R_a / {}^4R_{(solid)} \tag{19}$$

where
$$^4R_{(total)} = {}^4R_i + R_a \quad . \tag{20}$$

Since the fraction of radium in solution is small, it can be shown, from equations (19) and (20), that

$$\frac{1}{\emptyset_a} = 1 + \left(\frac{{}^4R_a}{{}^4R_{aq}}\right)\left(\frac{{}^4R_{aq}}{{}^4R_i}\right) \quad . \tag{21}$$

Since, $K_d = ({}^4R_a + {}^4R_i)/{}^4R_{aq}$ (22)

and $K_d^r = {}^6R_a/{}^6R_{aq} = {}^4R_a/{}^4R_{aq}$ (23)

it follows from equations (21), (22) and (23), that

$$\frac{1}{\emptyset_a} = 1 + \frac{K_d^r}{K_d - K_d^r} = 1 + \frac{1}{\rho - 1} \quad (24)$$

whence $\emptyset_a = 1 - (1/\rho)$

From Table 24, $\rho = 2$, and hence $\emptyset_a = \frac{1}{2}$.

From these experiments, there appears to be about a 50% probability that radium formed by α-decay on the surface of a clay particulate in dilute suspension will recoil into an inaccessible portion of the lattice.

7.4.3 An attempt to obtain experimental evidence for thorium recoil

An attempt is being made to seek experimental evidence for the effect of recoil on the adsorption of thorium, using the system $^{238}U/^{234}Th$ on the montmorillinite, kaolinite, illite suspensions discussed above. When equlibrated $^{238}U/^{234}Th$ is added to the suspension, the bulk of the uranium and thorium will essentially adsorb onto the clay surfaces. Two parameters are measured: U and ^{234}Th in the aqueous phase without treatment and following the addition of HCl to make 0.1 M solution.

The added ^{234}Th in all probability will not exist in solution because of its immediate total adsorption by the clay, but the fraction that will eventually appear in the liquid phase will be the recoiled ^{234}Th from the ^{238}U which is also completely adsorbed on the clay. If the consequences of α-recoil have a dominating effect on adsorption, the level of ^{234}Th in solution should vary with time in a predictable manner.

A liquid scintillation counting technique was used for this experiment. After addition of acid where appropriate, aliquots of the suspension are separated by filtration. The aqueous phase is counted under reproducible conditions using the commercial scintillating agent Instagel. It has been found experimentally that uranium α particles can be distinguished from $^{234}Th/^{234}Pa$ β particles by appropriately setting the discriminators.

References

1. A.H. Trusdell and B.F. Jones, WATEQ "A Computer Program for Calculating Chemical Equilibria of Natural Waters", J. Res. US Geol. Survey 2:223 (1974).

2. P.L. Airey, D. Roman, C. Golian, S. Short, T. Nightingale, R.T. Lowson, G.E. Calf, B.G. Davey, D. Gray and J. Ellis, "Radionuclide Migration around Uranium Ore Bodies - Analogues of Radioactive Waste Repositories", USNRC Contract NRC-04-81-172, Quarterly Report No. 7, AAEC Report C38, 1983.

3. Z. Borovec, "The Adsorption of Uranyl Species by Fine Clay", Chem. Geol. 32, 45-58 (1981).

4. A.M. Giblin, "The Role of Clay Adsorption in Genesis of Uranium Ores", in Proceedings of the International Symposium Uranium in the Pine Creek Geosyncline, Ed J. Ferguson and A.B. Goleby (IAEA, Vienna, 1980), pp.521-529.

5. T. Muto, S. Hironi and H. Kurata, "Some Aspects of Fixation of Uranium from Natural Waters", Min. Geol. Tokyo 15 (74), 287-298 (in Japanese), (1965).

6. G.A. Parks, "The Isoelectric Points of Solid Oxides, Solid Hydroxides and Aqueous Hydroxo Complex Systems", Chem. Rev. 65: 177-198 (1965).

7. R.L. Parfitt, "Anion Absorption by Soils and Soil Materials", Adv. Agron. 30:1-50 (1978).

8. A.G. Croft and C.W. Alexander, "Decay Characteristics of Once-through LWR and LMFBR Spent Fuels, High Level Wastes, and Fuel Assembly Structureal Material Wastes", Oak Ridge National Laboratory Report ORNL/TM-7431, 1980.

8. THE MIGRATION OF RADIONUCLIDES THROUGH CRYSTALLINE ROCK STRATA

8.1 Definition of the Problem

Another important aim of the project is to assess the extent to which crystalline rocks act as a barrier to the migration of radionuclides over extended periods. The mechanism of transport through crystalline rock is fundamentally different from that in the weathered clays (see Section 3). Groundwater flows principally through major fractures. In addition, diffusion into the bulk rock occurs via microscopic fractures. Solute transport is further complicated by physical and chemical interactions with accessible surface minerals.[1,2] This process, known as matrix diffusion, is shown schematically in Figure 18.

An analysis of the extent to which crystalline rocks act as geological barriers to the transport of radionuclides over long periods raises a number of questions :

(i) What is the microscopic rate of transport of groundwater through the system (i.e. the hydraulic age)?

(ii) What are the time-scales associated with the diffusion of water into the bulk rock via microscopic cracks and fissures?

(iii) What are the additional effects on solute transport of interaction with accessible minerals?

A geochemical analogue approach is applied to this problem; this involves study of the cumulative effect over geological time of the leaching uranium series nuclides from the crystalline rock matrix of the Jabiluka Two ore body.

8.2 Conceptual Approach

8.2.1 Procedure

In general, access to groundwater leads to the selective leaching or deposition of radionuclides. Isotope ratios depend on several factors :

- the initial values at the defined point of zero time;
- the relative rates of leaching or deposition; and
- the relative decay constants.

The time-scales over which perturbations due to leaching have occurred can be assessed by examining different parent/daughter pairs. For instance, systematic $^{226}Ra/^{230}Th$ disequilibria probably indicate leaching during the last 5000 y (half-life of ^{226}Ra = 1620 y). Further examples are shown in the following table :

Disequilibrium	Time-scale During which Leaching Occurred	Comment
$^{226}Ra/^{230}Th$	up to, say 5000 y	Ra leaching.
$^{234}U/^{238}U$	up to, say 5×10^5 y	Leaching probably leads to ^{234}U deficit in ore; authigenic uranium.
$^{207}Pb/^{235}U$ etc.	up to, say 10^9 y[a]	Both Pb and U are assumed to be mobile (see Section 8.2.3).

Interest in the lead/uranium ratios arises from the assumption that time-scales associated with diffusion into the bulk of the crystalline rock will almost certainly be much longer than those associated with transport in the weathered clay.

The following steps are involved in the investigation:

(1) A survey of the $^{234}U/^{238}U$, $^{230}Th/^{234}U$ and $^{226}Ra/^{230}Th$ activity ratios to establish whether there is evidence for leaching over the 10^3 to 10^5 year time-scale.

(2) Measurement of the $^{234}U/^{238}U$ activity ratios to acquire independent evidence of uranium leaching and, if possible, to draw conclusions on the mechanism.

(3) A systematic study of the $^{206}Pb/^{204}Pb$, $^{207}Pb/^{204}Pb$, $^{238}U/^{204}Pb$, $^{235}U/^{234}Pb$ ratios to obtain information on

- the relative rates of leaching of lead and uranium, and
- the time of commencement of leaching.

(4) Interpretation of the data in terms of present concepts of transport of solute through crystalline rocks - particularly the matrix diffusion model.

8.2.2 Potential application of $^{235}U/^{238}U$ ratios

Evidence for uranium leaching over geological time may, in principle, be obtained from a detailed study of $^{235}U/^{238}U$ variations in ore samples.

The absence of an isotopic effect does not necessarily imply an absence of leaching; it may simply indicate a mechanism independent of mass. In the following treatment, it is assumed that uranium is lost by radiogenic decay and by a first order leaching process; thus,

$$-d^5U/dt = \lambda_5 {}^5U + \upsilon_5 {}^5U \quad . \tag{25}$$

On integration,

$${}^5U(t) = {}^5U(t_w) \exp\left(-(\lambda_5+\upsilon_5)(t - t_w)\right) , \tag{26}$$

where ${}^5U(t_w)$ is the uranium level at time t_w, when the uranium first had access to leaching water. By analogy,

$${}^8U(t) = {}^8U(t_w) \exp\left(-(\lambda_8+\upsilon_8)(t - t_w)\right) . \tag{27}$$

Hence the isotope ratio

$$R = \left[\frac{{}^5U(t_w)\ \exp{-\lambda_5}\ (t-t_w)}{{}^8U(t_w)\ \exp{-\lambda_8}\ (t-t_w)}\right] \exp -(\upsilon_5-\upsilon_8)(t-t_w) \tag{28}$$

$$= R_{std} \exp\left(-\upsilon_5(1 - \upsilon_8/\upsilon_5)(t-t_w)\right)$$

$$= R_{std} \exp\left(-\upsilon_5\ \xi\ (t-t_w)\right) \tag{29}$$

$$= R_{std}\ (\text{leaching})^{\xi} \quad , \tag{30}$$

where $\upsilon_8/\upsilon_5 \simeq 1 - \xi$ (the isotope effect), and the 'leaching' (equation (30)) parameter is the fraction of remaining uranium, R_{std} is the expected isotope ratio in the absence of leaching, and 'leaching' is the cumulative extent of ^{235}U leaching.

Tabulated values of the parameter R/R_{std} (equation 30) are listed below:

Leaching[a]	ξ[b]	$\delta(R)$[c] (per mille)
0.9	0.006	- 0.6
0.5	0.006	- 4.2
0.1	0.006	-13.7

(a) fraction of uranium remaining;

(b) $\xi \sim \left[\frac{238}{235}\right]^{\frac{1}{2}} - 1 = 0.006$,

(c) $\{(R/R_{std})-1\} \times 100$ per mille.

The value chosen for the parameter ξ, and hence for the calculated ratio R/R_{std}, is a maximum.

8.2.3 A lead/lead, lead/uranium isotope method for studying leaching over geological time

Basic Equations

The treatment is based on the following assumptions:

(i) A zero point t_o (associated either with the formation of the deposit, or a later metamorphic event) may be relatively well-defined.

(ii) The leaching process commences some time later, at time t_w.

(iii) The leaching is a first order process and that any isotope effect may be ignored.

These assumptions are illustrated in Figure 19.

The generating equations are:

$$-dU_8/dt = \lambda_8 U_8 + \nu U_8 \qquad (31)$$

$$Pb_6/dt = \lambda_8 U_8 - \pi Pb_6 \qquad (32)$$

where U_8 = ^{238}U; Pb_6 = ^{206}Pb,
λ_8 = ^{238}U decay constant,
ν = rate of uranium leaching, and
π = rate of lead leaching.

The lead isotope ratio is calculated in two time intervals, $t_o - t_w$ and $t_w - t$ (Figure 19).

Period of No Leaching $t_o - t_w$

From equations (31) and (32) it can be shown that when $\nu = o$ and $\pi = o$,

$$Pb_6(t_w) = Pb_6(t_o) + \frac{\lambda_8 U_8(t_o)}{\pi-\nu-\lambda_8}\left[1 - \exp - \lambda_8 (t_w - t_o)\right] \qquad (33)$$

where $Pb_6(t_o)$ and $U_8(t_o)$ are the lead and uranium levels at time t_o. They reflect changes in the primordial levels up to t_o due to radiogenic decay and mobilization of the uranium.

Lead-204 is not formed through a decay chain. Hence,

$$Pb_4(t_w) = Pb_4(t_o) \quad . \qquad (34)$$

For ^{238}U, $$U_8(t_w) = U_8(t_o) \exp - \lambda_8(t_w - t_o) \quad . \qquad (35)$$

Period of Leaching $t_w - t$

When appreciable leaching occurs, the solutions of equations (31) and (32) take the form,

$$Pb_6(t) = Pb_6(t_w) \exp - \pi(t - t_w) -$$

$$- \frac{\lambda_8 U_8(t_w)}{(\pi-\nu-\lambda_8)} \left[\exp - \pi(t-t_w) - \exp - (\lambda_8+\nu)(t - t_w)\right] . \quad (36)$$

Since Pb_4 is not formed through the decay chain, but undergoes leaching,

$$Pb_4(t) = Pb_4(t_w) \exp - \pi(t-t_w) . \quad (37)$$

Combined Period $t_o - t$

The variation of ^{206}Pb and ^{204}Pb over the complete time interval $(t - t_o)$ (Figure 19) is found by substituting equations (33) and (35) into (36) and equation (34) into (37).

The results are:

$$Pb_6(t) = (Pb_6(t_o) \exp - \pi(t-t_w) + \frac{\lambda_8}{(\pi-\nu-\lambda_8)} U_8(t_o) \exp - \pi(t-t_w) -$$

$$- \frac{\lambda_8}{(\pi-\nu-\lambda_8)} U_8(t_o) \exp - \lambda_8(t-t_o) \exp - \nu(t-t_w) . \quad (38)$$

$$Pb_4(t) = Pb_4(t_o) \exp - \pi(t-t_w) . \quad (39)$$

From equations (38) and (39),

$$\frac{Pb_6(t)}{Pb_4(t)} = \frac{Pb_6(t_o)}{Pb_4(t_o)} + \frac{\lambda_8}{(\pi-\nu-\lambda_8)} \frac{U_8(t_o)}{Pb_4(t_o)}$$

$$- \frac{\lambda_8}{\pi-\nu-\lambda_8} \frac{U_8(t_o)}{Pb_4(t_o)} \frac{\exp - \lambda_8(t-t_o)}{\exp - \pi(t-t_w)} \exp - \nu(t-t_w) , \quad (40)$$

$$= \frac{Pb_6(t_o)}{Pb_4(t_o)} - \frac{1}{1-(\pi-\nu)/\lambda_8} \frac{U_8(t_o)}{Pb_4(t_o)} + \frac{1}{1-(\pi-\nu)/\lambda_8} \frac{U_6(t)}{Pb_4(t)} \quad (41)$$

From equation (41), it is predicted that $Pb_6(t)/Pb_4(t)$ will vary linearly with $U_8(t)/Pb_4(t)$, with the following parameters:

$$\text{slope} \quad 1/1-(\pi-\nu)/\lambda_8 \quad (42)$$

$$\text{intercept} \quad \frac{Pb_6(t_o)}{Pb_4(t_o)} - \text{slope} \frac{U_8(t_o)}{Pb_4(t_o)} . \quad (43)$$

Rate of Leaching

Equations exactly analogous to (33) to (41) can be written for the $^{235}U \rightarrow {}^{207}Pb$ system:

$$\text{slope} = 1/1-(\pi-\nu)/\lambda_5 \quad (44)$$

$$\text{intercept} = \frac{Pb_7(t_0)}{Pb_4(t_0)} - (\text{slope})\frac{U_5(t_0)}{Pb_4(t_0)} \quad (45)$$

From equations (42) and (44) it is possible to calculate independent values of π and ν. The values are the weighted average of the rate of leaching which has occurred since time t.

Complications can arise due to the leaching or deposition of uranium series intermediates. For instance, evidence of excess radium is presented in Table 25. Radium-226 will, of course, ultimately decay to ^{206}Pb. Mathematically, the effect of radium excess on the $^{238}U/^{206}Pb$ ratios is to decrease the apparent ^{238}U decay constant; the net leaching of an intermediate nuclide leads to an apparent increase in the decay constant.

8.3 Preliminary Results

8.3.1 Geological setting

An attempt is being made to test these concepts in the vicinity of a north-south fault zone intersecting the Jabiluka Two deposit. A general description of the geology of the Jabiluka region has been presented elsewhere. Of particular interest is that, immediately down-gradient of the fault zone, the average uranium levels are generally low, and tend to increase with distance from the fault. If it is assumed that the fault is a locus of groundwater recharge, and that the low uranium concentration close to the fault are the net effect of leaching over geological time, there is a possibility of evaluating theories of leaching and solute transport in crystalline rocks over geological time.

As part of a preliminary investigation, samples were collected from cores V153/V2, W/147/V and W/142/V2 which are at distances of 5 m, 30 m and 50 m, respectively, from the fault. The depths of the samples are shown in Table 25. Samples are assayed for uranium, thorium, $^{226}Ra/^{238}U$, $^{234}U/^{238}U$ and $^{230}Th/^{234}U$ activity ratios at the Lucas Heights Research Laboratories.

8.3.2 $^{234}U/^{238}U$, $^{230}Th/^{234}U$ and $^{226}Ra/^{230}Th$ activity ratios

The activity ratios are listed in Table 25. The most outstanding features of the data are the large $^{226}Ra/^{238}U$ disequilibria. The magnitude of the

disequilibria varies inversely with the total uranium concentration. It would appear that some uranium is leached from the regions of high concentrations and redistributed throughout the matrix. If this process has been occurring over geological time, it will have had a profound effect on the lead/lead and lead/uranium ratios.

The $^{230}Th/^{234}U$ data are much less variable. Only three of the nine samples have activity ratios that differ significantly from unity at the 2σ level. In all but one case, the ^{234}U is in secular equilibrium with ^{238}U. The general lack of mobility of the uranium is due to the reducing conditions found at depth within the Jabiluka Two ore body.

8.3.3 Other measurements

Measurements of $^{206}Pb/^{204}Pb$, $^{207}Pb/^{204}Pb$, $^{238}U/^{204}Pb$ and $^{235}U/^{238}U$ ratios are underway and will be reported as soon as they are available.

References

1. E. Gleuckauf, "The Movement of Solutes through Aqueous Fissures in Micro-porous rock during Borehole Experiments", Report AERE-R-10043, 1981.

2. I. Neretneiks, "Diffusion in the Rock Matrix : An Important Factor in Radionuclide Retardation?", J. Geophys. Res. 85:4379, 1980.

3. M.R. Hegge, D.V. Mosher, G.S. Eupene and P.S. Anthony, "Geologic Setting of the East Alligator Uranium Deposits and Prospects, in Proceedings of the International Uranium Symposium on the Pine Creek Geosyncline, Ed J. Ferguson and A.B. Goleby (IAEA, Vienna, 1980), p.259.

9. RADIONUCLIDE MIGRATION IN GROUNDWATER

9.1 Nabarlek

The geological setting of Nabarlek was described briefly in Section 5. The chemical and isotope data obtained from the sampling wells (Figure 6) are listed in Tables 26 and 27. Conventional units and the standards are given in Appendix B.

9.1.1 Tritium

Few conclusions can be drawn from the tritium data which are low and constant within experimental error. There is some evidence for a component of modern water in OB20.

9.1.2 Carbon isotopes

The $^{13}C/^{12}C$ ratios and the carbon-14 levels are interpreted as groundwater ages in accordance with the system model of Salem and co-workers.[1] The age patterns of groups of wells, such as OB19, OB20, OB25, RN20475 or OB21, TB36, TB40, are generally consistent with the picture of a mainly easterly flow of groundwater in the wet season perturbed by a component of flow to the south-west in the dry season. There are clearly some exceptions, such as RN4073 and TB33, which are modern. Care must be taken when interpreting the ages in unconfined systems. The radiocarbon ages simply reflect the average sub-surface residence time of the components of water comprising the sample.

9.1.3 Stable isotopes

Additional evidence for the significance of groundwater ages is derived from the D/H data. In general, it is found that the older the water, the more depleted it is in deuterium. The correlation coefficient is 0.86, which is significantly different from zero at the 99.5% level. Similar behaviour is found at Koongarra and in many other hydrological settings. It is not possible at this stage to provide a detailed explanation. Suffice it to say that *neither* mechanisms based on sub-surface mixing *nor* on palaeoclimatic effects can be excluded.

9.1.4 Uranium

The uranium concentration generally decreases with distance down-gradient of the mine. As with the groundwater in the vicinity of the major Ranger deposits, the $^{234}U/^{238}U$ isotope ratio increases with decreasing uranium concentration. Figure 20 should be compared with Figure 10 of the first Annual Report.[1]

The Ranger groundwater data were interpreted in terms of a two-component model: component 1, characterized by relatively high uranium concentration

and $^{234}U/^{238}U$ ratios close to unity, is the groundwater-intersecting deposit; component 2, with a low uranium concentration and high $^{234}U/^{238}U$, represents local infiltrating rainfall. If the fraction of component 2 is assumed to be proportional to the distance down-gradient of the deposit, it can be shown that

$$^{234}U(x)/^{238}U(x) = \xi + (^{238}U_2 - {}^{238}U_2\ \xi)/^{238}U(x)\ , \qquad (46)$$

where $^{234}U(x)$, $^{238}U(x)$ are the concentrations of the uranium isotopes at distance (x) from the deposit, $^{234}U_2$, $^{238}U_2$ are the concentrations in component 2 of the groundwater, and $\xi \sim {}^{234}U(o)/^{238}U(o)$.

The variation of $^{234}U(x)/^{238}U(x)$ with the reciprocal of the uranium concentration for the Nabarlek data is shown in Figure 21. The intercept, 0.9, corresponds to the isotope ratio of the groundwater intersecting the deposit. The slope (0.5 μg L^{-1}) is interpreted as $^{234}U_2 - \xi\ ^{234}U_2$, where $\xi = 0.9$. The most distant sampling well TB40 appears to be anomalous. There is insufficient detailed information to offer an explanation.

Levels of ^{230}Th were also measured (see Table 27). There is evidence that a substantial fraction of this radionuclide is associated with particulates (Section 10).

9.2 Koongarra

The groundwater hydrology of the area of the Koongarra deposits (Figure 1) has been studied extensively by Australian Groundwater Consultants and McMahon, Burgess and Yeates.[3] Their data, interpreted by Snelling[4], are shown schematically in Figure 22B. The groundwater is believed to recharge along a major fault line and to flow in a generally southerly direction away from the escarpment. The location of the sampling wells is shown in Figure 22A; the isotope data are listed in Table 28.

9.2.1 Tritium

Analysis of environmental tritium has shown that modern water is a significant component of water in wells 94 and KTD 1.

9.2.2 Carbon isotopes

The carbon isotope data listed in Table 28 are interpreted as groundwater ages, using the procedures of Salem et al.[1] Wells with appreciable levels of environmental tritium also have in excess of 100% modern ^{14}C.

The data are generally consistent with the concepts published by Snelling.[4] PH 78 and KD 1 are drilled into the Kombolgie sandstone up-gradient of the fault zone bounding the deposit. As was expected, the average residence time of the water reflects the depth. PH 7, which taps water from the weathered zone, is modern, and there is possibly a substantial component of local infiltration in this sample. The ^{14}C level in PH 49 is consistent

with the notion that the water is derived by infiltration through the sandstone sequence in the vicinity of the fault zone at a depth greater than that of KD 1. Samples from wells PH 55 and PH 94 further down-gradient appear to contain significant amounts of local recharge. As yet, no comment can be made on PH 7. The ^{14}C value is anomalous and has been resampled.

9.2.3 Deuterium/hydrogen

The deuterium/hydrogen ratios are listed in Table 28. As was the case for Nabarlek, there is a tendency for water with a longer mean residence time to be depleted in deuterium. The correlation coefficient is 0.79 which is significantly different from zero at the 99.5% level.

9.2.4 Uranium and thorium

There is no evidence for a systematic variation of $^{234}U/^{238}U$ ratios with uranium concentration (Figure 23). This is contrary to the findings down-gradient of Ranger One and Nabarlek (Section 4.2.2). Groundwater uranium is dominated by solution from the deposit and is not perturbed by local infiltration. As far as is practicable, further work is needed down-gradient of the deposit.

The groundwater thorium data (Table 28) are particularly interesting. Two samples (PH 14 and KTD 1) have relatively high thorium/uranium ratios (> 0.5); the remainder are low (< 0.06). There appears to be no correlation with uranium concentration and groundwater age, a correlation which might be likely if the actinides are dissolved in the groundwater and the rate of transport is controlled by adsorption coefficients. The notion that fully dispersed colloids may play an important role in transport is being further investigated.

9.3 Jabiluka

In the region of the ore bodies, the "rock permeabilities, fault zone transmissibilities, reservoir capacities and aquifer recharge were all extremely low".[5] It is assumed that the piezometric gradient generally follows the surface contours.

The location of the sampling wells is shown in Figure 24 and the isotope data are listed in Table 29. The tritium observed in well 170 is probably associated with the lack of water in the well after pumping. This sample is probably unrepresentative of the groundwater. As yet, there are insufficient data to make further comment.

9.4 Uranium Retardation Down-gradient of the Ranger Deposit

The $^{234}U/^{238}U$ activity ratios in groundwater close to the Ranger One deposit have values near unity. They increase with distance up to 4 km

down-gradient, due to mixing with a dispersed infiltrating groundwater characterized by large ^{234}U excess. Further down-gradient there is no environmental isotope evidence for local recharge. The $^{234}U/^{238}U$ activity ratios return to secular equilibrium due to a combination of radiogenic decay and the possibility of exchange with the host rock. Assuming that decay is the major process, the maximum relative retardation of the groundwater relative to the host rock is 1/250. Groundwater velocities were calculated from ^{14}C.

Qualitatively similar behaviour has recently been found in groundwater sampled from the Carizzo aquifer in Texas: "At distances from 0 to about 20 km, where the Carizzo is oxidizing and uranium dissolution is occurring, $^{234}U/^{238}U$ activity ratio (AR) values of 1.0±0.3 are found. Between 20 and 33 km, uranium concentrations drop dramatically and AR values as high as 9 occur. Below about 33 km, low dissolved uranium persists, accompanied by a regular decrease in the AR towards a secular equilibrium value of 1.".[6] A schematic representation of this behaviour is shown as an insert to Figure 15 of reference 1, reproduced as Figure 25.

Pearson[6] pointed out that

$$R_d = \frac{V_i}{V_c} = 1 + \frac{1 - \emptyset}{\emptyset} \rho_s K_d \quad , \tag{47}$$

where R_d is the retardation factor, V_i is the interstitial fluid velocity, V_c the solute velocity, $\emptyset$ the porosity of the sandstone, ρ_s the density, and K_d the adsorption coefficient. The systematic decrease in the $^{234}U/^{238}U$ activity ratios between 20 and 33 km is best explained with a K_d factor of 6, and a relative retardation factor of 30. The K_d factor is within the range of values calculated for particulate material collected from the pumped wells at Nabarlek (Table 30).

In the region of interest, down-gradient of Ranger One, there is possible contribution to groundwater flow from both the unweathered schists sequences and the upper weathered zone. It is thus not possible to define acceptable values for $\emptyset$ and K_d separately. Equation (47) can therefore only be expressed in the simple form

$$R_d = \frac{\text{mass of solute on the stationary phase}}{\text{mass of solute on the aqueous phase}} \tag{48}$$

References

1. O. Salem, J.H. Vissen, M. Dray and R. Gonfiantini, "Groundwater Flow Patterns in the Libyan Arab Jamahiriya Evaluated from Isotopic Data", in Proceedings of IAEA Advisory Group Meeting on Arid-zone Hydrology : Investigations with Isotope Techniques (IAEA, Vienna 1980), pp.165-173.

3. Australian Groundwater Consultants Pty Ltd and McMahon, Burgess & Yeates, "Report on Investigation of Groundwater and the Design of Water Management and Tailings Retention Systems for the Koongarra Project", Koongarra Project. Draft Environmental Impact Statement, (Noranda Australia Ltd, Melbourne, 1978), Appendix XI.

4. A.A. Snelling, "Uraninite and its Alteration Products, Koongarra Uranium Deposit", in Proceedings of Symposium Uranium in the Pine Creek Creek Geosyncline, Sydney, June 1979, IAEA Vienna, p.487.

5. Pancontinental Mining Ltd, "The Jabiluka Project Environmental Impact Statement", Vol. II, Chap. 5, Pancontinental Mining Ltd Sydney, 1979.

6. F.J. Jr Pearson, C.J. Norohne and R.W. Andrews, "Mathematical Modelling of the Distribution of Natural ^{14}C, ^{234}U and ^{238}U in a Regional Groundwater System", in Proceedings of Radiocarbon Conference, Seattle, 1981.

10. EVIDENCE FOR THE ROLE OF PARTICULATES IN RADIONUCLIDE TRANSPORT

The uranium and thorium isotopic data from the Nabarlek groundwater are listed in Table 30. During the sampling program, a significant level of particulate collected on the 0.45 μm Millipore filter, even after the well was pumped to constant groundwater conductivity.

When examined by X-ray diffraction, the particulates from well OB21 were found to contain 10% quartz, and the clay minerals kaolinite (medium level), $2M_1$ muscovite (medium level), smectite (medium level), and chlorite/vermiculite (small concentration).

The 2:1 clay minerals were primarily dioctahedral, although some trioctahedral clay was found. The iron oxide lepidocrocite was also present.

It can be seen from Table 30 that only between 0.8 and 11% of the uranium is associated with the particulates; the corresponding ratio for thorium varies between >0.22 and >5.7. Two important questions arise:

(i) Are the radionuclides on the particulate matter in equilibrium with those in 'solution'?

(ii) What fraction of the radionuclides is transported by particulates?

To address the first question, the $^{234}U/^{238}U$ activity ratios of the particulates were plotted against those in 'solution' (Figure 26). With the exception of TB40, the trend is adequately described by the isotopic equilibrium line of slope unity. The correlation coefficient for the six data points is 0.77 which has a greater than 90% probability of being significant. The 'particulate' and fully dispersed uranium appear to be in equilibrium.

The $^{230}Th/^{234}U$ ratios of the particulates vary substantially and do not appear to correlate with groundwater parameters. It is tentatively suggested that this variability is associated with the mineralogical composition of the particulates. It has been shown (Section 5) that the activity ratios vary markedly between different mineral phases of the ore assemblage in the weathered zone.

In principle, it should be possible to establish whether the 'particulate' and fully dispersed thorium are in isotopic equilibrium by comparing the $^{232}Th:^{228}Th:^{230}Th$ activity ratios. Unfortunately, there was insufficient 'dissolved' thorium to examine this parameter. The question is important and will be investigated further. If equilibrium conditions are found, the implication will be that the sub-surface migration of thorium can be predicted by an extension of the adsorption coefficient principle. If, on the other hand, the bulk of the thorium is associated with 'particulates' and not in equilibrium with the groundwater, two possibilities require examination:

(i) If the ratio of the particulate to groundwater migration velocities is very small, the bulk of the thorium will be *transported* by groundwater although associated with particulates. In this circumstance, it would be appropriate to apply the adsorption coefficient principle.

(ii) However, if particulate transport is the major mechanism, and the thorium is not in equilibrium with the solution, a different basis for predicting long-term migration must be developed.

Further work is clearly required. In particular, a detailed examination should be made of the distribution of uranium and thorium colloids with particle sizes in the range 0.005 to 1.0 μm. In addition, techniques for dating the rate of sub-surface transport of colloids should be considered.

11. RADIUM TRANSPORT*

11.1 Radium-226

Radium-226 is the daughter product of ^{230}Th. Since the thorium isotope is essentially immobile and has a longer half-life than radium, it is considered to be stable. Thus,

$$-dRa/dt = \lambda_a[Ra] - \lambda_i[I] - R_{geol} \quad (49)$$

where λ_a, and λ_i are the decay constants of ^{226}Ra (Ra) and ^{230}Th (I) respectively, and R_{geol} is the rate of leaching/deposition. It was shown in the first Annual Report[1] that equation (49) may be integrated

$$\frac{\lambda_a Ra - \lambda_i I - R_{geol}}{\lambda_a Ra(to) - \lambda_i I - R_{geol}} = \exp(-\lambda_a t) \quad (50)$$

where $Ra(t_o)$ is the radium level at zero time. The definition of zero time must be the same as that chosen for the uranium series model (Section 3). Since the time interval is at least an order of magnitude greater than the ^{226}Ra half-life, $\exp(-\lambda_a t) \approx 0$ and the activity ratio

$$\frac{\lambda_a Ra}{\lambda_i I} = 1 + \frac{R_{geol}}{\lambda_i I} \quad (51)$$

Thus, activity ratios in excess of unity imply deposition, and those less than unity, leaching. The available data for Ranger One, Ranger Three, Jabiluka One, Jabiluka Two and Nabarlek drill cores are listed in Tables 31 to 33.

In some cases (S1/185, Ranger One; DH 35, DH 16 Jabiluka One; and V153/V2, Jabiluka Two) there appear to be relationships between the $^{226}Ra/^{230}Th$ activity ratios and the total uranium concentration. The lower the concentration, the higher the activity ratio, i.e. the higher propensity for radium deposition. The correlation coefficients are 0.75, 0.73, 0.88, and 0.71 (>90%) respectively. The value in parenthesis is the significance of the correlation, i.e. the probability that the correlation coefficients are greater than zero. A simple explanation could be sought in terms of the redistribution of radium from high concentration regions to those that are lower. However, it is important to note that the correlation does not hold for the Nabarlek samples nor for some other cores (S1/146, DH 3, W/147/V).

* Drill core locations are shown in Figure 1.

11.2 The Distribution of Radium through the Iron and Clay/Quartz Phases of the Core S1/146, Ranger One

A detailed description of the distribution of uranium and thorium throughout phases selectively leached from core S1/146 samples is presented in Section 6.4.2. Radium measurements were made on the total sample and on the clay/quartz resistate phases. The data are presented in Table 20. In all cases, the $^{226}Ra/^{230}Th$ activity ratios in the clay/quartz phases are greater than unity, whereas those in the other selectively leached phases (mainly amorphous and crystalline iron) are less than unity.

Interpretation is complex. Although much of the radium is authigenic, i.e. generated *in situ* by thorium decay, there is significant redistribution of radium throughout many cores. The accumulation of radium in the clay/quartz phases would be due to a combination of

(i) preferential adsorption from groundwater solution; and

(ii) a tendency for ^{226}Ra formed by α-recoil to be ejected into the clay/quartz phase, which comprises >95% of the dry mass.

The large radium deficits in the other (predominately iron) phases are interesting. Loss of ^{226}Ra by recoil to the clay/quartz phase, could, in principle, account for much of the effect. However, if this were the dominating cause, a similar $^{230}Th/^{234}U$ deficit would be expected. In fact, substantial excesses are observed. It will be recalled that the explanation was based on the uptake of nuclides from the groundwater by the amorphous iron, and a dynamic equilibrium between the amorphous and the crystalline iron. A similar explanation could be used to elucidate the radium data. Clearly, more detailed experiments involving the assay of radium in all the separated phases are needed.

However, the possibility of a trivial explanation involving the adsorption onto the clay/quartz phases of the radium mobilized during the sequential leaching process cannot be excluded at this stage. To examine this possibility further, the experiment will be repeated using magnetic/mechanical separation of phases.

11.3 The Distribution of Short-lived Radium Isotopes

(Section 11.3 has been contributed by Drs B. Dickson and R. Meakins of CSIRO Division of Mineral Physics, and is reproduced with permission.)

11.3.1 Introduction

Four radium isotopes are present in the decay series of uranium and thorium: ^{226}Ra (half-life = 1620 y) in the uranium series, ^{223}Ra (half-life = 11.4 days) in the actinium series, and ^{228}Ra and ^{224}Ra (half-lives = 5.75 y and 3.64 days respectively) in the thorium series. The relationship of these isotopes to their parents is shown in Figure 27. The CSIRO Division of Mineral Physics is studying the application of radium isotope analysis to uranium exploration.

Though the use of ^{226}Ra in waters for uranium exploration has been described frequently; the use of multiple isotopes is a more recent development[2]. Measurement of ^{226}Ra and ^{228}Ra istopes has been proposed as a means of locating buried uranium deposits[3-4]; the use of ^{223}Ra has been described[5], and an empirical scheme proposed for rating the significance of a water to uranium exploration.

This section presents the results obtained from analysis of radium isotopes in water samples collected from the locality of the Ranger and Koongarra uranium deposits in the East Alligator Rivers region of the Northern Territory.

11.3.2 Samples and analysis

11.3.2.1 Sample collection

Twenty-two groundwater samples were collected from a number of water bores and drill holes (Figure 28) by members of the AAEC's Nuclear Geohydrology Group. For 17 of the samples, a sample was collected by pumping between 50 and 250 L through a manganese-impregnated acrylic filter. This selectively removed trace heavy metals and radionuclides from the water.[7-8] A water sample was also collected at the same time to enable the recovery efficiency of the filters to be estimated. This sample was filtered and acidified. Samples were then sent to the CSIRO laboratory at North Ryde, New South Wales, for radium analysis.

Acrylic filter cartridges were used (Curo Micro-Kleen II, 50 μm, Code G78L2). These are treated in 0.5 M potassium permanganate at room temperature (22°C) for 14 days, washed with deionized water and dried. The filter is mounted in a Millipore 101 housing and an untreated 10 μm filter is mounted in an upflow housing to remove particulate matter from the water.

The filter is processed in the laboratory to strip the adsorbed radionuclides for analysis. The filter is heated with 1 M hydrozylaminehydrochloric acid in 1 M HCl at 50°C for 30 minutes. The resulting solution is filtered and may be analyzed as described below to determine radium or any other radionuclide of interest.

The high concentration of manganese can sometimes interfere with the chemical procedures and, if necessary, the uranium, radium and thorium may be separated from the manganese by a BIO-RAD AG1X4 anion exchange column. The solution is added to the column in 9 M HCl. The thorium and radium pass through the column whereas the uranium must be eluted with 1 M HCl. The column may be cleaned of iron and manganese with 10 column volumes of water.

11.3.3 Radium analysis

Apart from ^{228}Ra, naturally occurring radium isotopes may be determined in water samples by alpha spectrometry after chemical extraction and deposition of the radium in a thin layer of barium sulphate carrier.[9] The radium is

extracted by co-precipitation with $Pb/BaSO_4$. After purification, the radium and carrier are deposited in a thin layer[10] of $BaSO_4$ (approximately 200 $\mu g/cm^{-2}$) on a 0.45 μm filter paper.[10] The $BaSO_4$ carrier contains ^{133}Ba, with a gamma emission at 356 keV which is used to measure the efficiency of the extraction procedure for radium.

An example of an α-spectrum obtained using a 400 mm^2 diffused junction detector in a Nucleus model 5300 alpha spectrometer (Figure 29) illustrates the complexity of the spectra. The various isotopes may be identified by their α-energy. The amounts of ^{226}Ra, ^{224}Ra and ^{223}Ra are estimated with a computer program that uses the shape of the leading ^{226}Ra peak at 4.77 MeV to obtain the stripping factors and fractions of other peaks in the spectrum to 7.8 MeV. The concentration of ^{228}Ra is obtained by storing the prepared sources and counting them again after four to six months, when the ^{228}Ra concentration can be estimated from the ingrown ^{212}Pb.

The results for ^{223}Ra and ^{224}Ra were corrected for decay between the time of sampling and analysis. This assumes that no radionuclides higher in the respective decay series were present.

The accuracy of the radium analyses is dependent on the calibration standard, the estimate of the sample recovery and the counting statistics. Generally, the estimates for ^{226}Ra have an uncertainty of approximately ±5% for samples with ^{226}Ra in excess of 0.2 pCi L^{-1}. For lower activities, the error is determined by counting statistics.

The radium results obtained for the water filter samples are listed in Tables 34 and 35 respectively. The recovery efficiencies are given in Table 36.

11.3.3 Discussion

11.3.3.1 Effectiveness of the filters

The estimated recovery of ^{226}Ra from the waters by the Mn-filters ranged from 11 to 92%. Generally, these recoveries were lower than previously reported[8] and from our own previous experience. This may be due to the flow rates being higher (>8 L/min) than the recommended (5 L/min). Consequently, the use of only 10-15% of the filter for the radium analyses led, in some cases (9252, 9722, PH73), to unsatisfactory statistical accuracy in the filter results. However, samples such as 20361, PH94 and XPH-8 illustrate the value of the filters. Had the total filter been analyzed, all results would have been satisfactory.

11.3.3.2 Ranger samples

Radium-226 in the Ranger area samples ranged from 35 pCi L^{-1} in sample 79/1 (which interesects the Ranger One No 3 ore body) to 0.16 pCi L^{-1} in water bore 9252. Sample 79/1 also had the highest activity of ^{224}Ra of the Ranger samples. Sample 20361, the furthest north of the Ranger deposit, also had a high ^{224}Ra activity,but sample OB29 alone had ^{224}Ra

in excess of ^{226}Ra. The $^{226}Ra/^{223}Ra$ ratio of the filters ranged from 11 to 47. Sample 79/6a, for which only a water sample was analysed, had a low $^{226}Ra/^{223}Ra$ ratio of 3.2. (The natural activity ratio of $^{226}Ra/^{223}Ra$ for a uranium ore in the radioactive equilibrium is 21.7.)

11.3.3.3 Koongarra area

Radium-226 in the Koongarra area samples ranged from 280 pCi/L^{-1} (in PH49 from the Koongarra ore body) to 0.04 pCi/L^{-1} (in PH94). Generally, there appear to be higher activities of the short-lived radium isotopes in waters from the Koongarra area than from the Ranger area. Whereas only 2 out of 10 samples from the Ranger area have ^{224}Ra greater than or comparable to ^{226}Ra 10 out of the 13 Koongarra samples do. Similarly for ^{223}Ra, only one Ranger area sample had a $^{226}Ra/^{223}Ra$ ratio below 10, whereas 8 of the 13 Koongarra samples had ratios below 10. None of the Koongarra samples had a ratio greater than the natural ratio of 21.7. The low ratio of 1.8 recorded in XPH-8 is similar to that recorded in a sample collected in November 1982 (i.e. 1.5).

References

1. P.L. Airey, D. Roman, C. Golian, S. Short, T. Nightingale, R.T. Lowson and G.E. Calf, "Radionuclide Migration around Uranium Ore Bodies - Analogues of Radioactive Waste Repcsitories", USNRC Contract NRC-04-81-172, Annual Report 1981-82, AAEC Report C29, 1982.

2. A.A. Levinson, C.J. Bland and R.S. Lively, "Ore Deposits and Prospecting", in M. Ivanovich and R.S. Harmon (Eds), Uranium Series Disequilibrium, Chap. 14,(Oxford Science Publ., 1982).

3. S. Block and R.M. Key, "Modes of Formation of Anomalously High Radioactivity in Oil Field Brines", Am. Assoc. Pet. Geol. Bull., 154-159 (1980).

4. M. Asikainen, "Radium Content and the $^{226}Ra/^{228}Ra$ Activity Ratio of Groundwater from Bedrock", Geochim. Cosmochim. Acta, 45, pp.1375-1381.

5. J.R. Dean, C.J. Bland and A.A. Levinson, "^{226}Radium/^{223}Radium Ratio in Groundwater as a Uranium Exploration Technique", J. Geochem. Expl. (in press)(1983).

6. B.L. Dickson, R.L. Meakins and C.J. Bland, "Evaluation of Radioactive Anomalies using Radium Isotopes in Groundwaters", J. Geochem. Expl. (in press) (1983).

7. W.S. Moore and D.F. Reid, "Extraction of Radium from Natural Waters using Manganese-impregnated Acrylic Fibres", J. Geophys. Res. 78:8880-8886 (1973).

8. D.F. Reid, R.M. Key and D.R. Schink, "Radium, Thorium and Actinium Extraction from Seawater using an Improved Manganese-oxide-coated Fiber", Earth Planet. Sci. Lett. 43:223-226 (1979).

9. C.W. Sill, K.W. Puphal and F.D. Hindman, "Simultaneous Determination of Alpha-emitting Nuclides of Radium through Californium in Soil", Anal. Chem. 46:1725-1737 (1974).

10. A.S. Goldin, "Determination of Dissolved Radium", Anal. Chem. 33:406-409 (1961).

12. FURTHER INVESTIGATIONS

There are two principal areas in need of further investigation:

(i) the analysis of new insights into transport and adsorption behaviour; and

(ii) extension of the analogue, particularly to man-made elements such as ^{239}Pu, ^{237}Pu, ^{129}I and ^{99}Tc.

12.1 New Tasks Arising Out of Previous Work

12.1.1 The role of colloids in the transport of radionuclides in groundwater

There is evidence that a significant proportion of uranium and most of the thorium in groundwater pumped from the Nabarlek area is associated with particulates (see Section 10). The 'particulate' uranium appears to be in equilibrium with the 'solution'; however, this could not be determined for thorium because of its low levels in solution. Three questions need to be addressed:

(a) What is the proportion of uranium and thorium associated with particulates and colloids of defined size ranges?

(c) What is the relative rate of transport of 'dissolved' and 'colloidal' radionuclides?

(c) Are 'solute' and 'colloidal' radionuclides in equilibrium?

These matters are extremely important. If the bulk of a radionuclide is transported by a colloid *not* in equilibrium with the 'solution', the validity of conventional adsorption coefficients as predictors of transport is called into question. On the other hand, if equilibrium can be established, only a redefinition of the use of the adsorption isotherm concept will be needed.

12.1.2 The role of iron minerals in the transport of radionuclides

Selective phase separation techniques associated with careful X-ray diffraction have confirmed the importance of iron minerals in the accumulation of uranium and thorium in weathered ores. Separation techniques are being combined with batch adsorption experiments to study differences in the distribution of ^{238}U (and ^{234}U) present over geological time with ^{236}U added as a tracer. These experiments are important in establishing a relationship between laboratory isotherms and data needed for long-term prediction. However, the need to measure isotopic disequilibria on four phases greatly increases the amount of analytical work.

Two extensions to this approach are envisaged, both of which will involve significant research:

(a) Crystalline Rocks. Selective phase separation techniques will be developed to study the distribution of uranium series nuclides on separable components within the reduced zones. As a further extension, a particular study will be made of material grading from fully altered minerals at the surfaces of major cracks and fissures to the unweathered bulk rock. Attempts will be made to interpret the data in terms of the adsorption/leaching behaviour near major fractures over geological time.

(b) Organic Phase. Because of the potential significance of such complexing agents as humic and fulvic acids in determining the mobility of actinides, selective phase separation techniques will be extended to include complex organic acids.

Preliminary evidence of the possible importance of iron minerals in the transport of colloids will be investigated further. Because of the small quantity of material available and the inherent difficulty in identifying different iron minerals, the diffractometer is being modified to allow the collection of differential spectra.

12.1.3 Interpretation of correlated parent/daughter ratios

Important information on the relationship between adsorption and transport kinetics can be deduced from systematic measurements of similar parent/daughter pairs.[1] The principle has been demonstrated for the Th/Ra system by Dr J.C. Laul of Battelle Pacific N W Laboratories.[2] Experiments are under way to measure $^{232}Th/^{228}Ra$, $^{228}Th/^{224}Ra$, $^{230}Th/^{226}Ra$ and $^{227}Th/^{223}Ra$ in groundwater samples from Koongarra and Ranger. At equilibrium, the ratios should simply reflect the relationship between the adsorption coefficients. If, on the other hand, the time for establishing an adsorption coefficient is comparable to the half-lives of the nuclides, systematic differences in the Th/Ra ratios might be observed which should correlate with the appropriate half-lives and with groundwater parameters. The principle could be extended to the $^{238}U/^{230}Th$, $^{234}U/^{230}Th$ systems, if there is sufficient activity for measurement.

12.2 Major Extensions of the Geochemical Analogue

The geochemical analogue approach is useful (i) in establishing correlations between laboratory parameters and those appropriate to geological time-scales, and (ii) in ensuring that significant parameters have not been omitted from the transport models.

Geochemical analogues usually have two important limitations. Firstly, they are inevitably site specific. In the present case, findings arising out of studies of uranium deposits in the Northern Territory of Australia need to be related to sites being considered as possible locations of high

level radioactive waste repositories. To some extent, the problem of relating one site to another is being answered by correlating transport parameters with detailed mineralogy. If, for instance, the extent to which iron mineralogy determines the migration rate of radionuclides in the weathered zone can be quantified, an important basis will be established for relating findings from one alluvial setting to another. Again, if the role of colloids in groundwater transport can be determined, this will provide another basis for interrelating transport at different sites.

The second limitation of the current work is that measurements are restricted to major actinides. Important components of high-level radioactive waste repositories, such as ^{237}Np, ^{239}Pu, ^{129}I and ^{99}Tc, have not been included. However, the power of the concept of using uranium deposits as HLW repository analogues is that these nuclides may be included, provided that

- the rates of formation may be calculated with sufficient accuracy; and
- measurements may be undertaken with sufficient precision.

12.2.1 Iodine-129

Iodine-129 is one of the more significant fission products. The environmental component is generated by the spallation of atmospheric xenon and by sub-surface fission processes. Relevant information on the input function was obtained from a recent survey of the levels of the isotope in groundwater from the Great Artesian Basin, Australia.[3]

In an endeavour to incorporate iodine-129 into the geochemical analogue, groundwater and ore samples will be collected from Ranger, Jabiluka, Nabarlek and Koongarra. The principal aims of the investigation are:

(i) to study the mobilization of the isotope associated with the advance of the weathering front through the metamorphic host rocks, and with the evolution of the weathered profiles; and

(ii) to identify factors affecting the mobility of ^{129}I in groundwater down-gradient of the deposits.

An important simplification to data interpretation arises from the fact that the time for the evolution of the weathered zone is probably less than 500,000 y. Since the half-life of ^{129}I is 17,000,000 y, very little isotope will be generated subsequent to weathering. The ratio

$$(^{129}I/^{238}U)_{\text{weathered zone}}/(^{129}I/^{238}U)_{\text{crystalline zone}}$$

will thus reflect the net effect of mobilization induced by weathering, and a small input from ^{129}I in rainfall. The ratio should be small unless there is appreciable association of iodide with the minerals of the weathered profile.

12.2.2 Neptunium-237

The formation of ^{237}Np is initiated by the ^{238}U (n,2n) reaction. As with ^{129}I

(a) it should be mobilized by the passage of the weathering front through the metamorphosed host rock;

(b) since the model of the analogue indicates that the passage of the weathering front occurred less than, say, 500,000 y before present, the generation of the nuclide (half-life 2.14×10^6 y) is small and the ratio

$$(^{237}Np/^{238}U)_{\text{weathered zone}}/(^{237}Np/^{238}U)_{\text{crystalline zone}}$$

can be interpreted in terms of the mobilization of neptunium following the passage of the weathering front.

On the basis of analogy with ^{239}Pu measurements, it has been assessed that it should be possible to detect 10^7 atoms of ^{237}Np using mass spectrometry. Assuming a useful level of 10^9 atoms, and an equilibrium $^{237}Np/^{238}U$ ratio of 2.2×10^{-12} found for Katanga One, less than 1 g uranium would be required.[4]

It is therefore proposed, if possible, to study the mobilization of ^{237}Np from the Northern Territory ore deposits using state-of-the-art mass spectrometry. There are two logical extensions of this work:

(i) to investigate the groundwater-induced migration of neptunium, and

(ii) to measure the distribution of the isotope through selectively extracted phases to establish whether iron mineralogy plays an analogous role in neptunium transport to uranium and thorium.

In the case of groundwater, the work will probably be precluded by the size of the groundwater sample required (approximately 10^6 L per g U).

12.2.3 Plutonium-239/chlorine-36

The scientific basis for incorporating ^{239}Pu into the geochemical analogue is similar to that for ^{129}I and ^{237}Np. However, it is inherently more complex because the time-scales associated with the evolution of the

weathered profile are comparable to the half-life of the isotope. Account must therefore be taken, not only of the rate of mobilization, but also the rate of formation within the weathered profile. Because of the inherent complexity of the processes, there is advantage in normalizing the ^{235}Pu data to a second isotope which is also formed by neutron activation in both the unweathered and weathered zones and will be mobilized by the weathering. Chlorine-36 seems suitable and it is therefore proposed to measure $^{239}Pu/^{36}Cl$ ratios.

12.2.4 Other fission products

It is proposed to extend the analogue to include ^{99}Tc. Technetium/iodide mobility ratios will be compared by monitoring $^{99}Tc/^{129}I$.

12.3 Site Evaluation

As was discussed in Section 2, the aim of the project is to establish the scientific principles for the long-term prediction of radionuclide migration. In particular, correlations are sought between

- laboratory sorption and matrix properties (relation 3, Figure 2),
- laboratory leaching and radionuclide distribution throughout the mineral phases (correlation 2), and
- radionuclide distribution and long-term transport behaviour (correlation 1).

The generality of the correlations should be investigated by seeking to apply them to other classes of geochemical analogue. For instance, the distribution of radionuclides through the linings of old tailings dams could be studied.

If the validity of the correlations is established in a number of these settings, an attempt could be made to apply them to an appropriate potential repository site. The following steps would be involved:

- the mineralogy of the host rock would be studied and a separation into defined phases undertaken;
- the distribution of indicator elements such as uranium, thorium and radium through the different phases would be established;
- laboratory adsorption/leaching experiments would be undertaken and correlated with the distribution of uranium throughout the separated phases;
- on the basis of insights obtained from the geochemical analogue, predictions would be made of the long-term transport of uranium series elements and more relevant transuranics and fission products.

References

1. S. Krishnaswami, W.C. Graustein, K.K. Turikian and J.F. Dowd, "Radium, Thorium and Radioactive Lead Isotopes in Groundwater : Application to the in situ Determination of Adsorption-Desorption Rate Constants and Retardation Factors", Water Res. Res., 18, 1633-1675 (1982).

2. J.C. Laul, R.W. Perkins and N. Hubbard, "An Aspect of Th and Ra Chemistry in the Wolfcamp and Granite Wash Aquifers, Palo Duro Basin, Texas", EOS, 64(18), p.227 (1983).

3. P.L. Airey, H. Bentley, G.E. Calf, S.N. Davis, D. Elmore, H. Gore, M.A. Habermehl, F. Phillips, J. Smith and T. Torgersen, "Isotope Hydrology of the Great Artesian Basin", in Proceedings of the International Conference on Groundwater and Man (Sydney, 1983), Vol. 1 p.1.

4. W.A. Myers and M. Lindren, "Precise Determination of the Natural Abundance of ^{237}Np and ^{239}Pu in Katanga Pitchblende", J. Inorg. Nucl. Chem., 1971, 33:3233-3238.

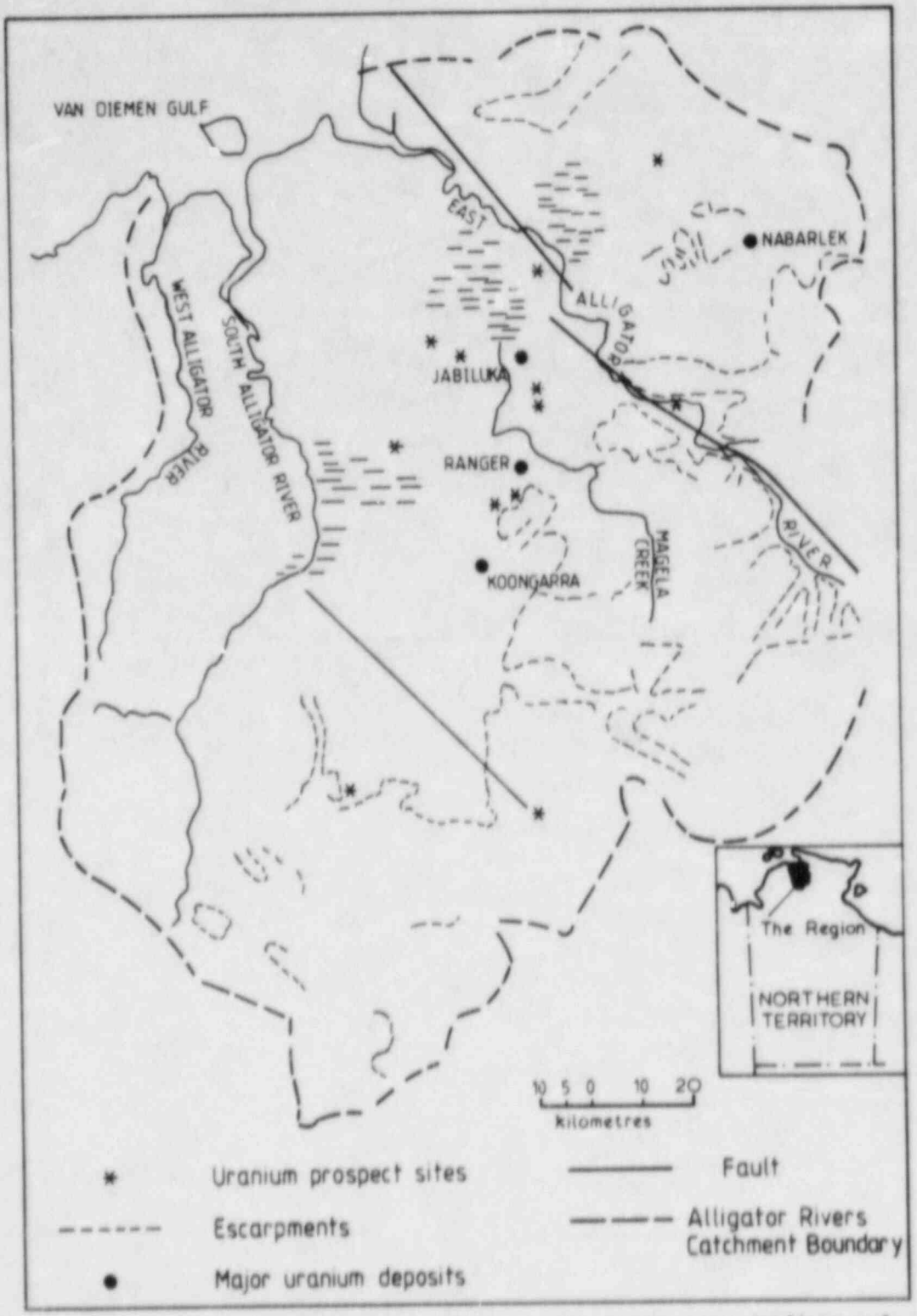

FIGURE 1 The location of the principal uranium ore bodies and prospects in the East Alligator River area of the Northern Territory of Australia. (Map 9, reference [15], Section 1.)

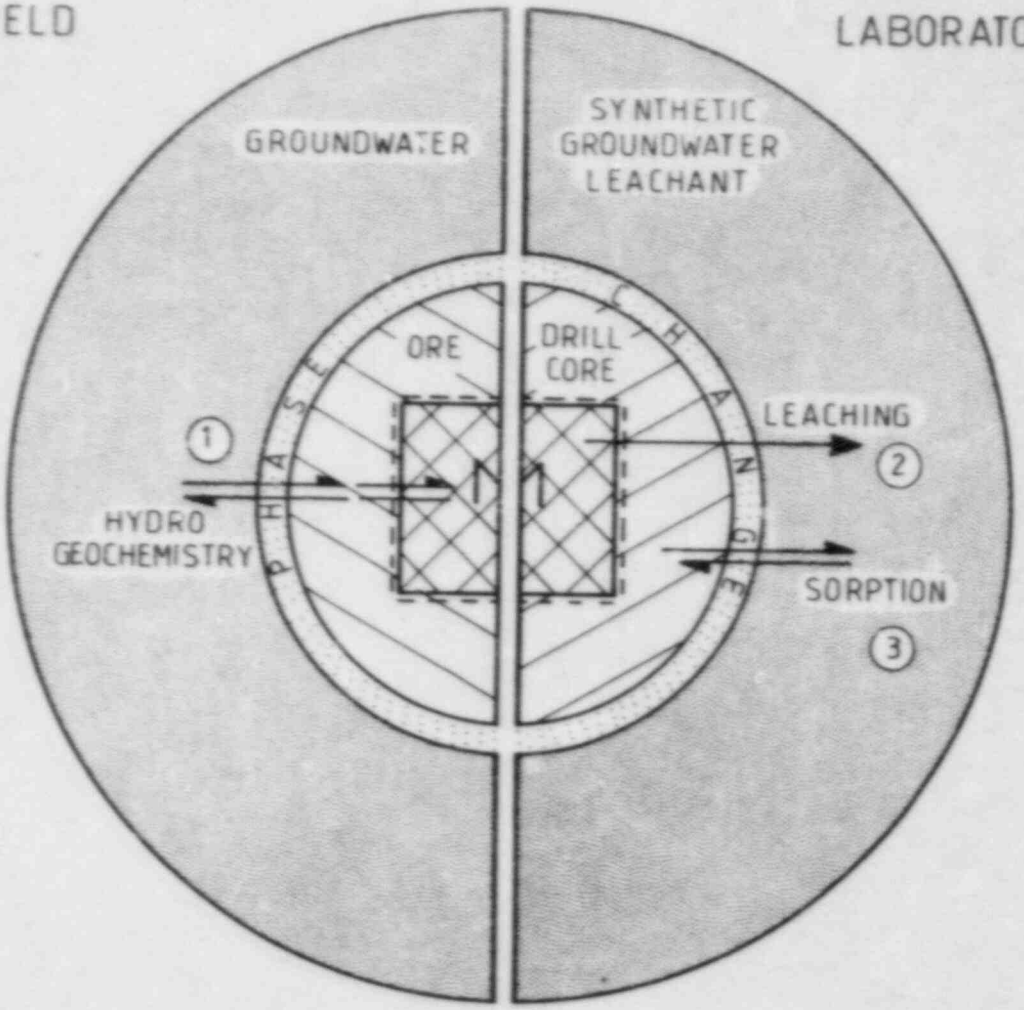

FIGURE 2 Schematic representation of the geochemical analogue approach. The relationship between field observations and laboratory studies is shown.

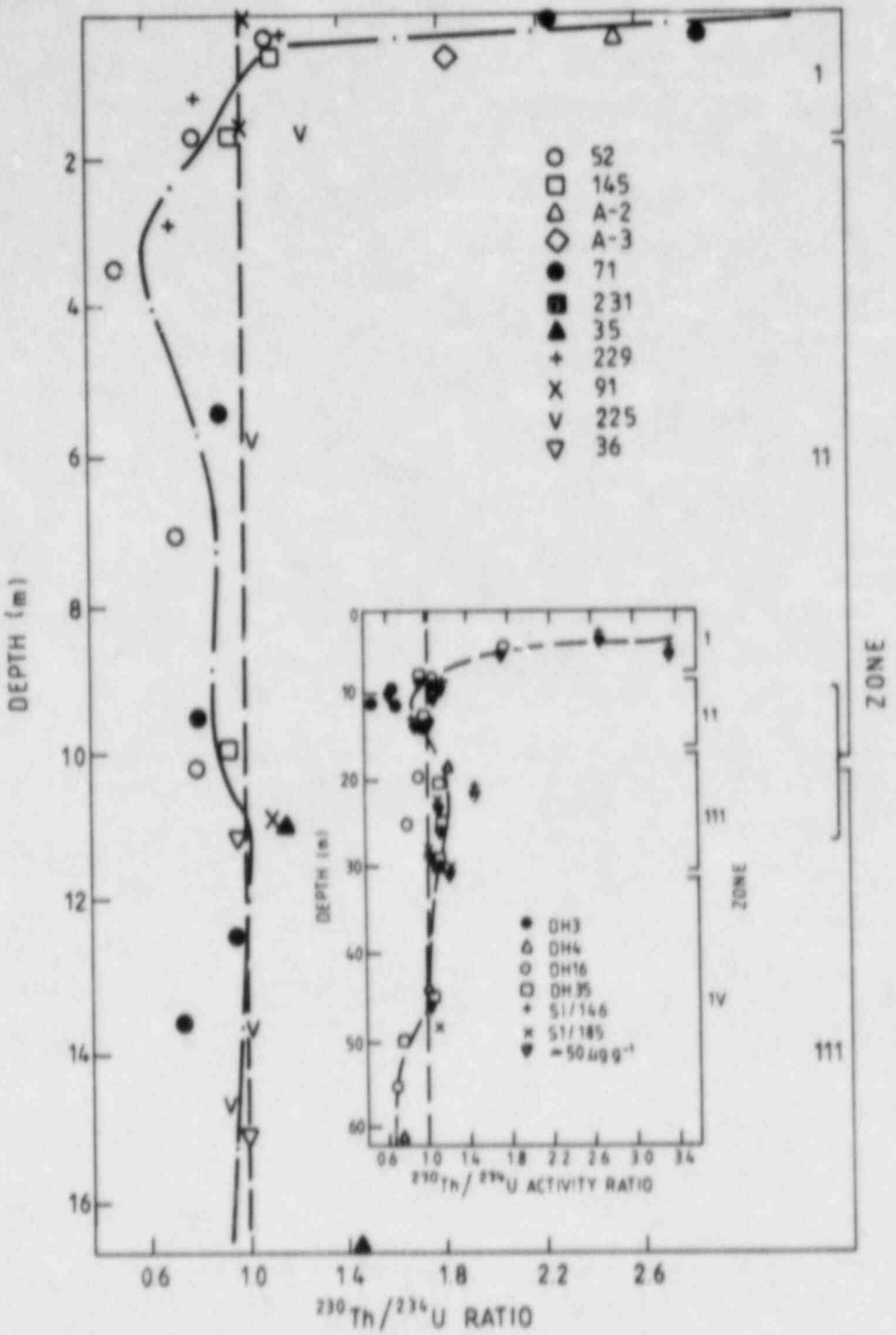

FIGURE 3 Composite illustration of the variation with depth of the $^{230}Th/^{234}U$ ratios for the Nabarlek drill holes listed in the key. The three-zone classification is illustrated. The analogous variation for Ranger One and Jabiluka One deposits is shown as an insert.

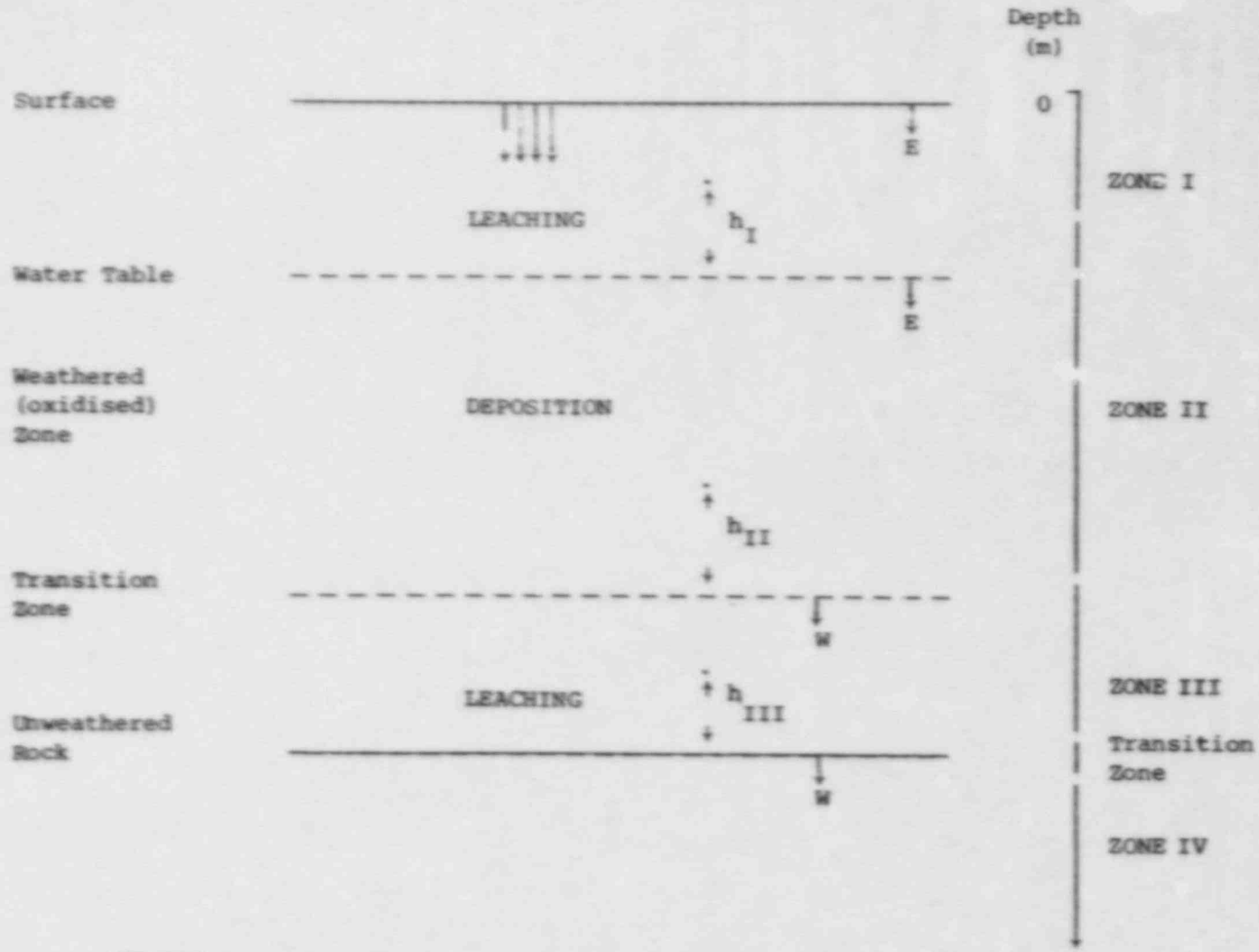

FIGURE 4 Schematic representation of the four-zone model (Nabarlek). Note: zones III and IV cannot be distinguished from isotopic evidence.

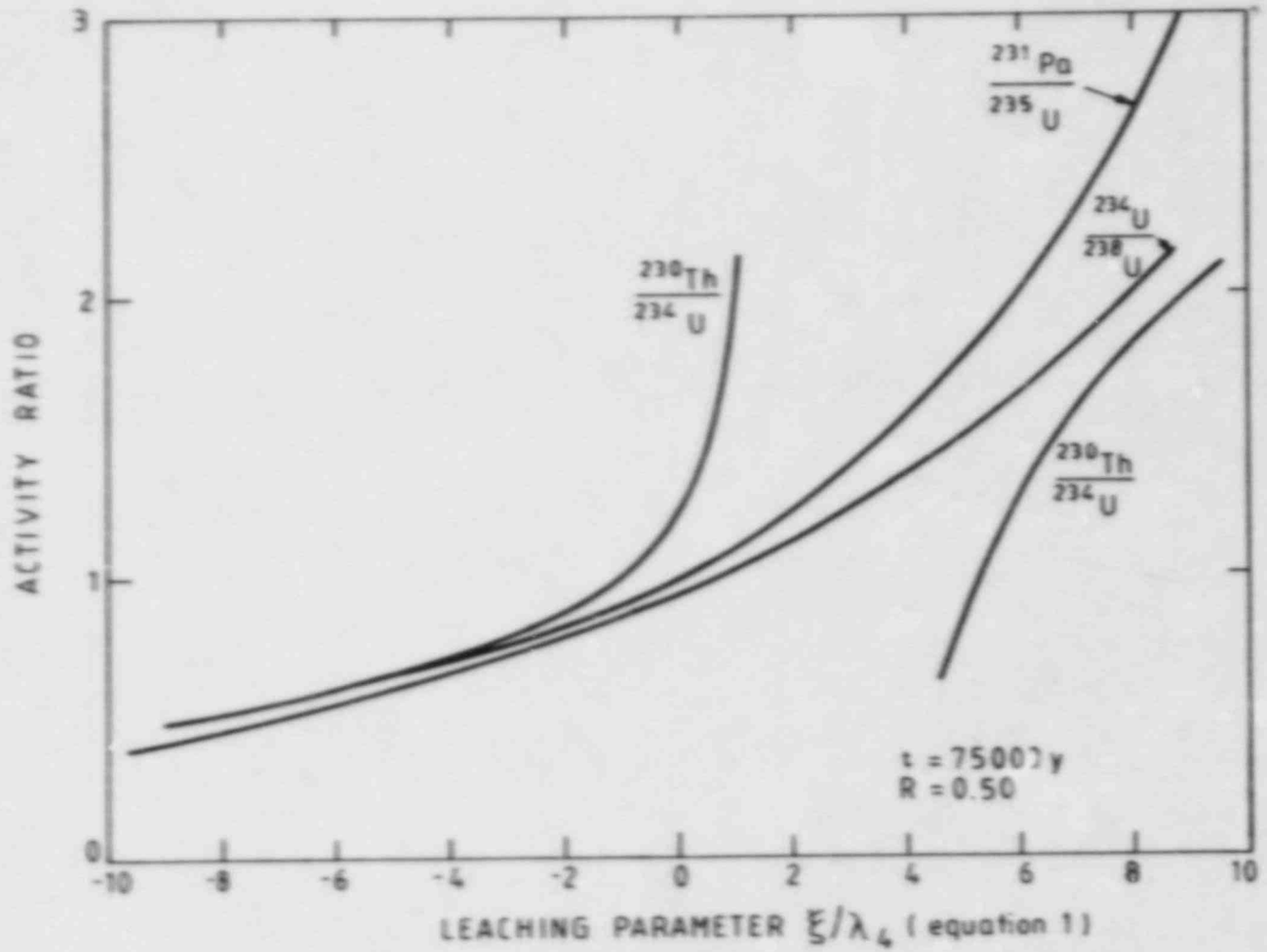

FIGURE 5 Variation of the isotope ratios with the erosion parameter ξ/λ_4 (equation (1)). Positive values indicate leaching, negative values, deposition. In the calculation, a value of 0.5 is assumed for the $^{234}U/^{238}U$ ratios and 75 000 y for the time.

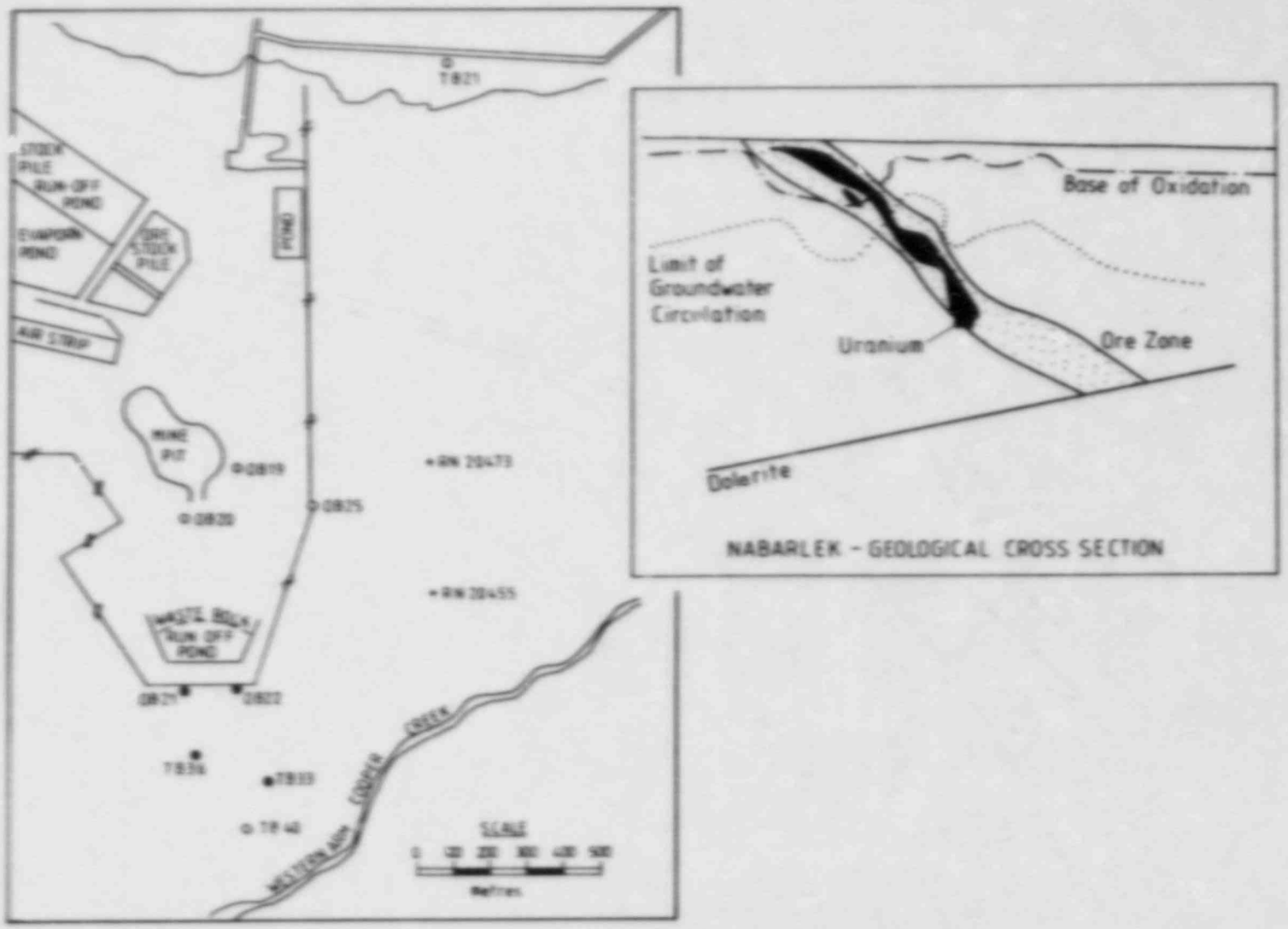

FIGURE 6 Location of the sampling wells at Nabarlek. Insert: general geological cross-section.

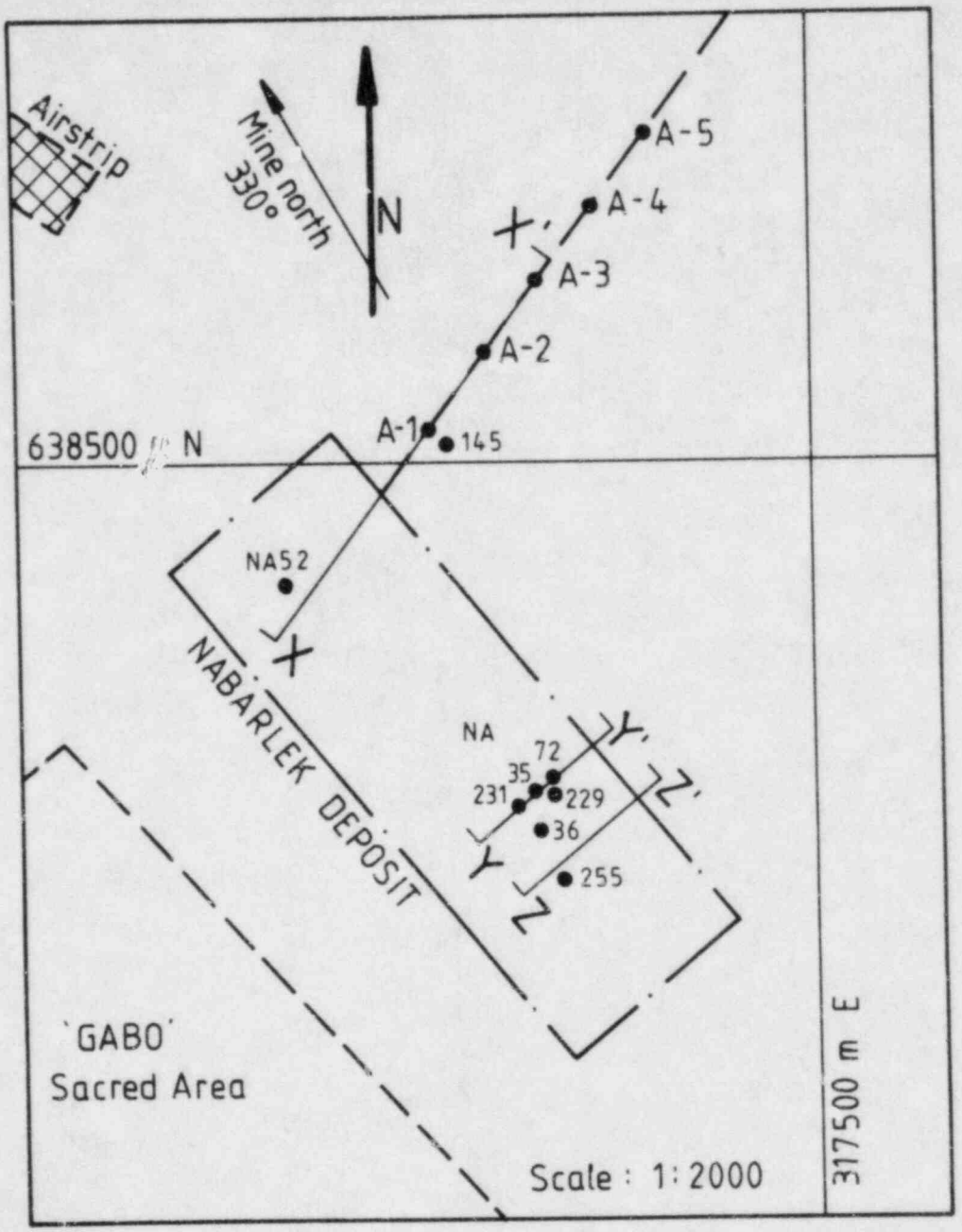

FIGURE 7 Spatial location of Nabarlek drill core samples. The transects XX', Y'' and ZZ' shown in Figures 8, 9 and 10, respectively, are also indicated.

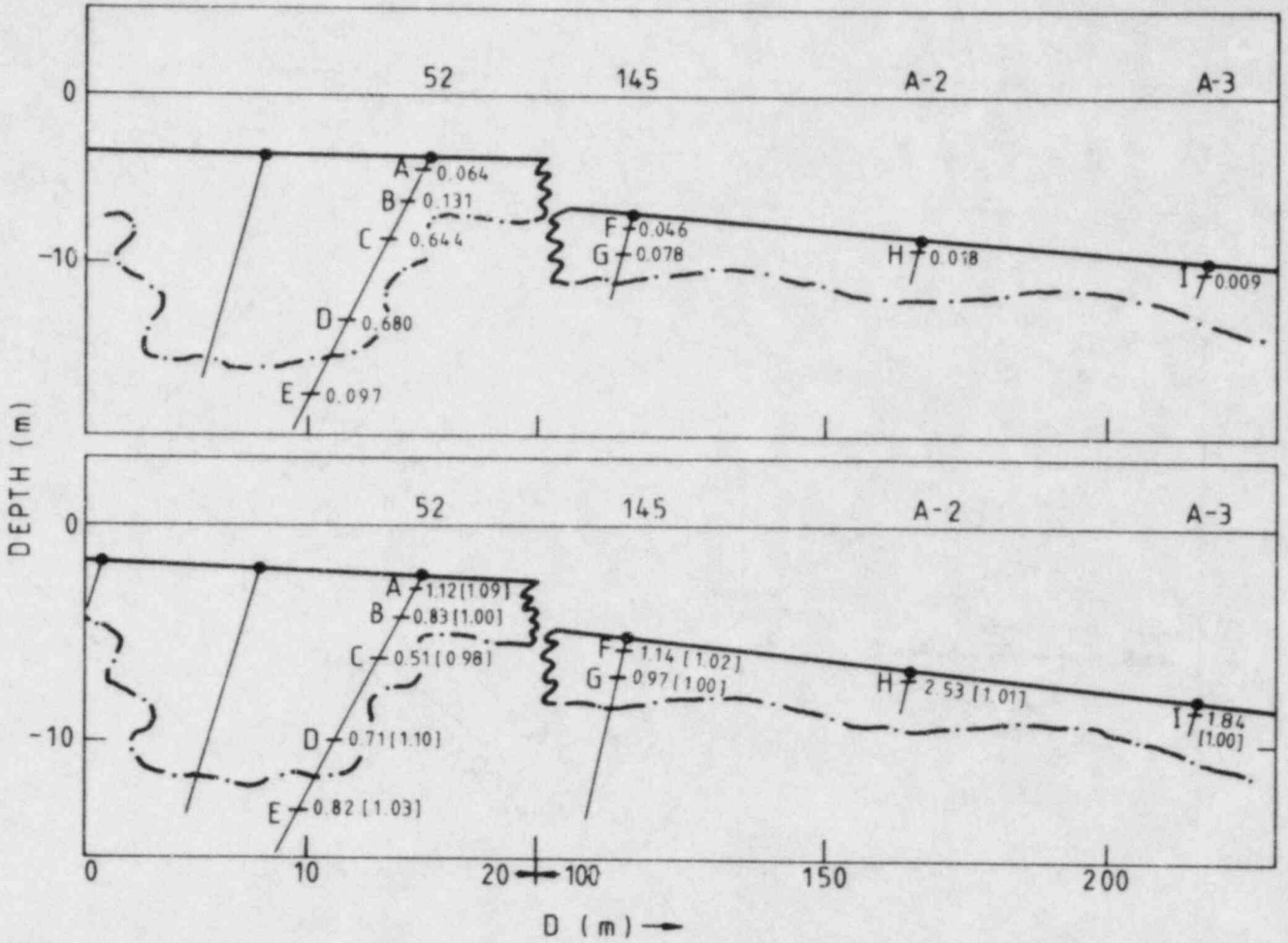

FIGURE 8 Transverse section XX' (Figure 7). Top : weight per cent uranium concentration. Individual samples are identified. Bottom : $^{230}Th/^{234}U$ activity ratios in ore samples; $^{234}U/^{238}U$ ratios are shown in parenthesis. —·—·— base of weathering zone. ∿∿∿ boundary of schist crust (deformation) zone.

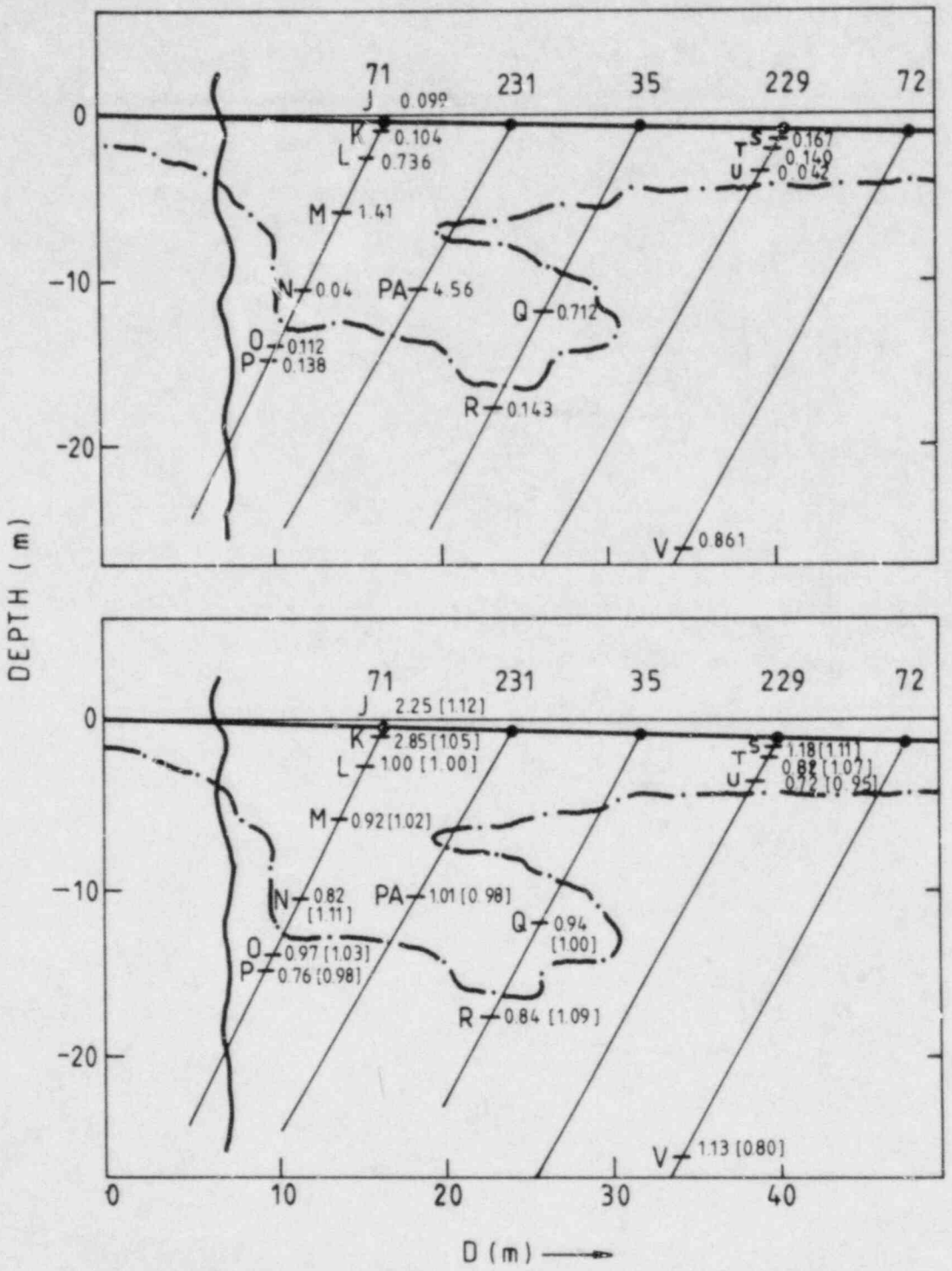

FIGURE 9 Transverse section YY' (Figure 7). Top : weight per cent uranium concentration. Individual samples are identified. Bottom : $^{230}Th/^{234}U$ activity ratios in ore samples; $^{234}U/^{238}U$ ratios are shown in parenthesis. —·—·— base of weathering zone. ∿∿∿ boundary of schist crust (deformation) zone.

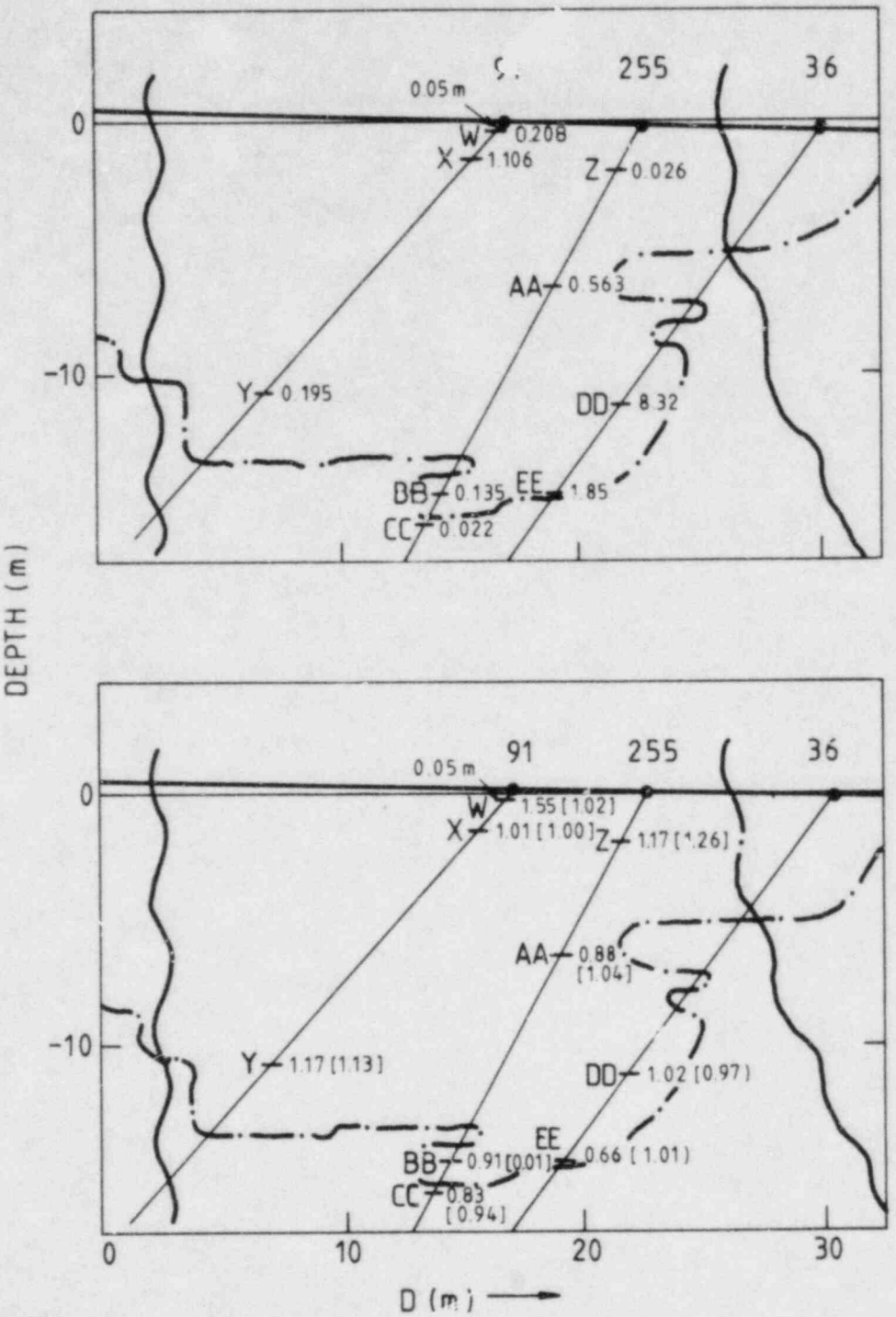

FIGURE 10 Transverse section ZZ' (Figure 7). Top : weight per cent uranium concentration. Individual samples are identified. Bottom : $^{230}Th/^{234}U$ activity ratios in ore samples; $^{234}U/^{238}U$ ratios are shown in parenthesis. —·—·— base of weathering zone. ∿∿∿ boundary of schist crust (deformation) zone. Note : diamond drill hole 255 is 19 m S.E. of the transect.

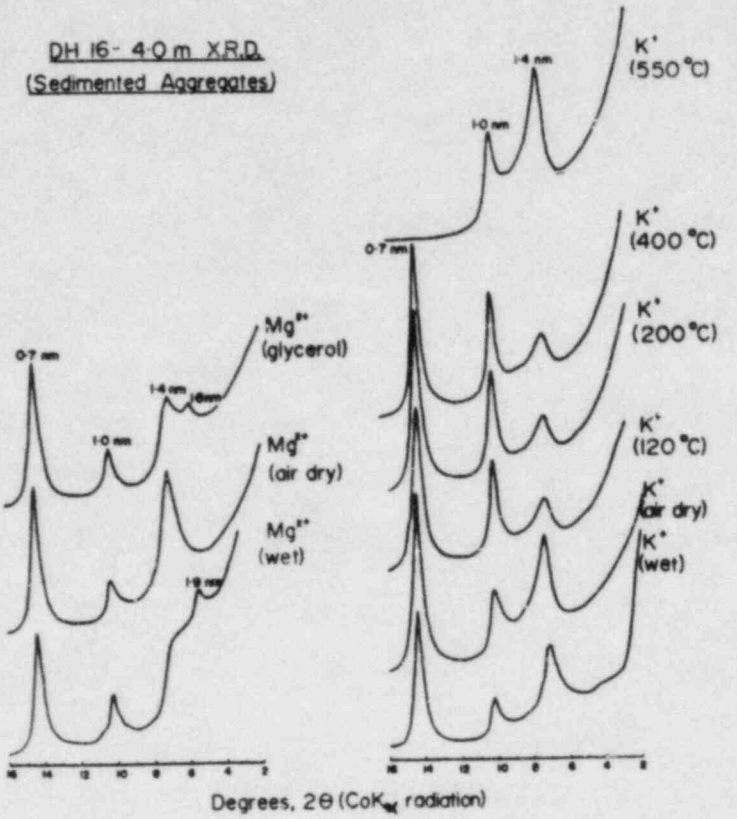

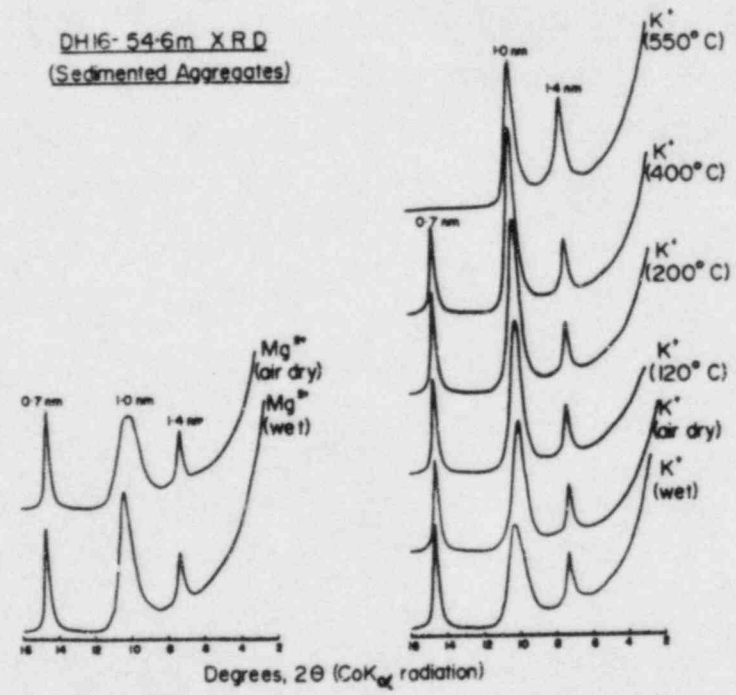

FIGURE 11 X-ray diffraction analysis of DH 16 samples (sedimented aggregates).

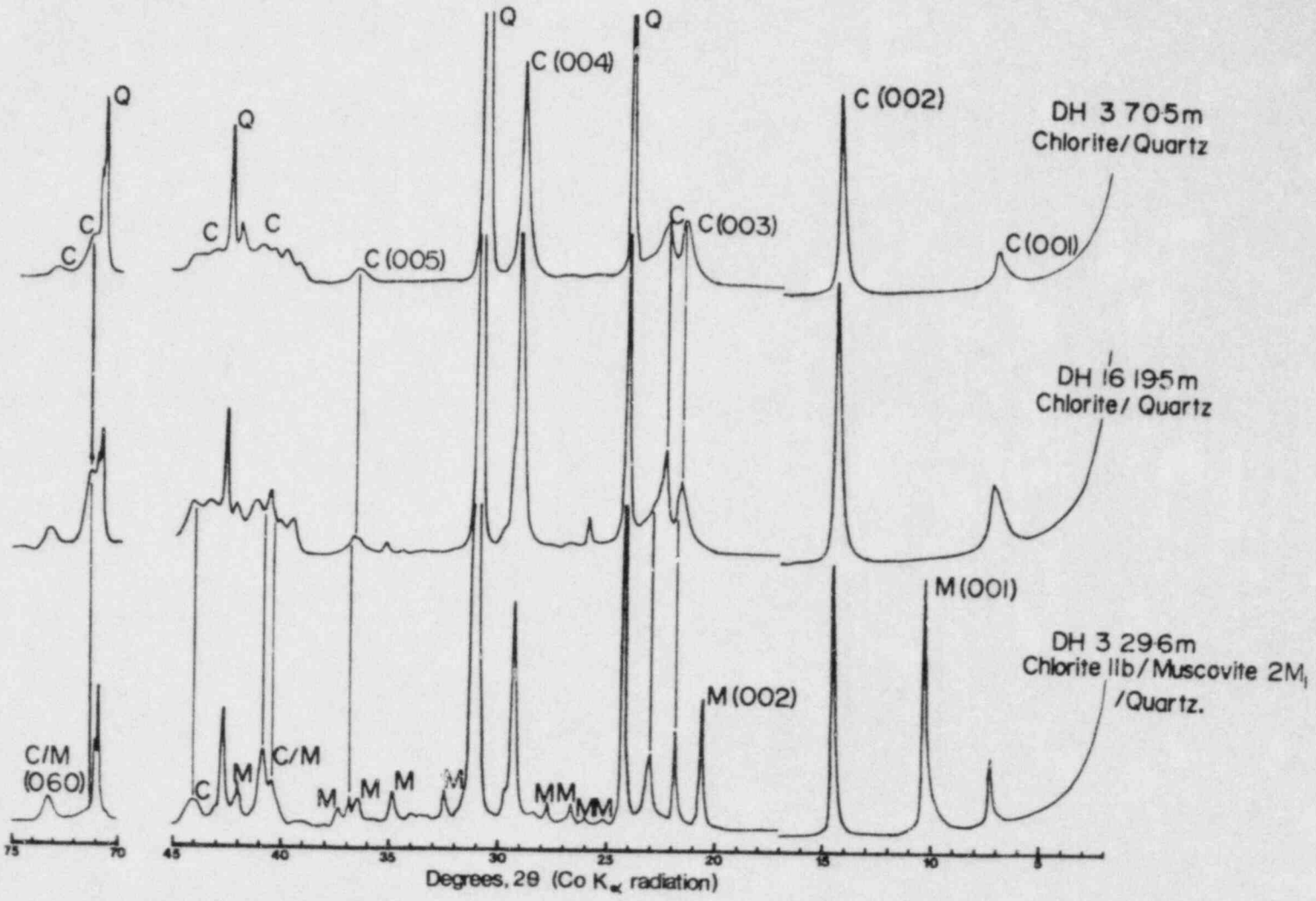

FIGURE 12 X-ray diffraction analysis of Jabiluka DH 3 and DH 16 samples (random powders).

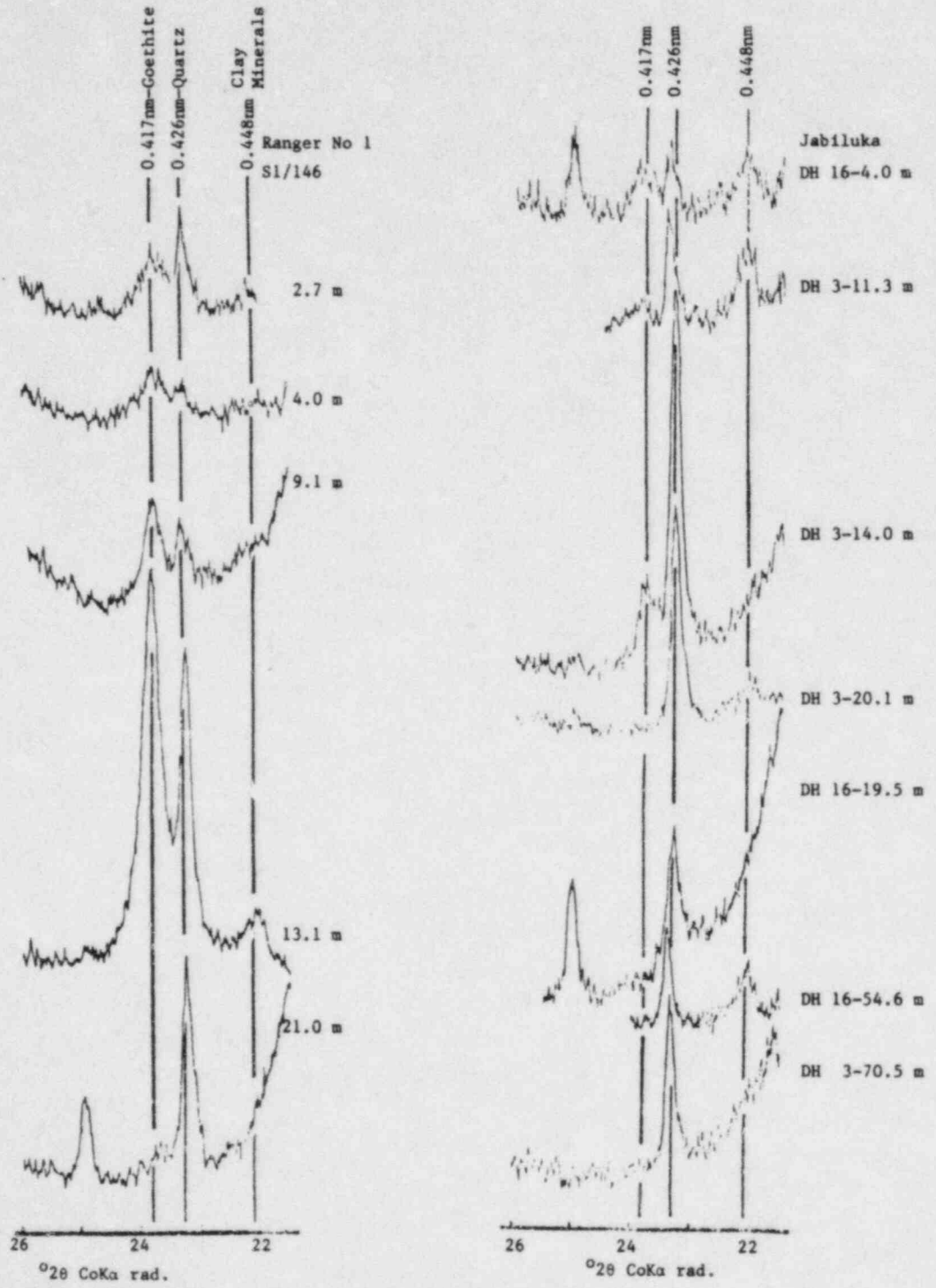

FIGURE 13 X-ray diffraction analysis of Ranger One and Jabiluka samples (sedimented aggregates).

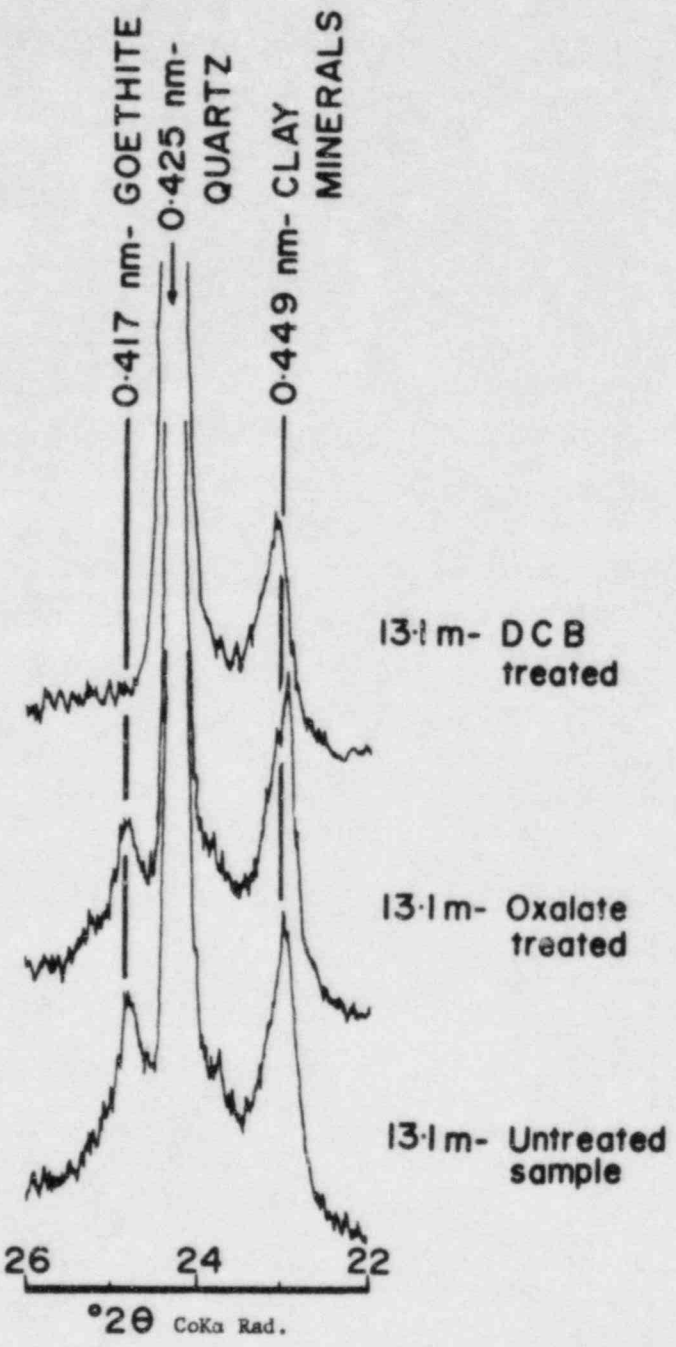

FIGURE 14 S1/146 - 13.1 m: Effect of Tamm's acid oxalate and diothionite-citrate-bicarbonate on the 22-26° 2θ region of the random powder diffraction pattern.

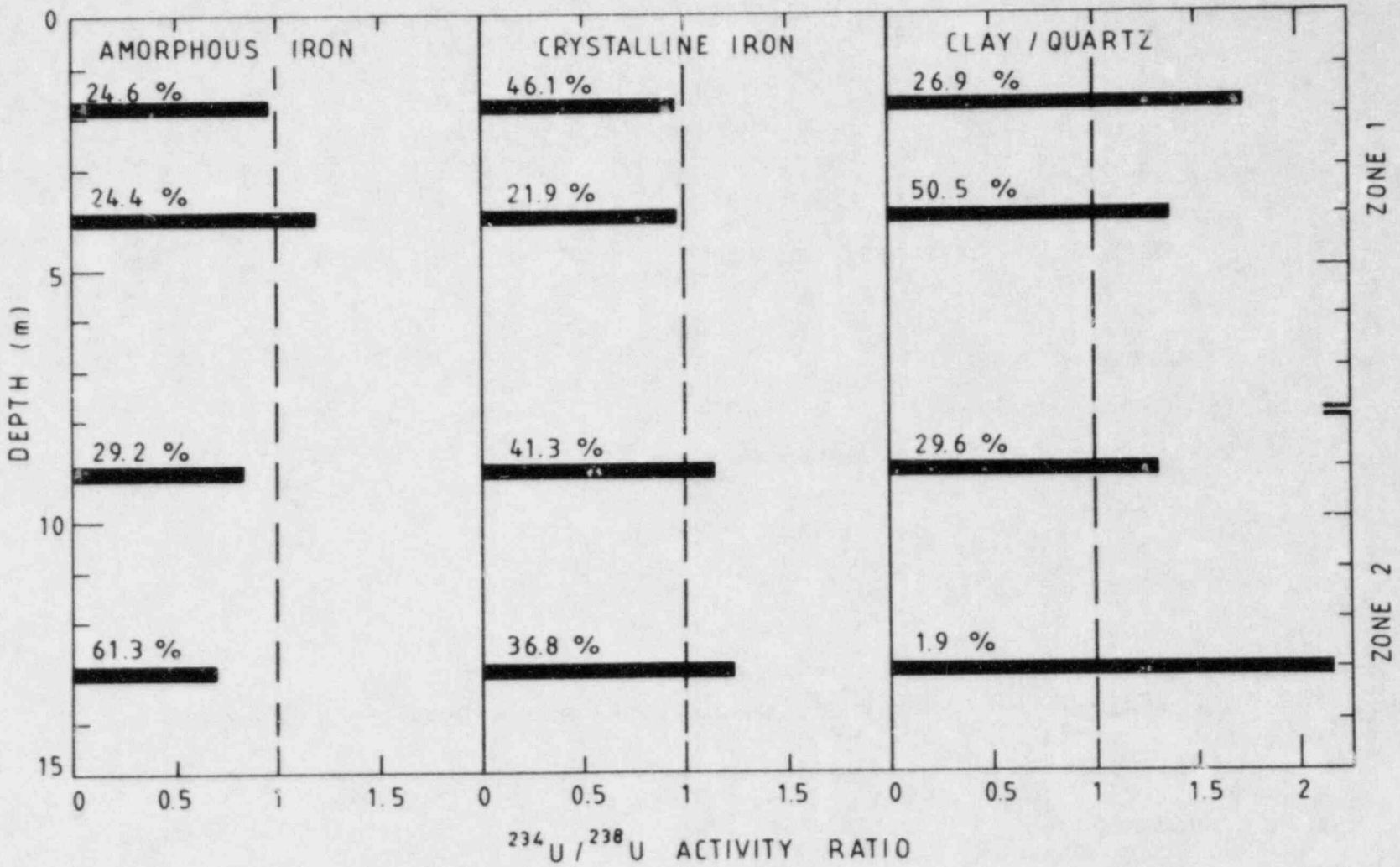

FIGURE 15 Variation of the $^{234}U/^{238}U$ activity ratios in selectively extracted phases from samples from the S1/146 core of the Ranger One ore body. (a) amorphous iron, (b) crystalline iron, (c) clay and quartz phases.

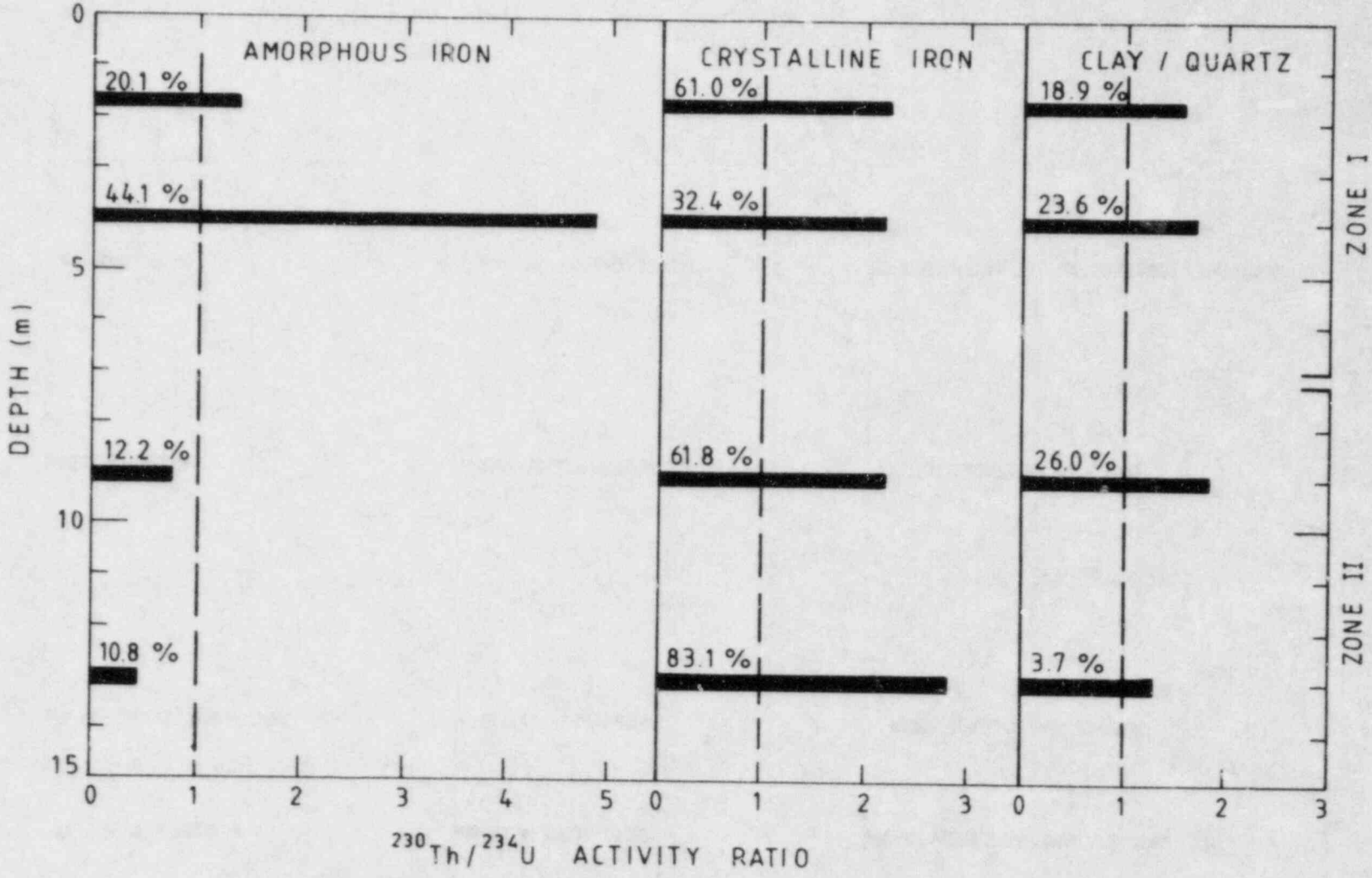

FIGURE 16 Variation of the $^{230}Th/^{234}U$ activity ratios in selectively extracted phases from samples from the S1/146 core of the Ranger One ore body. (a) amorphous iron, (b) crystalline iron, (c) clay and quartz phases.

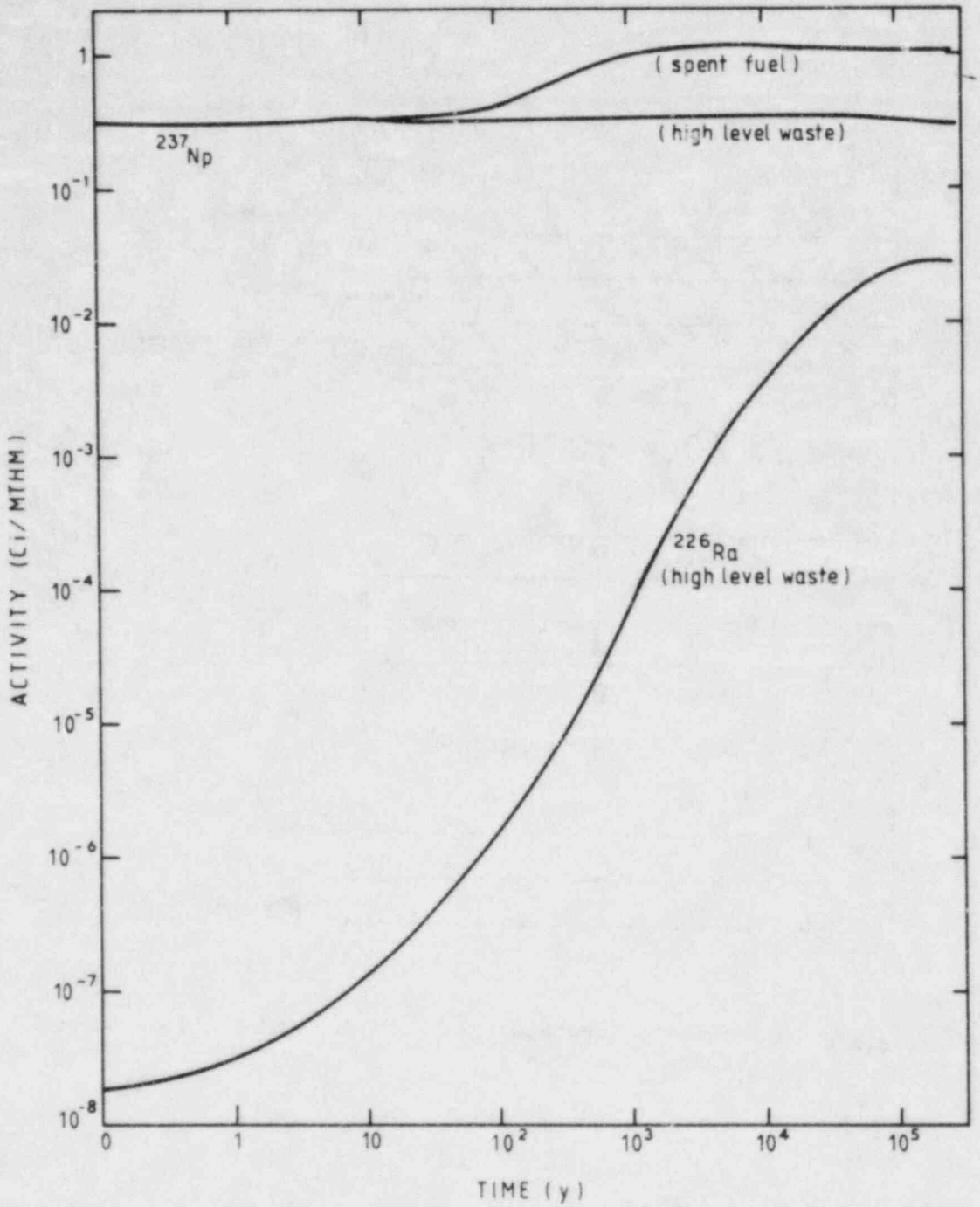

FIGURE 17 Variation with time of the relative activities of ^{237}Np and ^{226}Ra in high level waste and spent fuel (after Croft and Alexander, reference [8], Section 7.)

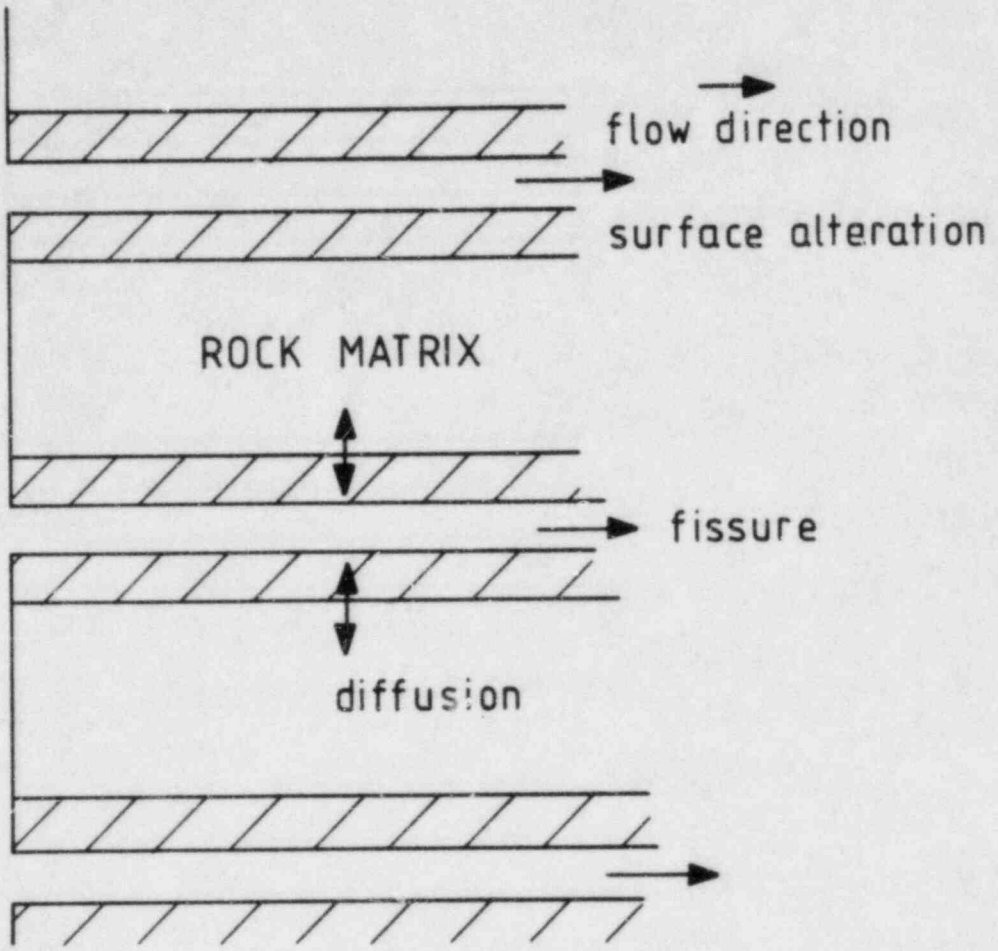

FIGURE 18 Schematic representation of groundwater flow through crystalline rock.

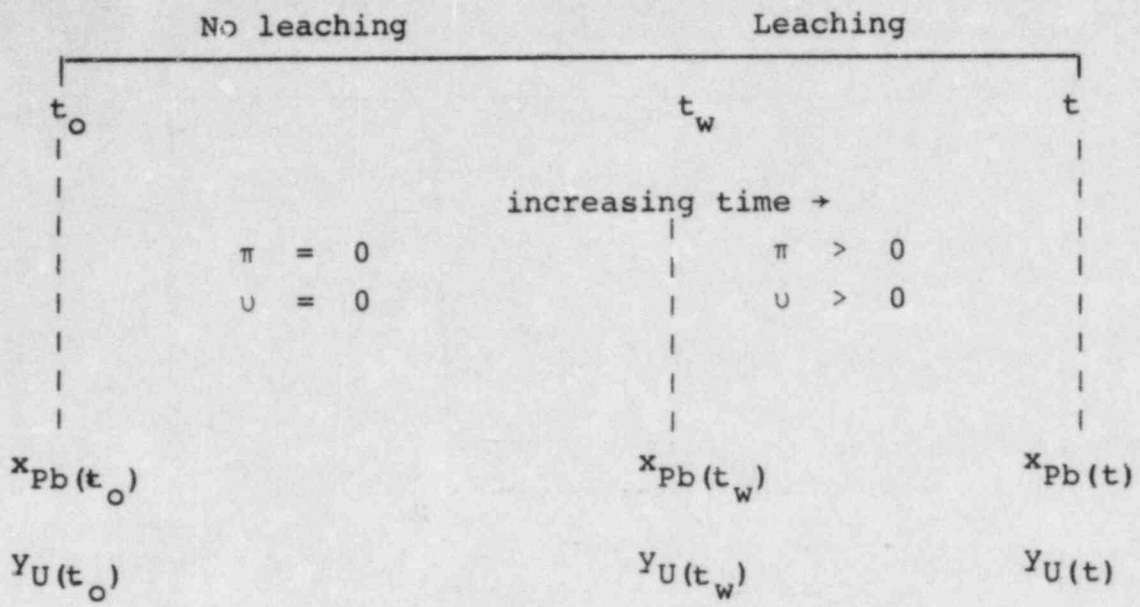

Note : x = 204, 205, 206 or 207.
y = 235 or 238.

FIGURE 19 Schematic representation of variable parameters.

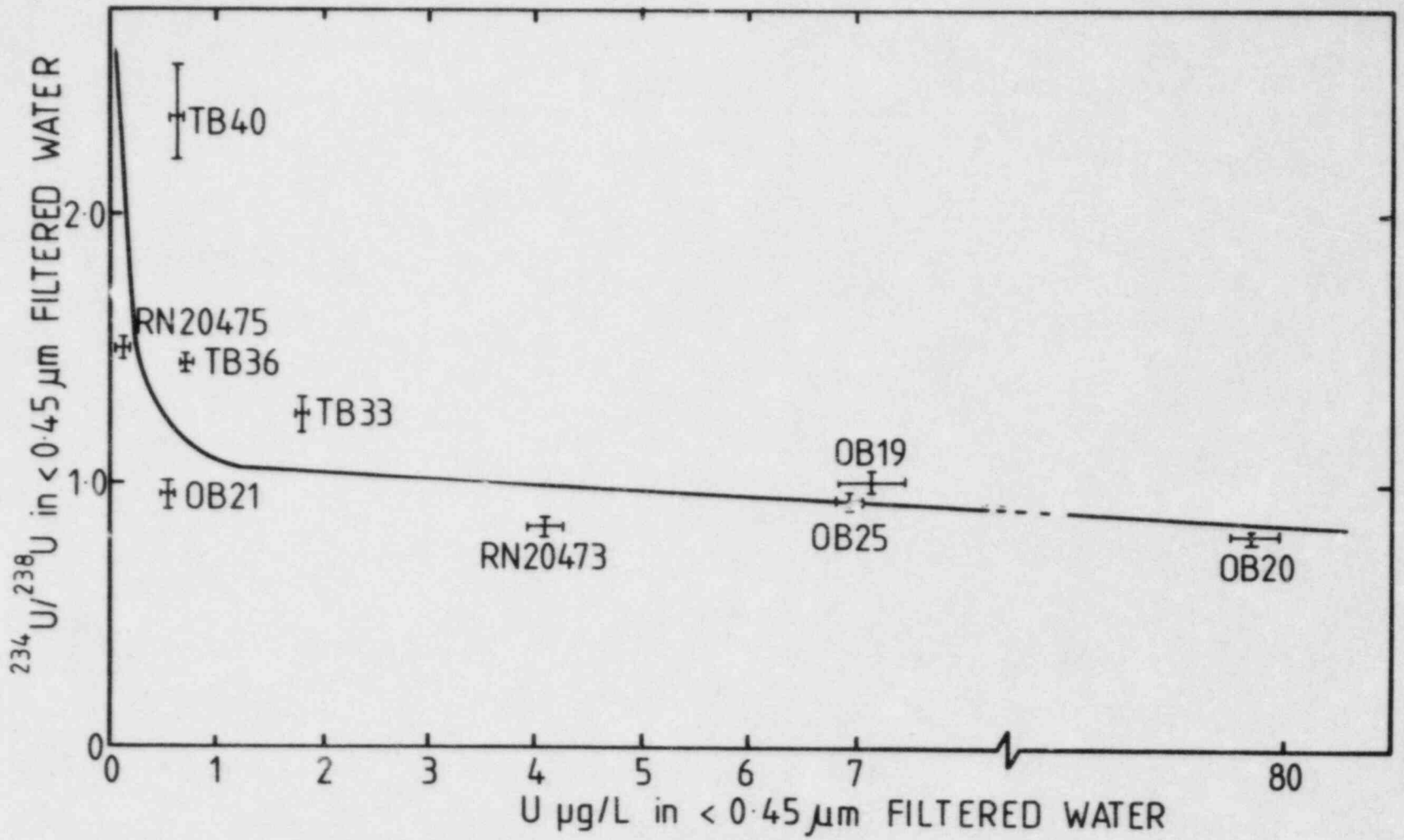

FIGURE 20 Variation of $^{234}U/^{238}U$ ratios with uranium concentration in Nabarlek groundwater (<0.45 µm).

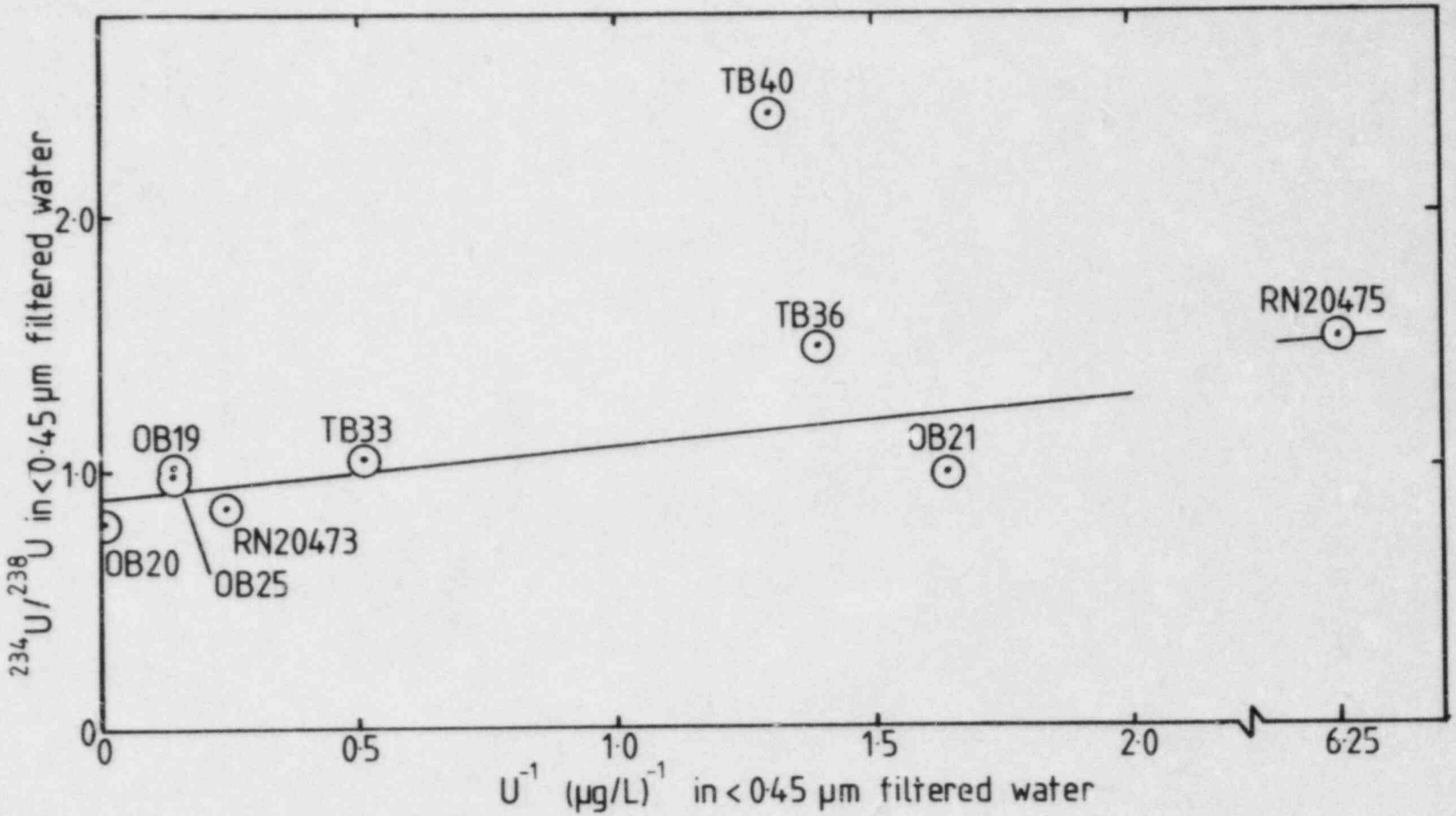

FIGURE 21 Variation of $^{234}U/^{238}U$ ratios with the reciprocal of the uranium concentration in Nabarlek groundwater (<0.45 µm).

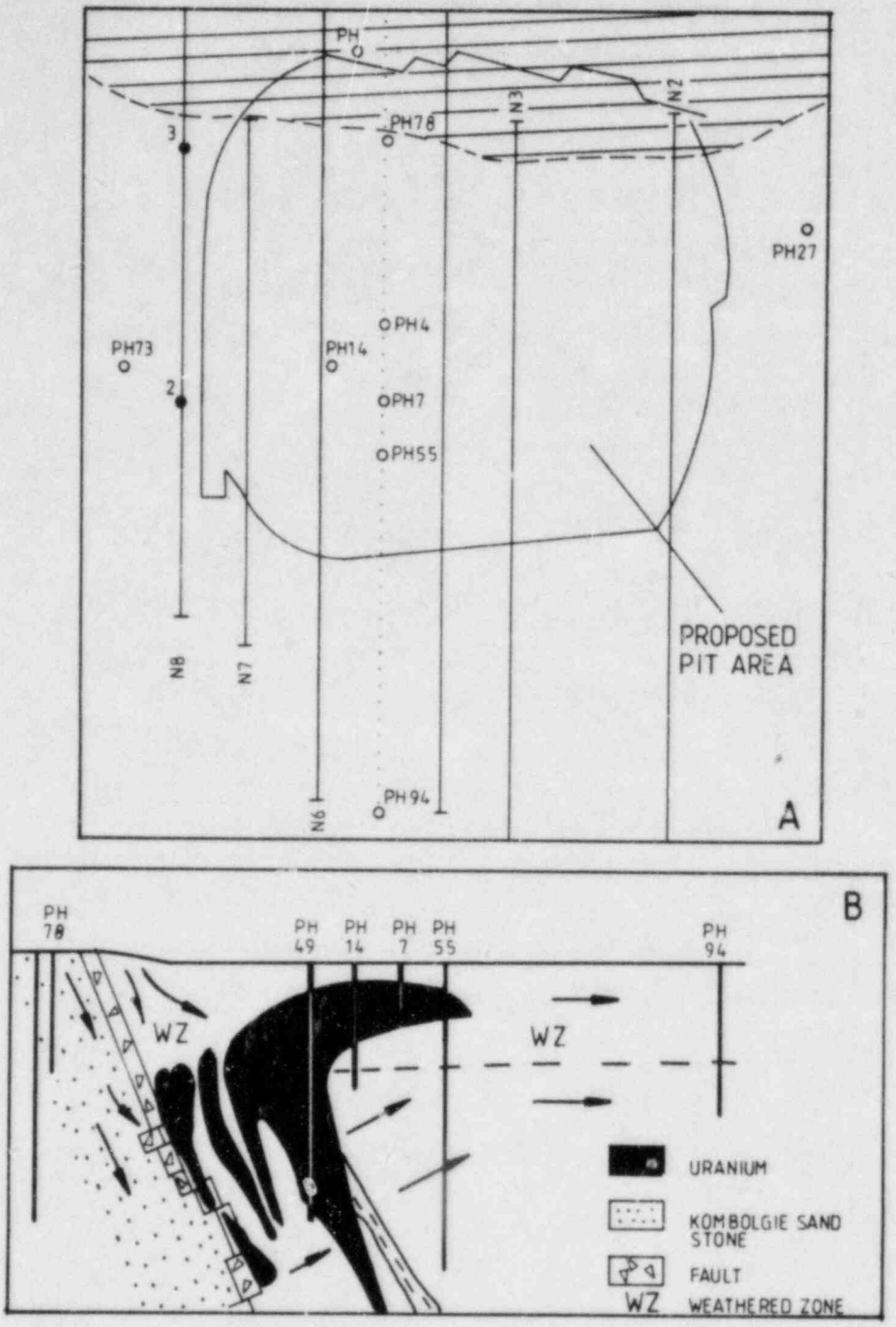

FIGURE 22 A. Location of the sampling wells at the Koongarra deposit (adapted from Figure 10, reference [3], Section 9).
B. A section between wells PH 78 and PH 94 showing the location of a major fault, the extent of the uranium deposits, the boundary of surface oxidation and the groundwater flow paths (adapted from Figure 1, reference [4], Section 9).

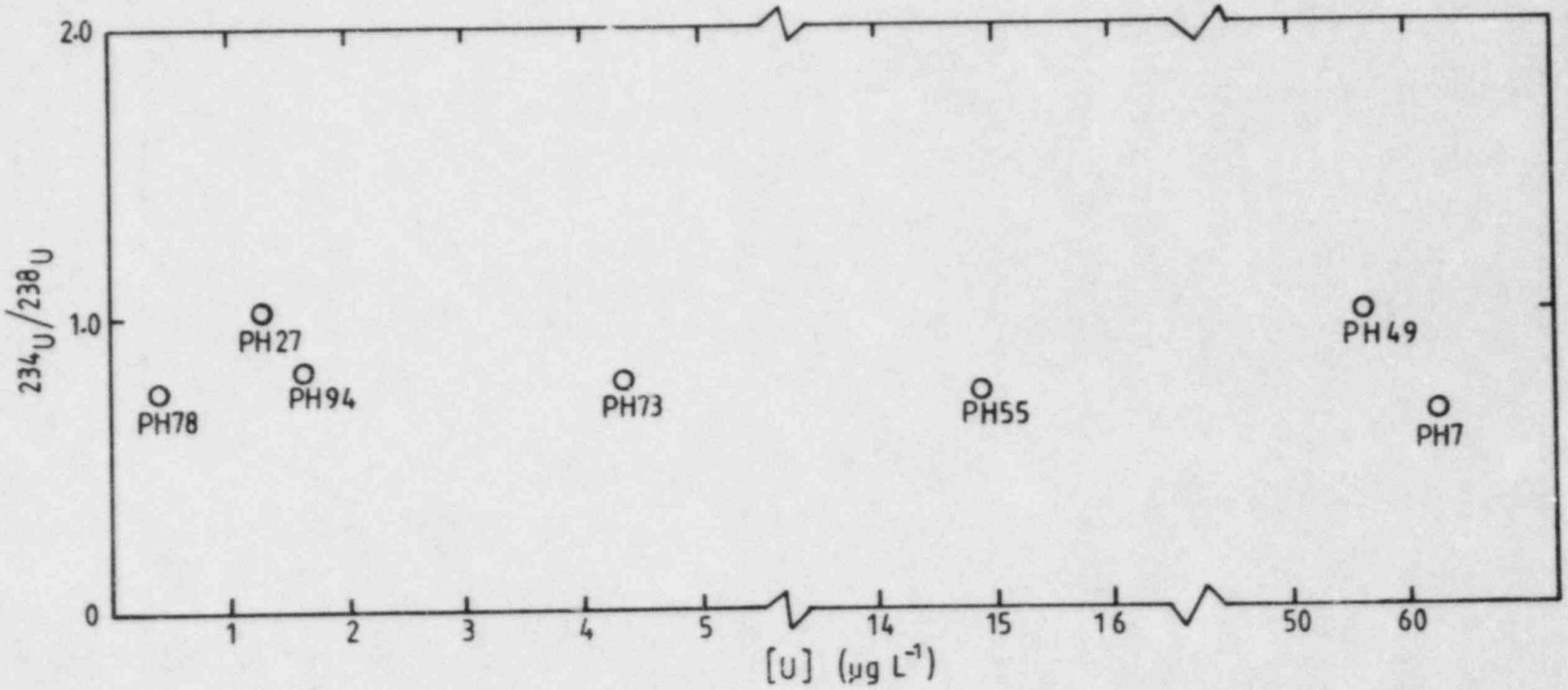

FIGURE 23 Variation of the $^{234}U/^{238}U$ ratios with uranium concentration in Koongarra groundwater.

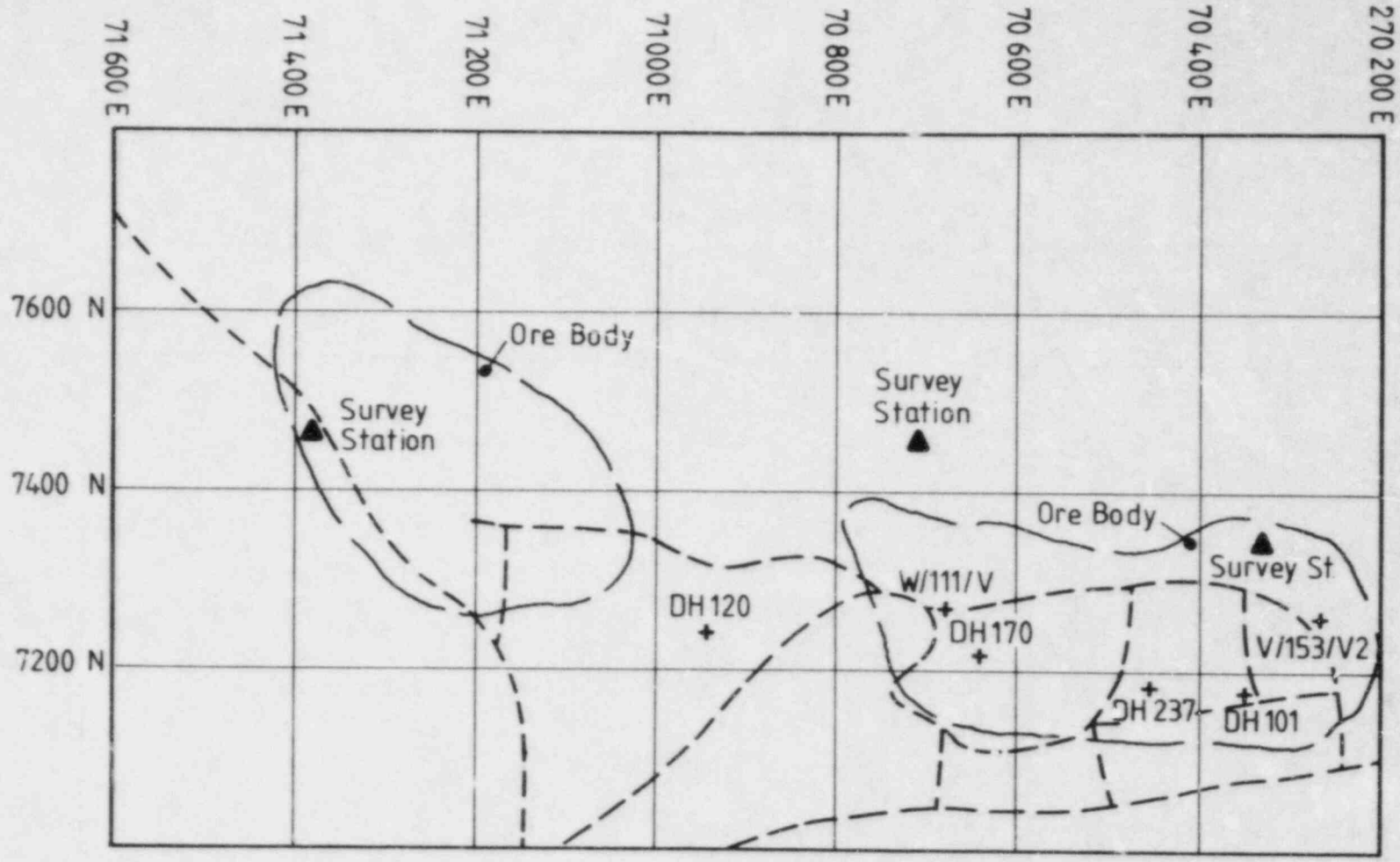

FIGURE 24 Location of sampling wells at the Jabiluka One and Two deposits.

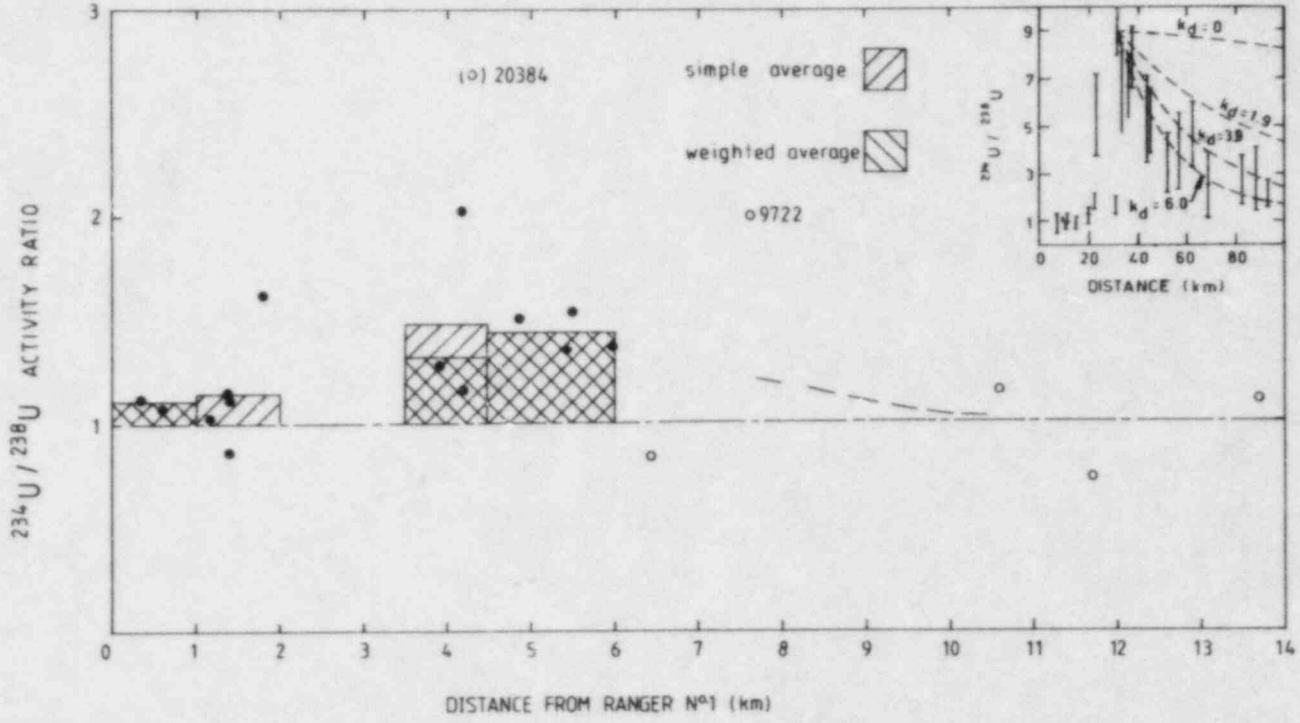

FIGURE 25 Variation with distance from the Ranger One ore body of the $^{234}U/^{238}U$ activity ratios. Where appropriate simple averages and weighted averages are shown.
Insert : Schematic representation of the variation of $^{234}U/^{238}U$ ratios down-gradient from the outcrop of the Carizzo sandstone aquifer, Texas (reference [6], Section 9).

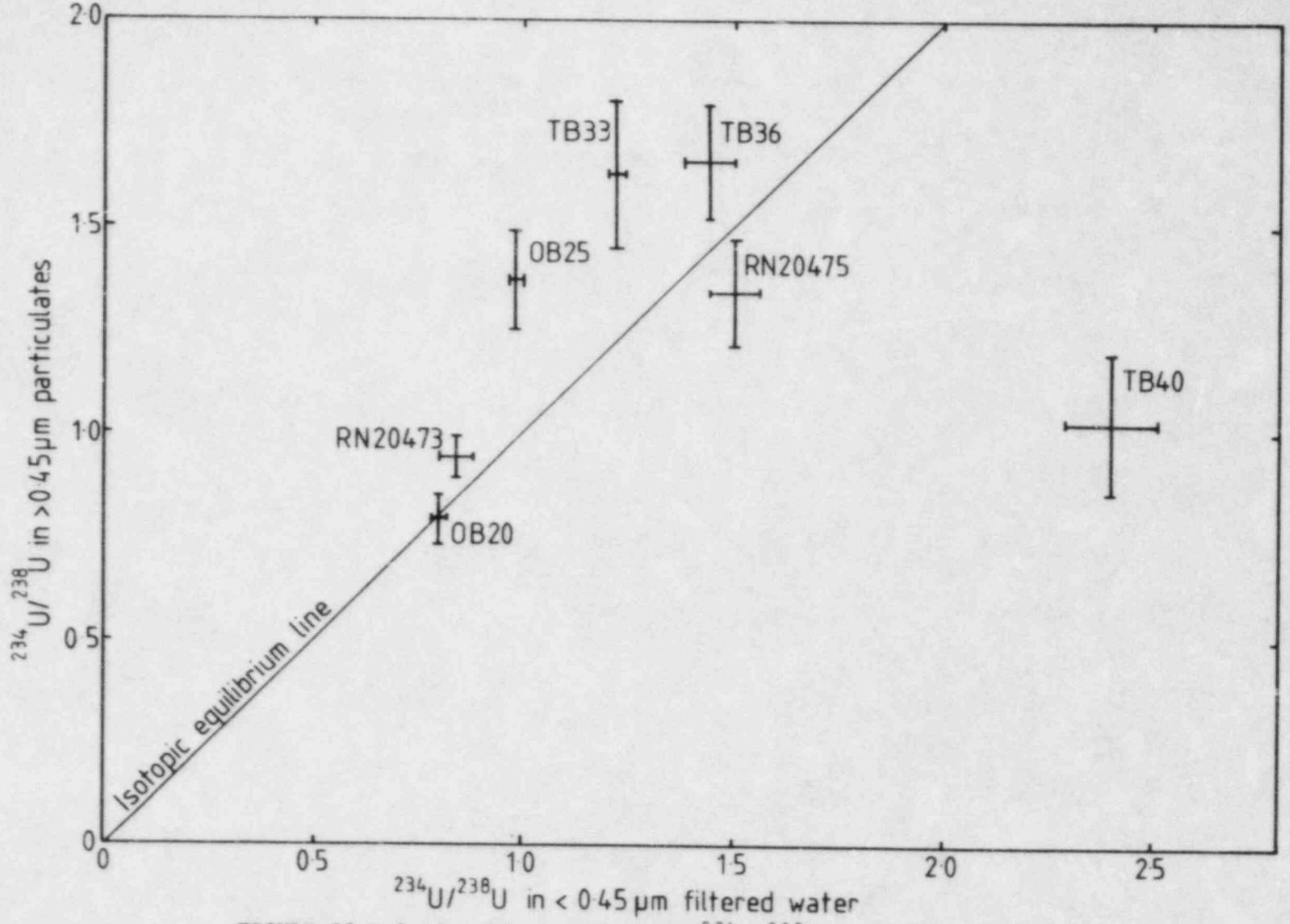

FIGURE 26 Relationship between the $^{234}U/^{238}U$ ratios in particulates and in the groundwater sampled at Nabarlek.

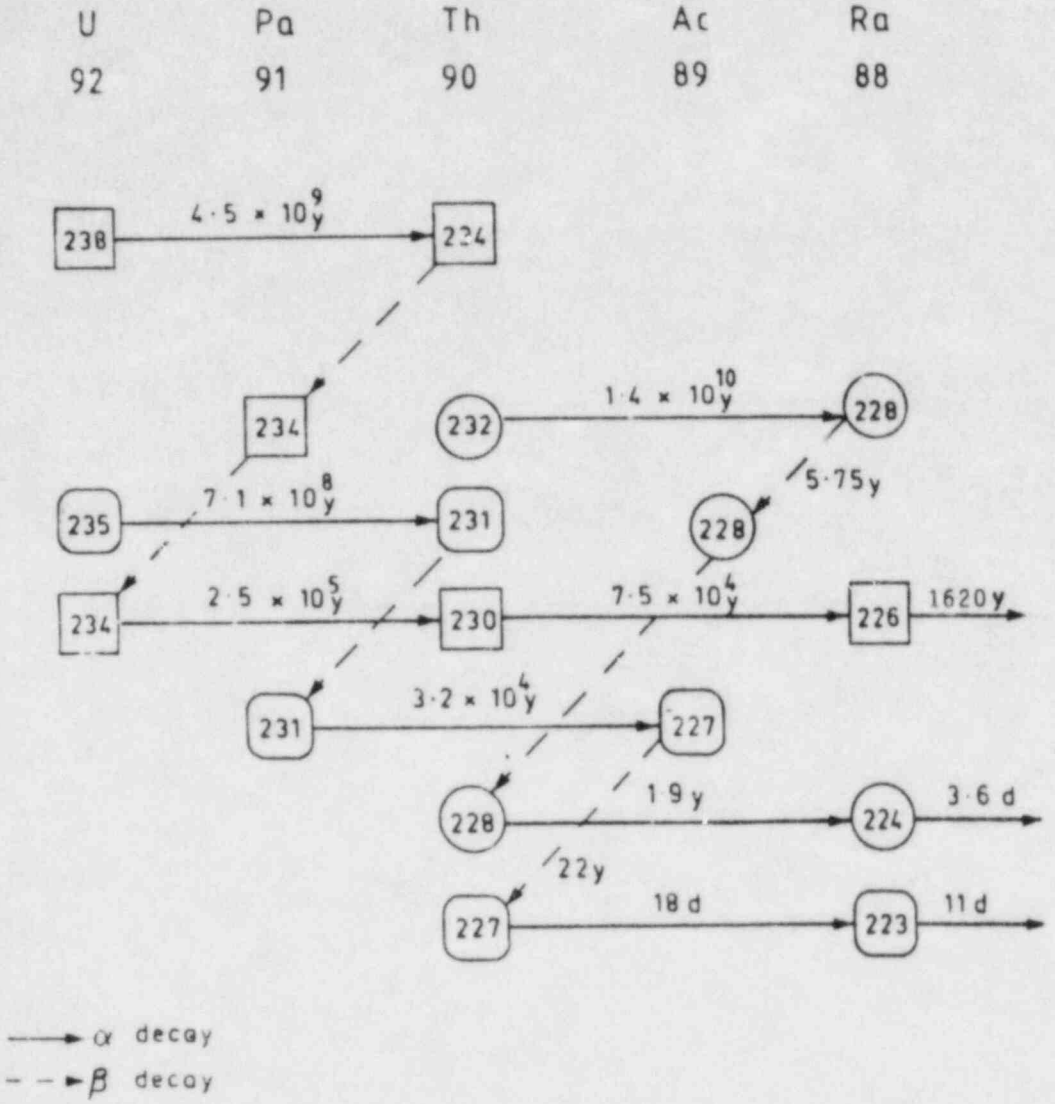

FIGURE 27 Decay series for ^{238}U, ^{235}U and ^{232}Th.

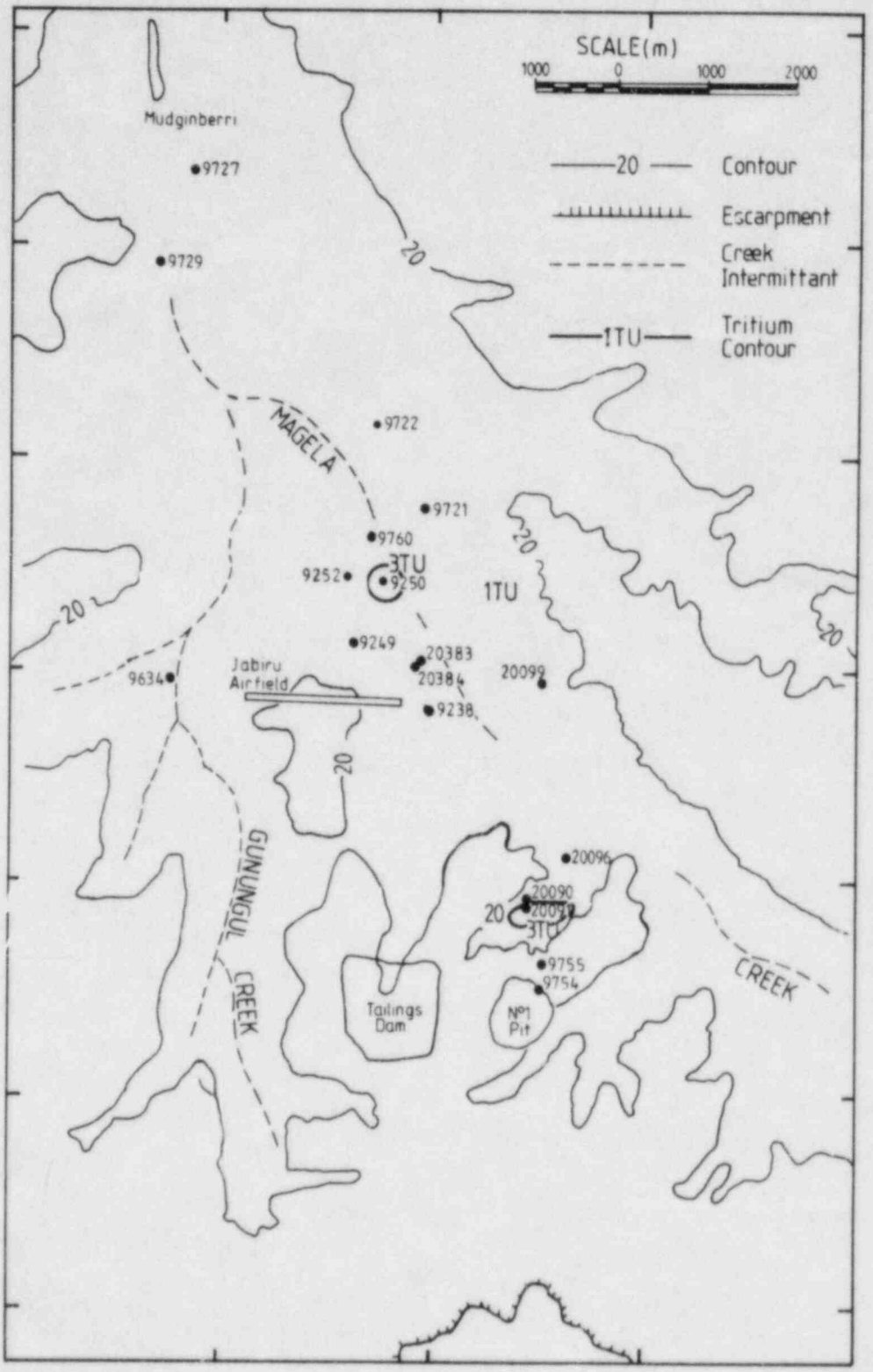

FIGURE 28 Location of the sampling wells. Well locations supplied by the Northern Territory Department of Transport and Works.

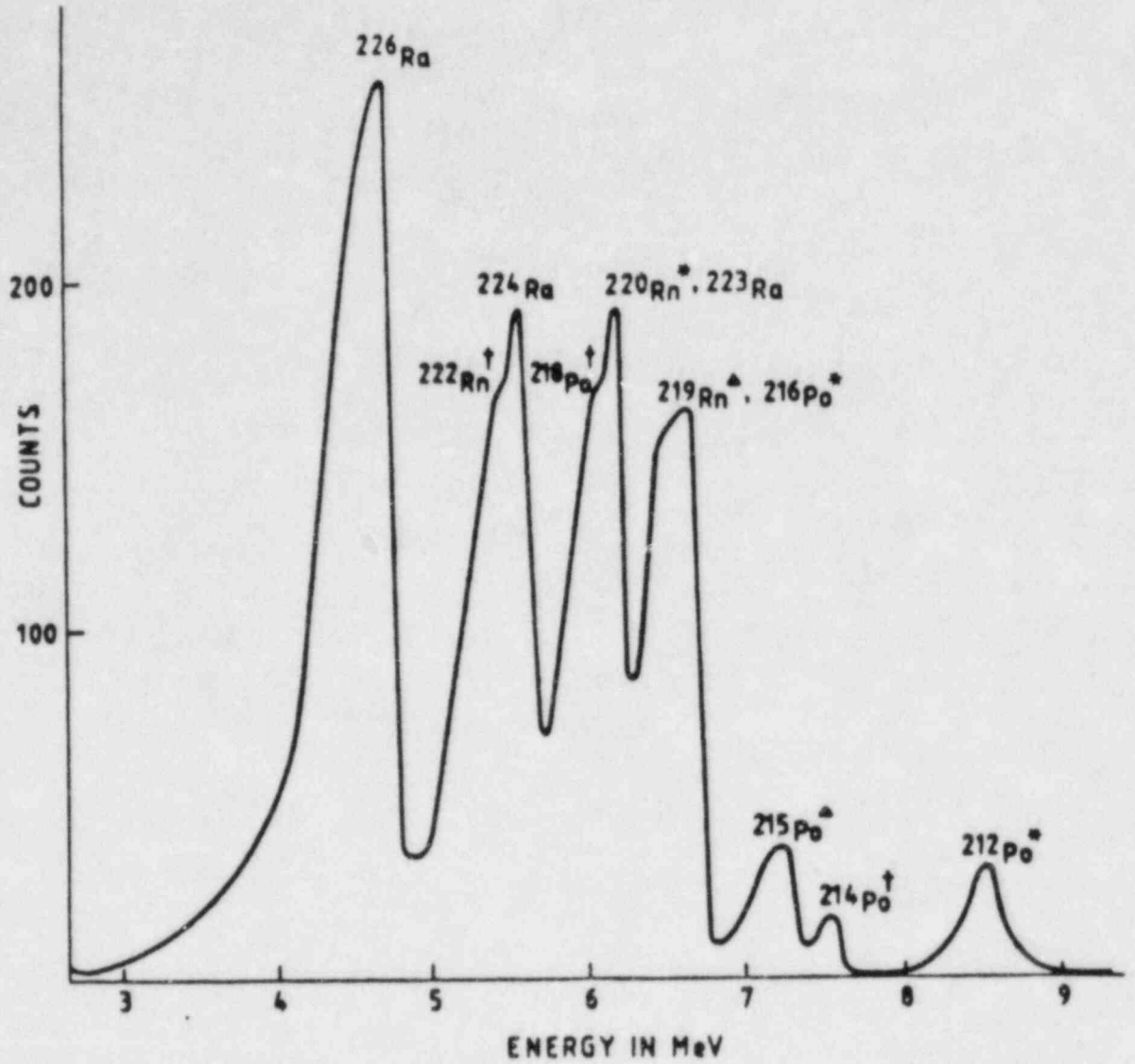

FIGURE 29 An α-particle spectrum of Ra extracted from a groundwater. The daughters of ^{226}Ra and ^{224}Ra grow in during the counting period. These are indicated by † for the daughters of ^{226}Ra, and * for the daughters of ^{224}Ra.

TABLE 1

FOUR-ZONE MODEL OF THE UPPER SEQUENCES OF THE ORE BODIES

Zone	Hydrology	Mineralogy	Comments
I	Unsaturated in the dry season; oscillating table	Oxidized ferricrete or ferruginous zone grading into a mottled zone	Uranium leaching
II	Permanently saturated	Generally corresponds to the pallid zone	Some U deposition
III	Saturated	Transition zone between weathered and unweathered rock; oxidized material; evidence of layering inherited from Cahill formation; in lower region weathering away from pre-existing cracks and fissures observed	Region of some U leaching
IV	Saturated	Unweathered rock from Cahill formation	

TABLE 2

DRILL CORE SAMPLES - ISOTOPIC DATA AND MODEL PARAMETER VALUES -

DRILL HOLE S1/146 - RANGER ONE

Sample			Activity Ratios (observed)				Consistent Parameter Values[1]					
U Concentration ($\mu g\ g^{-1}$)	Depth (m)	Zone (Fig. 4)	$\frac{^{234}U}{^{238}U}$	$\frac{^{230}Th}{^{234}U}$	$\frac{^{226}Ra}{^{230}Th}$[4]	$\frac{^{231}Pa}{^{235}U}$	U Leaching (L) (or Depn) Rate (D) (% per 1000 y) [2]	Time x 1000 (y)	$\frac{^{234}U(o)}{^{238}U(o)}$	$\frac{^{230}Th(o)}{^{234}U(o)}$	R[3]	Rate Erosion (E) or Adv. Weathering Front (W) (m per 1000 y)
51	2.7	I	0.96±0.03	1.76±0.06	0.58±0.02		1.5 (L)	43	0.9	0.9	1.0	0.12 (E)
81	4.0	I	0.75±0.03	3.31±0.13	0.40±0.01		0.8 (L)	87	0.9	0.9	1.0	0.96 (E)
35	9.1	I	0.96±0.03	1.13±0.04	0.81±0.02		0.3 (D)	11	0.9	0.9	1.0	0.02 (E)[5]
378	13.1	II	0.99±0.03	0.90±0.04	0.55±0.08		0.3 (D)	86	0.9	1.2	1.0	0.05 (W)
36	21.0	III	0.68±0.03	1.45±0.08	0.80±0.02		0.6 (L)	171	1.0	1.0	1.5	0.05 (W)

NOTES

(1) A selection only of values is presented. Further development will permit evaluation of all data sets from all samples on a profile.
(2) The rate of leaching (or deposition) is defined by equation (1).
(3) R, the relative rate of leaching (or deposition) of ^{234}U to ^{238}U, is defined by equation (1).
(4) Relative values only are reported.
(5) For samples close to the postulated zone boundary, the parameter values should be considered as a guide only.

TABLE 3

DRILL CORE SAMPLES - ISOTOPIC DATA AND MODEL PARAMETER VALUES -

DRILL HOLE S1/185 - RANGER ONE

Sample			Activity Ratios (observed)				Consistent Parameter Values[1]					
U Concentration ($\mu g\ g^{-1}$)	Depth (m)	Zone (Fig. 4)	$\frac{^{234}U}{^{238}U}$	$\frac{^{230}Th}{^{234}U}$	$\frac{^{226}Ra}{^{230}Th}$[4]	$\frac{^{231}Pa}{^{235}U}$	U Leaching (L) (or Depn) Rate (D) (% per 1000 y) [2]	Time x 1000 (y)	$\frac{^{234}U(o)}{^{238}U(o)}$	$\frac{^{230}Th(o)}{^{234}U(o)}$	R[3]	Rate Erosion (E) or Adv. Weathering Front (W) (m per 1000 y)
47	22.4	III	0.94±0.03	1.07±0.06	0.64±0.01		0.3 (D)	32	1.0	1.0	1.0	0.18 (W)
74	28.0	III	0.91±0.03	1.00±0.06	0.60±0.08		0.3 (D)	22	1.0	1.0	1.0	0.06 (W)
93	30.0	III	0.95±0.04	1.18±0.06	0.62±0.08		0.6 (D)	32	1.0	1.0	1.0	0.02 (W)
35	48.4	IV	0.84±0.03	1.08±0.06			(5)					
10	110.0	IV	0.90±0.08	0.69±0.05	1.55±0.08							
21.7	142.0	IV			0.98±0.03							

NOTES

(1) A selection only of values is presented. Further development will permit evaluation of all data sets from all samples on a profile.

(2) The rate of leaching (or deposition) is defined by equation (1).

(3) R, the relative rate of leaching (or deposition) of ^{234}U to ^{238}U, is defined by equation (1).

(4) Relative values only are reported.

(5) Parameters cannot be deduced for zone IV.

TABLE 4

DRILL CORE SAMPLES - ISOTOPIC DATA AND MODEL PARAMETER VALUES -

DRILL HOLE DH 3 - JABILUKA ONE

Sample			Activity Ratios (observed)				Consistent Parameter Values[1]					
U Concentration ($\mu g\ g^{-1}$)	Depth (m)	Zone (Fig. 4)	$\frac{^{234}U}{^{238}U}$	$\frac{^{230}Th}{^{234}U}$	$\frac{^{226}Ra}{^{230}Th}$[4]	$\frac{^{231}Pa}{^{235}U}$	U Leaching (L) (or Depn) Rate (D) (% per 1000 y) [2]	Time x 1000 (y)	$\frac{^{234}U(o)}{^{238}U(o)}$	$\frac{^{230}Th(o)}{^{234}U(o)}$	R[3]	Rate Erosion (E) or Adv. Weathering Front (W) (m per 1000 y)
6.9	9.3	II	1.01±0.08	0.64±0.05			1.0 (D)	109	0.9	1.2	1.0	0.07 (W)
6.2	11.0	II	0.96±0.05	0.45±0.04			2.0 (L)[5]	171	0.9	1.2	1.0	0.03 (W)
5.0	11.3	II	0.94±0.05	0.68±0.05			2.0 (D)	64	0.9	1.2	1.0	0.05 (W)
2.7	14.0	II	0.92±0.08	0.92±0.05			1.1 (D)	43	0.9	1.2	1.0	0.07 (W)
3.5	20.1	III	0.97±0.05	0.31±0.11			0.0 (D)[5]	43	0.9	1.2	1.0	0.18 (W)
7.8	29.6	III	1.00±0.04	1.07±0.11			0.03 (D)	92	0.9	1.2	1.0	0.009 (W)
524.5	70.5	IV	0.96±0.02	0.84±0.04			[6]					

NOTES

(1) A selection only of values is presented. Further development will permit evaluation of all data sets from all samples on a profile.
(2) The rate of leaching (or deposition) is defined by equation (1).
(3) R, the relative rate of leaching (or deposition) of ^{234}U to ^{238}U, is defined by equation (1).
(4) Relative values only are reported.
(5) This result does not conform to the normal pattern.
(6) Parameters cannot be calculated for zone IV.

TABLE 5

DRILL CORE SAMPLES - ISOTOPIC DATA AND MODEL PARAMETER VALUES -

DRILL HOLE DH 4 - JABILUKA ONE

Sample			Activity Ratios (observed)				Consistent Parameter Values[1]					
U Concentration ($\mu g\ g^{-1}$)	Depth (m)	Zone (Fig. 4)	$\frac{^{234}U}{^{238}U}$	$\frac{^{230}Th}{^{234}U}$	$\frac{^{226}Ra}{^{230}Th}$[4]	$\frac{^{231}Pa}{^{235}U}$	U Leaching (L) (or Depn) Rate (D) (% per 1000 y) [2]	Time x 1000 (y)	$\frac{^{234}U(o)}{^{235}U(o)}$	$\frac{^{230}Th(o)}{^{234}U(o)}$	R[3]	Rate Erosion (E) or Adv. Weathering Front (W) (m per 1000 y)
52.0	9.8	II	1.10±0.07	1.05±0.08			0.3 (D)	107	0.9	1.2	2.0	0.06
6.0	18.6	III	0.96±0.08	1.18±0.15			0.3 (L)	65	1.0	1.0	1.0	0.25
9.2	36.0	IV	0.92±0.05				(5)					
0.7	43.9	IV	0.98±0.09	0.99±0.15								
6.6	61.3	IV	1.10±0.11	0.77±0.08								

NOTES

(1) A selection only of values is presented. Further development will permit evaluation of all data sets from all samples on a profile.
(2) The rate of leaching (or deposition) is defined by equation (1).
(3) R, the relative rate of leaching (or deposition) of ^{234}U to ^{238}U, is defined by equation (1).
(4) Relative values only are reported.
(5) Parameters cannot be calculated for zone IV.

TABLE 6

DRILL CORE SAMPLES - ISOTOPIC DATA AND MODEL PARAMETER VALUES -

DRILL HOLE DH 16 - JABILUKA ONE

Sample			Activity Ratios (observed)				Consistent Parameter Values[1]					
U Concentration ($\mu g\ g^{-1}$)	Depth (m)	Zone (Fig. 4)	$\frac{^{234}U}{^{238}U}$	$\frac{^{230}Th}{^{234}U}$	$\frac{^{226}Ra}{^{230}Th}$[4]	$\frac{^{231}Pa}{^{235}U}$	U Leaching (L) (or Depn) Rate (D) (% per 1000 y) (2)	Time x 1000 (y)	$\frac{^{234}U(o)}{^{238}U(o)}$	$\frac{^{230}Th(o)}{^{234}U(o)}$	R[3]	Rate Erosion (E) or Adv. Weathering Front (W) (m per 1000 y)
1147	4.0	I	1.02±0.06	1.72±0.06			0.15 (L)	43	0.9	0.9	1.0	0.09
1822	8.2	I	0.97±0.01	1.05±0.03			0.3 (D)	22	0.9	0.9	1.0	0.02 (E)
1145	13.1	II	0.93±0.04	0.97±0.04			0.3 (D)	96	0.9	1.2	1.0	0.04 (W)
15	19.5	III	0.99±0.02	0.90±0.04			0.3 (D)	86	1.0	1.0	1.0	0.18 (W)
11.7	25.0	III	1.05±0.05	0.78±0.04			0.3 (D)	86	1.0	1.0	1.0	0.11 (W)
6.9	45.1	IV	1.09±0.09				(6)					
1.7	54.6	IV	0.92±0.06	0.67±0.05								

NOTES
(1) A selection only of values is presented. Further development will permit evaluation of all data sets from all samples on a profile.
(2) The rate of leaching (or deposition) is defined by equation (1).
(3) R, the relative rate of leaching (or deposition) of ^{234}U to ^{238}U, is defined by equation (1).
(4) Relative values only are reported.
(5) The computer program produced no output.
(6) Parameter values cannot be calculated for zone IV.

TABLE 6a

DRILL CORE SAMPLES - ISOTOPIC DATA AND MODEL PARAMETER VALUES -

DRILL HOLE DH 35 - JABILUKA ONE

Sample			Activity Ratios (observed)				Consistent Parameter Values[1]					
U Concentration ($\mu g\ g^{-1}$)	Depth (m)	Zone (Fig. 4)	$\frac{^{234}U}{^{238}U}$	$\frac{^{230}Th}{^{234}U}$	$\frac{^{226}Ra}{^{230}Th}$[4]	$\frac{^{231}Pa}{^{235}U}$	U Leaching (L) (or Depn) Rate (D) (% per 1000 y) (2)	Time x 1000 (y)	$\frac{^{234}U(o)}{^{238}U(o)}$	$\frac{^{230}Th(o)}{^{234}U(o)}$	R[3]	Rate Erosion (E) or Adv. Weathering Front (W) (m per 1000 y)
256	8.2	I	1.08±0.05	0.93±0.04			0.3 (D)	64	0.9	0.9	1.5	0.03 (W)
616	12.5	II	1.06±0.04	0.97±0.04			0.3 (D)	65	0.9	1.2	1.5	0.08 (W)
30.3	20.3	III	1.04±0.06	1.10±0.17			0.3 (L)	65	1.0	1.0	1.0	0.23 (W)
123	25.0	III	1.05±0.03	1.12±0.04			0.3 (L)	43	1.0	1.0	0.5	0.23 (W)
7.6	29.2	III	1.16±0.07	1.07±0.06			(6)					
74.1	45.0	IV	0.85±0.04	1.03±0.05								
5.4	50.0	IV	0.95±0.04	0.76±0.05								

NOTES

(1) A selection only of values is presented. Further development will permit evaluation of all data sets from all samples on a profile.
(2) The rate of leaching (or deposition) is defined by equation (1).
(3) R, the relative rate of leaching (or deposition) of ^{234}U to ^{238}U, is defined by equation (1).
(4) Relative values only are reported.
(5) As there were no samples from the upper (leaching) zone, no attempt could be made to assess mass balance.
(6) Leaching parameters cannot be calculated for zone IV.

TABLE 7

DESCRIPTION OF CORE SAMPLES FROM RANGER ONE S1/146

Depth (m)	Colour	Comments	Zone of the Laterite Profile	Aquifer ystem
2.7	Mottled 80% 10YR 5/6 (dry) red 20% 5YR 5/1 (dry) white	Inhomogeneous - large quartz veins present (3 cm length 0.5 cm wide), matrix easily crushed, no evidence of layering.	Mottled zone of laterite	Shallow upper aquifer system
4.0	Mottled 80% 5Y 8/1 (dry) white 20% 10YR 4/6 (dry) white	Quartz grains 3 mm diameter, matrix easily crushed with fingers, no evidence of layering.	Mottled zone of laterite	
9.1	Slightly mottled 95% 5Y 8/1 (dry) white 5% 10YR 7/8 (dry) white	No quartz grains visible, matrix easily crushed with fingers, no evidence of layering.	Pallid zone of laterite	
13.1	Only ground sample available 2.5 Y 7/6 (dry) yellow	-	Oxidized material	Deep ore body aquifer system
14.6	Slightly mottled 95% 7.5 YR 8/4 (dry) pink 5% Black and green veins	No quartz grains visible, matrix easily crushed with fingers. Some evidence of layering inherited from Cahill formation.	Oxidized material	
19.7	Whole coloured 10YR 8/3 (dry) very pale	Quartz grains 1-2 nm diameter visible. Definite layered structure inherited from Cahill formation visible.	Oxidized material	
21.0	Whole coloured 10Y 6/2 ( ) greenish olive	No quartz grains visible. Well consolidated material showing layer structure of Cahill formation.	Slightly weathered rock	

TABLE 8

NABARLEK DRILL CORE SAMPLES - ISOTOPIC DATA AND MODEL PARAMETER VALUES

Sample				Activity Ratios (measured)				Consistent Parameter Values					
Sample	U Concentration ($\mu g\ g^{-1}$)	Depth (m)	Zone (Fig. 4)	$\frac{^{234}U}{^{238}U}$	$\frac{^{230}Th}{^{234}U}$	$\frac{^{226}Ra}{^{230}Th}$	$\frac{^{231}Pa}{^{235}U}$	U Leaching (L) (or Depn) Rate (D) (% per 1000 y)	Time x 1000 (y)	$\frac{^{234}U(o)}{^{238}U(o)}$ *	$\frac{^{230}Th(o)}{^{234}U(o)}$ *	R †	Rate Erosion (E) or Adv. Weathering Front (W) (m per 1000 y)
52/A	640	0.44	I	1.09	1.12	0.93		2.1 (L)	11	1.0	0.7	1.0	0.06 E
B	1310	1.78	II	1.00	0.83	0.99		0.3 (D)	98	1.0	1.0	1.0	0.08 W
C	6440	3.56	II	0.98	0.51	0.86		0.3 (D)	87	1.0	1.0	1.0	0.08 W
D	6800	7.10	II	1.10	0.71	1.12		0.3 (D)	43	1.0	1.0	1.0	0.08 W
E	970	10.2	II	1.03	0.82	1.12		0.3 (D)	43	1.0	1.0	1.0	~0.02 W
145/F	460	0.67	I	1.02	1.14	1.21		2.1 (L)	22	1.0	0.7	1.0	0.05 E
G	730	1.78	II	1.00	0.97	1.15		0.3 (D)	43	1.0	1.0	1.0	
A-2/H	180	0.44	I	1.01	2.53	1.24		2.5 (L)	39	1.0	0.7	1.0	0.04 E
A3/I	90	0.66	I	1.00	1.84	1.71		2.1 (L)	32	1.0	0.7	1.0	0.03 E
71/J	990	0.10	I	1.12	2.25	0.88		2.4 (L)	33	1.0	0.7	1.0	0.05 E
K	1040	0.32	I	1.05	2.85			1.5 (L)	54	1.0	0.7	1.0	0.03 E
L	7360	2.01	II	1.00	1.00	0.92		0	108	1.0	1.0	1.0	0.08 W
M	14100	5.51	II	1.02	0.92	1.01		0	65	1.0	1.0	1.0	0.08 W
N	400	9.75	II	1.11	0.82	1.16		0.3 (D)	65	1.0	1.0	1.0	0.01 W
O	1190	12.5	III	1.03	0.97	1.04							
P	1380	13.6	III	0.98	0.76	1.37							

(Continued)

TABLE 8 (Continued)

Sample				Activity Ratios (measured)				Consistent Parameter Values					
Sample	U Concentration ($\mu g\ g^{-1}$)	Depth (m)	Zone (Fig. 4)	$\frac{^{234}U}{^{238}U}$	$\frac{^{230}Th}{^{234}U}$	$\frac{^{226}Ra}{^{230}Th}$	$\frac{^{231}Pa}{^{235}U}$	U Leaching (L) (or Depn) Rate (D) (% per 1000 y)	Time x 1000 (y)	$\frac{^{234}U(o)}{^{238}U(o)}$ *	$\frac{^{230}Th(o)}{^{234}U(o)}$ *	R †	Rate Erosion (E) or Adv. Weathering Front (W) (m per 1000 y)
231/FA	45600	10.0	II	0.98	1.01	0.94		0	43	1.0	1.0	1.0	0.01 W
35/Q	7120	11.0	III	1.00	0.94	1.16							
R	1430	16.3	IV	1.09	0.84	1.45							
229/S	1670	0.42	I	1.11	1.18	0.98		2.1 (L)	21	1.0	0.7	1.0	0.06 E
T	1400	1.28	I	1.07	0.82	1.11		1.8 (L)	11	1.0	0.7	1.0	0.04 E
U	420	2.97	II	0.95	0.72	1.16							
72/V	8610	25.0	IV	0.80	1.13	1.02							
91/W	2080	0.05	I	1.15	1.02	1.18		1.2 (L)	21	1.0	0.7	1.0	0.08 E
X	11060	1.67	I	1.01	1.00	0.97		2.1 (L)	11	1.0	0.7	1.0	<0.01 E
Y	1950	10.9	III	1.17	1.13	0.88							
255/Z	260	1.76	I	1.17	1.26	0.69							
AA	5630	5.87	II	0.88	1.04	1.61		0	65	1.0	1.0	1.0	0.07 W
BB	1350	13.7	III	0.91	1.01	0.94							
CC	220	14.7	III	0.83	0.94	1.85							
36/DD	83200	11.4	III	1.02	0.97								
EE	18500	15.1	III	0.66	1.01	1.06							

* $^{234}U(o)/^{238}U(o)$ and $^{230}Th(o)/^{234}U(o)$ are the initial values of the respective ratios, i.e. the value before the evolution of the zone in question (column 4).

† R is the $^{234}U/^{238}U$ activity ratio in the transporting medium (infiltrating water).

TABLE 9

COMPUTATION OF VERTICAL URANIUM FLUX

Sample	Depth (m)	Zone	U Conc. (av.) ($\mu g\ g^{-1}$)	Leaching (L) Deposition (D) Rate (% per 1000 y)	Total leaching (L) Deposition (D) ($mg\ y^{-1}\ m^{-2}$)
52/	0	I	640	2.1 (L)	15.4 (L)
A	0.44	I	975	0.3 (D)	10.6 (D)
B	1.78	II	3875	0.3 (D)	54.3 (D)
C	3.56	II	6660	0.3 (D)	186 (D)
D	7.10	II	3925	0.3 (D)	95 (D)
E	10.2				
71/	0	I	990	2.4 (L)	6.2 (L)
J	0.1	I	1015	1.5 (L)	7.9 (L)
K	0.32	II	4200	0	0
L	2.01	II	10730	0	0
M	5.51	II	7250	0.3 (D)	238 (D)
N	9.75	III	795	*	
O	12.5	III	1285	*	
P	13.6				
91/	0	I	2080	1.2 (L)	3.2 (L)
W	0.05	I	6570		
X	1.67	II	1950	*	
Y	10.9				

TABLE 10

MINERALOGY OF JABILUKA ONE DH 3

Sample	% Quartz	>2 µm Fraction						Other Minerals
		Chlorite	Mica	Vermiculite	Smectite	Kaolinite	Goethite	
11.0 R	55							
11.3 S	50	30	50	10	15	?	-	
14.0 S	70	50	30	10	10	?	2	
20.1 S	50	30	70[I]	-	-	-	-	
29.6 R	45	✓	✓	-	-	-	-	
70.5 S	60	100	-	-	-	-	-	

TABLE 11

MINERALOGY OF JABILUKA ONE DH 16

Sample	% Quartz	>2 µm Fraction						Other Minerals
		Chlorite	Mica	Vermiculite	Smectite	Kaolinite	Goethite	
4.0 S	30	25	20	5	20	25	2	
8.2 R	60							
13.1 R	90							
19.5 S	35	100	-	-	-	-	-	Anatase
45.1 R	40	✓	✓	-	-	-	-	Pyrite
54.6 S	45	50	50[I]	-	-	-	-	

S - sample investigated using sedimented aggregates and random powders.
R - sample investigated as random powder.
I - interstratified material pr sent.
✓ - present.
? - may be present.

TABLE 12

MINERALOGY OF RANGER ONE S1/146

Sample	% Quartz	>2 µm Fraction						Other Minerals
		Chlorite	Mica	Vermiculite	Smectite	Kaolinite	Goethite	
2.7 S	35	-	5	-	25	70	0	Hematite (Anatase)
4.0 S	10	-	10	-	40	50	L	Anatase (Hematite)
9.1 S	30	-	10	-	50	40	L	Anatase
13.1 S	50	-	40	-	25	30	10	Anatase
21.0 S	60	60	25	15	-	-	-	

S - sample investigated using sedimented aggregates and random powders.
R - sample investigated as random powder.
I - interstratified material present.
✓ - present.
L - present in low concentration.
? - may be present.

TABLE 13

COLOUR AND IRON MINERALOGY OF CORE SAMPLES FROM

RANGER ONE S1/146

Depth (m)	Colour	Hematite	Goethite	Magnetic Component (%)
2.7	Red	Present	?	0.5
4.0	White	Low	?	0.6
9.1	White	n.d.	Low	2.0
13.1	Yellow	n.d.	Present	1.0

n.d. - not detectable.

? - may be present in low levels.

TABLE 14

S1/146 : DEPTH 2.7 m : URANIUM (^{238}U) AND THORIUM (^{230}Th)

EXTRACTIONS AND ASSOCIATED ISOTOPE ACTIVITY RATIOS

Extractant	% ^{238}U	$^{234}U/^{238}U$	% ^{230}Th	$^{230}Th/^{234}U$
0.1 M NH_4Cl (24-hour shake)	1.3±0.1	1.27±0.08	<0.2	n.d.
Acid oxalate (4 hours in dark)	24.6±0.9	0.98±0.03	20.1±1.4	.31±0.09
CDB-2 extracts (½ hour; 80°C)	46.1±1.0	0.99±0.08	61.0±2.6	2.15±0.23
5% Na_2CO_3 (16-hour shake)	1.0±0.2	1.00±0.15	<0.2	n.d.
$HNO_3/HF/HClO_4$ digestion + Na_2O_2 fusion	26.9±0.5	1.78±0.08	18.9±0.6	1.56±0.14

All errors quoted are one standard deviation.

n.d. - not determined.

TABLE 15

S1/146 : DEPTH 4.0 m : URANIUM (^{238}U) AND THORIUM (^{230}Th) EXTRACTIONS AND ASSOCIATED ISOTOPE ACTIVITY RATIOS

Extractant	% ^{238}U	$^{234}U/^{238}U$	% ^{230}Th	$^{230}Th/^{234}U$
0.1 M NH_4Cl (24-hour shake)	0.8±0.1	1.17±0.12	<0.2	n.d.
Acid oxalate (4 hours in dark)	24.4±1.0	1.14±0.04	44.1±4.2	4.74±0.46
CDB-2 extracts (½ hour; 80°C)	21.9±0.4	0.96±0.04	32.4±1.9	1.92±0.10
5% Na_2CO_3 (16-hour shake)	2.4±0.2	0.95±0.11	<0.2	n.d.
$HNO_3/HF/HClO_4$ digestion + Na_2O_2 fusion	50.5±1.6	1.32±0.04	23.6±1.7	1.73±0.17

All errors quoted are one standard deviation.

n.d. - not determined.

TABLE 16

S1/146 : DEPTH 9.1 m : URANIUM (^{238}U) AND THORIUM (^{230}Th) EXTRACTIONS AND ASSOCIATED ISOTOPE ACTIVITY RATIOS

Extractant	% ^{238}U	$^{234}U/^{238}U$	% ^{230}Th	$^{230}Th/^{234}U$
0.1 M NH_4Cl (24-hour shake)	<0.2	n.d.	<0.2	n.d.
Acid oxalate (4 hours in dark)	29.2±0.6	0.80±0.02	12.2±0.8	0.75±0.04
CDB-2 extracts (½ hour; 80°C)	41.3±0.5	1.08±0.07	61.8±3.4	2.17±0.17
5% Na_2CO_3 (16-hour shake)	0.2	n.d.	0.2	n.d.
$HNO_3/HF/HClO_4$ digestion + Na_2O_2 fusion	29.6±3.6	1.27±0.07	26.0±1.5	1.85±0.14

All errors quoted are one standard deviation.

n.d. - not determined.

TABLE 17

S1/146 : DEPTH 13.1 m : URANIUM (^{238}U) AND THORIUM (^{230}Th)

EXTRACTIONS AND ASSOCIATED ISOTOPE ACTIVITY RATIOS

Extractant	% ^{238}U	$^{234}U/^{238}U$	% ^{230}Th	$^{230}Th/^{234}U$
0.1 M NH_4Cl (24-hour shake)	<0.2	n.d.	<0.2	n.d.
Acid oxalate (4 hours in dark)	61.3±3.7	0.67±0.02	10.8±0.2	0.37±0.02
CDB-2 extracts (½ hour; 80°C)	36.8±1.8	1.21±0.06	83.1±2.9	2.85±0.17
5% Na_2CO_3 (16-hour shake)	<0.2	n.d.	2.4±0.2	n.d.
$HNO_3/HF/HClO_4$ digestion	1.9±0.1	2.15±0.12	3.7±0.2	1.26±0.11

TABLE 18

REPRODUCIBILITY : DUPLICATION OF SOME EXTRACTIONS TO VERIFY REPRODUCIBILITY OF THE TECHNIQUE

Extract	Depth (m)	% ^{238}U	$^{234}U/^{238}U$
0.1 M NH_4Cl	4.0	0.6±0.04	0.95±0.08
(24-hour shake)	4.0	0.8±0.1	1.17±0.12
CDB-1st extract	4.0	16.3±0.4	0.95±0.02
(½ hour; 80°C)	4.0	15.7±1.0	0.87±0.04
CDB-1st extract	13.1	30.4±0.6	1.20±0.05
(½ hour; 80°C)	13.1	33.5±1.6	1.17±0.03

All errors quoted are one standard deviation.

TABLE 19

A MASS BALANCE : COMPARISON OF TOTAL ^{238}U OBTAINED BY SUMMATION OF ALPHA SPECTROMETRIC ASSAYS OF ALL EXTRACTS AND BY DELAYED NEUTRON ACTIVATION (DNA) ANALYSIS OF WHOLE SAMPLE (RANGER ONE S1/146 PROFILE)

Depth (m)	^{238}U all extracts ($\mu g\ g^{-1}$)	^{238}U by DNA ($\mu g\ g^{-1}$)
2.7	47.2	51.3
4.0	84.3	81.1
9.1	35.6	35.6
13.1	352	378

TABLE 20

^{226}Ra LEVELS AND $^{226}Ra/^{230}Th$ ACTIVITY RATIOS IN PHASES SEPARATED FROM S1/146 RANGER ONE

Depth (m)	Total Uranium ($\mu g\ g^{-1}$)	Clay/Quartz		Other Phases (predominantly Fe)	
		^{226}Ra ($dpm\ g^{-1}$)	$^{226}Ra/^{230}Th$	^{226}Ra ($dpm\ g^{-1}$)	$^{226}Ra/^{230}Th$
2.7	47.2	38.7	1.47	26.8	0.33
4.0	84.3	74.3	1.03	36.3	0.33
9.1	35.6	43.0	2.31	<1	<0.03
13.1	352	74.7	5.5	173.4	0.42

TABLE 21

SYNTHETIC GROUNDWATER COMPOSITION

JABIRU[(a)]

Component	Concentration ($mg\ L^{-1}$)
SiO_2	38.7± 4.5
Na^+	11.5± 1.8
K^+	3.2± 0.6
Ca^{2+}	11.5± 1.6
Mg^{2+}	16.8± 2.4
Cl^-	9.5± 1.6
SO_4^{2-}	4.2± 0.9
HCO_3	143.0±12.0

(a) Uncertainties quoted to a 95% confidence level.

TABLE 22

LONG-TERM LEACHING EXPERIMENTS

Sample : 13.1 m S1/146, Ranger One
Solution oxidizing, pH 5.5
Weight of sample : 0.5 g
Sample preparation : crushed to -100 BS
Added ^{236}U : 6 aliquots of 150 dpm
Uranium content : 378 µg g^{-1}, i.e. 189 µg or 142 dpm
$^{234}U/^{238}U$ ratio : 0.99±0.03

Day	Isotope	Activity Solution (dpm)	Activity Ore (dpm)	K_d *
1	^{238}U			$>10^4$
	^{236}U			$>10^4$
	^{234}U			$>10^4$
26	^{238}U	0.043	142	3.3×10^3
	^{236}U	0.01	900	9×10^4
	^{234}U	0.047	141	3×10^3

* See text for definition of K_d.

dpm - disintegrations per minute

TABLE 23

FOURTEEN DAY LEACHING/ADSORPTION EXPERIMENTS

Sample : 4.0 S1/146, Ranger One
Mass of sample : 2.00 g
Volume of aqueous phase : 100 mL
Sample preparation : crushed to -100 BS with rotary mill
Uranium content : 84.3 $\mu g\ g^{-1}$
$^{234}U/^{238}U$ activity ratio : 1.19±0.04

Experimental Conditions (1)	^{236}U:K_d of (2) Adsorption	U:K_d of (2) Desorption (3)	$\frac{K_d(^{236}U)}{K_d(^{238}U)}$ (2)
pH 5.5, oxidizing	2.2×10^3	9.9×10^3	0.22
pH 5.5, reducing	4.0×10^3	3×10^4	0.13
pH 8.5, oxidizing	4.2×10^3	2×10^4	0.21
pH 8.5, reducing	8.1×10^3	7×10^4	0.11

(1) See section 7.2.1.

(2) See text for definition of K_d.

(3) Values are rounded to one significant figure if the standard deviation associated with measurements exceeds 10%.

TABLE 24

THE EFFECT OF α-RECOIL ON RADIUM ADSORPTION COEFFICIENTS

Volume of suspensions - 100 mL
Total ^{226}Ra added to each suspension - 4700 dpm
Total ^{228}Th added to each suspension - 4736 dpm
pH - 7.5

Suspension	Loading ($mg\ mL^{-1}$)	% Activity in 'Solution' (1)(2)			$\rho = \frac{K_d}{K_d^r}$ (3) (eqn 18)	ϕ_a
		^{226}Ra	^{228}Th	^{224}Ra		
montmorillinite (4)	119	4.6	2.4	2.4	2.0	0.5
illite	103	15	14	7.5	2.0	0.5
kaolinite	137	1.5	0.7	0.7	2.0	0.5

(1) The ^{226}Ra, ^{228}Th solutions in this experiment were added on 15 September; the $^{224}Ra/^{226}Ra$ assay was undertaken between 30 September and 11 October 1982.

(2) Dissolved, i.e. 'non-filterable' activity, was estimated by passing a 1 mL aliquot through a 0.22 μm membrane filter.

(3) The values of ρ are slight underestimates, as no attempt has been made to correct for the small fraction of ^{224}Ra formed from the dissolved ^{228}Th.

(4) Sodium forms of the clays were prepared.

dpm = disintegrations per minute.

TABLE 25

URANIUM SERIES DISEQUILIBRIA WITHIN JABILUKA TWO ORE BODY

Sample	Depth (m)	U (µg/g)	$^{226}Ra/^{238}U$	$^{234}U/^{238}U$	$^{230}Th/^{234}U$	$^{231}Pa/^{235}U$
V152/V2	60.5	6.83	3.68±0.24			
	81.1	2.64	8.00±0.96			
	99.0	5.34	5.32±0.42			
	117.6	6.51	7.04±0.35			
	138.2	13.40	3.30±0.16			
	150.5	9.79	5.79±0.29			
W/147/V	65.3	22.89	1.77±0.07			
	87.9	2451.3	1.30±0.01	1.00	0.68±0.04	
	110.0	21.25	6.87±0.25			
	130.2	5.05	5.81±0.47			
	148.5	1768.5	1.20±0.01	1.00	0.74±0.04	
	172.0	108.0	1.15±0.01			
W/141/V2	75.9	3.92				
	91.8	7.30				
	103.8	4.64	6.25±0.50			
	118.9	52.81	1.13±0.03			
	137.0	1269.5	0.97±0.01			
	149.7	4424.4	1.03±0.01			

TABLE 26

NABARLEK GROUNDWATER - CHEMICAL COMPOSITION

Sample	Sample (Date)	T (°C)	pH	Na ($mg\ L^{-1}$)	K ($mg\ L^{-1}$)	Ca ($mg\ L^{-1}$)	Mg ($mg\ L^{-1}$)	Fe ($mg\ L^{-1}$)	H_2CO_3 ($mg\ L^{-1}$)	HCO_3^- ($mg\ L^{-1}$)	Cl ($mg\ L^{-1}$)	SO_4 ($mg\ L^{-1}$)	PO_4 ($mg\ L^{-1}$)	SiO_2 ($mg\ L^{-1}$)	F ($mg\ L^{-1}$)
OB 19	15.9.82	33.2	6.75	16.9	1.5	5.4	79	0.02		358.5	115.7	1.20	0.41	23	1.0
OB 20	15.9.82	32.8	6.70	10.5	1.0	6.6	55	0.02		241.9	65.1	1.72	0.02	33	0.5
OB 21	15.9.82	31.0	6.25	10.8	1.12	8.5	50	0.077		241.4	171.2	1.72	0.02	40	0.5
OB 25	16.9.82	33.9	6.90	11.2	2.3	12.0	49	0.02		243.0	844.0	1.72	0.02	39	0.5
TB 33	16.9.82	32.0	7.00	12.7	1.2	11.6	33	0.02		379.3	67.5	1.80	0.02	39	0.5
TB 36	16.9.82	31.6	6.85	9.9	0.93	5.0	55	0.02		229.4	44.4	0.2	0.02	35	0.5
TB 40	15.9.82	32.0	6.95	14.4	0.67	10.5	58	0.77		275.5	62.7	1.72	0.095	43	0.5
20473	16.9.82	33.2	6.40	5.5	1.4	4.7	29	0.02		98.9	53.0	21.96	0.02	39	0.5
20475	16.9.82	33.2	6.95	9.8	1.5	12.2	40	0.02		202.8	41.0	0.2	0.02	45	0.5

TABLE 27

NABARLEK GROUNDWATER - ISOTOPIC DATA

Bore No.	Tritium (TU)*	D/H	^{14}C (% mod. C)	[U] ($\mu g\ L^{-1}$)	$^{234}U/^{238}U$	$^{230}Th/^{234}U$
OB 19	1.5±0.4	-37.5±0.8	85.1±0.5	7.13±0.32	1.05±0.05	
OB 20	2.7±0.4	-37.9±0.5	96.5±0.7	77.3±2.6	0.80±0.017	< 0.0045
OB 25	0.8±0.4	-38.9±0.5	84.9±0.9	6.96±0.14	0.97±0.021	
OB 21	1.7±0.4	-35.5±0.7	96.9±0.8	0.61±0.032	0.97±0.09	< 0.06
TB 36	1.8±0.3	-34.8±0.6	87.3±0.7	0.72±0.032	1.44±0.06	< 0.02
TB 33	1.7±0.3	-32.7±0.5	99.3±0.7	1.81±0.05	1.22±0.023	0.04±0.02
TB 40	1.7±0.3	-34.8±0.4	85.4±0.7	0.74±0.03	2.40±0.11	0.02±0.01
RN20475	0.7±0.3	-38.6±0.5	87.5±1.0	0.16±0.01	1.50±0.06	
RN20473	1.2±0.3		138.5±1.2	4.11±0.17	0.84±0.04	0.014±0.003

* By definition, 1 TU is the ratio of 1 tritium atom per 10^{18} hydrogen atoms.

TABLE 28

KOONGARRA GROUNDWATER - ISOTOPIC DATA

Well No.	Tritium (TU)	D/H	[U] ($\mu g\ L^{-1}$)	$^{234}U/^{238}U$	$^{230}Th/^{234}U$
PH 78	*	-34.8±0.4	0.41±0.02	0.76±0.07	<0.06
PH 27	1.4±0.4	-34.8±0.4	1.30±0.03	1.02±0.03	0.05±0.01
PH 73	*	-33.2±0.3	4.34±0.14	0.78±0.03	
PH 49	0.9±0.4	-37.1±0.7	55.8±1.7	0.99±0.09	
PH 14	0.6±0.4	-36.3±0.4	29.1±1.4	0.74±0.04	0.55±0.10
PH 7	0.8±0.4	-33.5±0.3	62.3±1.1	0.65±0.02	<0.0025
PH 55	0.9±0.4	-34.1±1.2	14.9±0.04	0.74±0.04	0.05±0.01
PH 94	4.7±0.5	-30.5±0.8	1.66±0.07	0.82±0.06	
KTD 1	2.3±0.4	-32.0±0.4	0.9±0.5	> 1	0.7±0.07
KD1	1.0±0.4	-36.0±0.5	0.085±0.006	1.42±0.20	

* Samples broken in transit.

TABLE 29

JABILUKA GROUNDWATER - ISOTOPIC DATA

Well No.	Tritium (TU)	D/H	[U] ($\mu g\ L^{-1}$)	$^{234}U/^{238}U$	$^{230}Th/^{234}U$
170	2.2±0.4	-31.1±0.5			
DH 237	0.7±0.3	-35.0±1.3			
101	1.5±0.3	-35.2±1.0	0.30±0.02	1.27±0.06	
V/153/V2	1.0±0.4	-33.6±0.6	3.60±0.19	1.17±0.05	
W/111/V	0.4±0.4	-34.8±0.2	0.401±0.018	2.00±0.08	
120	0.5±0.4	-37.4±0.1	0.23±0.014	3.67±0.16	

TABLE 30

DISTRIBUTION OF URANIUM AND THORIUM BETWEEN NABARLEK GROUNDWATER AND PARTICULATES

Location (Bore No.)	Uranium $\mu g\ L^{-1}$ in <0.45 µm filtered water	$^{234}U/^{238}U$ in <0.45 µm filtered water	$^{230}Th/^{234}U$ in <0.45 µm filtered water	Uranium $\mu g\ L^{-1}$ in >0.45 µm particulates	$^{234}U/^{238}U$ in >0.45 µm particulates	$^{230}Th/^{234}U$ in >0.45 µm particulates	^{238}U in >0.45 µm/ ^{238}U in <0.45 µm	^{230}Th in >0.5 µm/ ^{230}Th in <0.5 µm	K_d
OB 19	7.13±0.32	1.05±0.05	BDL	ND	ND	ND	ND	-	-
OB 20	77.32±2.6	0.80±0.02	<0.0045	2374±51	0.79±0.06	0.75±0.10	3.05×10^{-2}	>5.7	0.15
OB 21	0.61±0.03	0.97±0.09	<0.06	ND	ND	ND	ND	-	-
OB 25	6.96±0.14	0.97±0.02	BDL	54.5±3.3	1.37±0.12	0.25±0.04	0.78×10^{-2}	>2.8*	0.7
TB 33	1.81±0.05	1.22±0.02	0.04±0.02	57.7±11.5	1.63±0.18	TBD	3.2×10^{-2}	-	3
TB 36	0.72±0.03	1.44±0.06	<0.02	27.5±1.6	1.66±0.14	0.11±0.02	3.8×10^{-2}	>0.22	4
TB 40	0.74±0.03	2.40±0.11	0.02±0.01	69.9±3.9	1.02±0.17	1.04±0.19	9.4×10^{-2}	>2	1.4
RN 20473	4.11±0.17	0.84±0.04	0.014±0.003	189±7	0.94±0.05	0.42±0.11	4.6×10^{-2}	>1.5	5
RN 20475	0.16±0.01	1.50±0.06	BDL	17.7±1.0	1.34±0.13	0.39±0.14	11.3×10^{-2}	>3.9*	10

BDL = Below Detection Limit

ND = Not Determined

TBD = Yet to Be Determined

* Assume DL 0.01

TABLE 31

REDISTRIBUTION OF RADIUM IN DRILL HOLES S1/146 AND S1/185, RANGER ONE

Drill Hole	Depth (m)	U ($\mu g\ g^{-1}$)	$^{226}Ra/^{230}Th$	U_{eq}/U	Ra Leaching L (or Deposition D) x 10^{-13} g/g ore per 1000 y	Rel. Leaching L (or Deposition D) Rate (% per 1000 y)	
						Ra	U
S1/146	2.7	51.3	1.07	1.73	8.8	5 D	0.8 L
	4.0	81.1	0.74	1.84	56.5	19 L	0.8 L
	9.1	35.6	1.52	1.64	85.5	67 D	0.6 L
	13.1	378	1.03	0.89	15.2	1.1 D	0.6 D
	21.0	36.5	1.50	1.47	39.4	30 D	0.3 L
S1/185	22	46.8	1.20	1.21	16.5	10 D	0.3 L
	28	74.3	1.12	1.02	13.2	5 D	0.3 L
	30	93.4	1.16	1.28	28.4	8 D	0.6 L
	48	34.9	1.29	1.23	17.3	14 D	
	110	10.4	2.90	2.39	49.9	135 D	
	142	21.7	1.84	1.51			

TABLE 32

RADIUM DISEQUILIBRIA, DRILL HOLES S1/149 (RANGER ONE)

AND S3/32 (RANGER THREE)

Drill Hole	Depth (m)	U ($\mu g\ g^{-1}$)	^{226}Ra (dpm g^{-1})	U_{eq}/U
S1/149	0.0	679	1172.3	1.30
	3.0	107	554.2	3.88
	6.0	793	1124.1	1.06
	9.0	1465	1525.6	0.78
	10.0	2008	2784.3	1.04
	11.0		33184.7	
	14.7	1028	1396.4	1.02
	15.7	2642	3529.8	1.00
	18.2	759	1099.1	1.09
	21.0		52435.5	
	21.6	15352		
	25.0	873	3746.7	3.22
S3/32	0.0	41.6	67.92	2.18
	2.0	191.5	124.0	0.86
	3.0	17.1	22.9	1.79
	3.4	152.7	107.9	0.94
	4.0	28.1	32.5	1.54

dpm = disintegrations per minute

TABLE 33

REDISTRIBUTION OF RADIUM IN DRILL HOLES DH 3, DH 4, DH 8, DH 16 AND DH 35

JABILUKA ONE

Drill Hole	Depth (m)	U ($\mu g\ g^{-1}$)	$^{226}Ra/^{230}Th$	U_{eq}/U	Ra Leaching L (or Deposition D) x 10^{-13} g g^{-1} ore per 1000 y	Rel. Leaching L (or Deposition D) rate (% per 1000 y)	
						Ra*	U+
DH 3	9.3	6.9	5.22	3.51	142	568 L	1.1 D
	11.0	6.2	5.03	1.63	77	352 D	2.5 L
	11.3	5.0	4.28	2.82	65	360 D	1.1 D
	14.0	2.7	9.20	7.97		2546 D	1.1 D
	15.6	3.2	10.45	7.15			
	20.1	3.5	10.03	7.09		1061 D	0.1 D
	29.6	7.8	3.04	3.31		286 D	0.1 L
	70.5	524	2.25	1.84		92 D	
DH 4	9.8	52.1	1.15±0.04	1.35	13.4 D	7.5 D	0.3 D
	18.6	6.0	1.19±0.16	1.37	2.6 D	12.3 D	0.3 L
	43.9	0.7	6.87±0.81	6.8	5.8 D	242 D	
	61.3	6.6	3.55±0.19	3.1	28.4 D	123 D	
DH 8	1.8	3.0	8.48±0.67	4.7			
	2.9	6.3	7.73±0.64	3.7			
DH 16	4.0	1147	0.76	1.33	443	8 L	
	8.2	1822	0.87	0.89	253	4 L	0.3 L
	13.1	1145	0.80	0.77	239	6 L	0.3 D
	19.5	19.5	2.63	1.97	84	120 D	0.3 D

(Continued)

TABLE 33 (Continued)

Drill Hole	Depth (m)	U ($\mu g\ g^{-1}$)	$^{226}Ra/^{230}Th$	U_{eq}/U	Ra Leaching L (or Deposition D) x 10^{-13} g g^{-1} ore per 1000 y	Rel. Leaching L (or Deposition D) rate (% per 1000 y)	
						Ra*	U+
DH 35	8.2	256.2	1.06±0.04	1.07	22.7 D	2.6 D	0.3 D
	17.0	6.4		5.16			
	12.5	615.7	0.93±0.04	0.95	65.7 L	3.1 L	0.3 D
	20.3	30.3	5.60±0.56	6.29	236 D	229 D	0.3 L
	25.0	122.9	2.02±0.06	2.45	201 D	48 D	0.3 L
	29.2	7.6	8.54±0.38	10.2	105 D	403 D	

* The value calculated is an instantaneous rate averaged over 1000 y, to allow comparison with geochemical timescales.

+ See Tables 5 and 6(a)

TABLE 34

RADIUM ANALYSES OF WATER SAMPLES

Sample No.	Delay (h)	^{226}Ra	^{224}Ra	^{223}Ra	$^{226}Ra/^{223}Ra$
		pCi L^{-1}			
(a) Ranger Area					
79/1	650.8	34.02±1.16	102.94±22.27	5.34±0.63	6.4
82/3	722.9	1.23±0.05	-3.89± 2.02	0.13±0.05	9.6
OB 29	655.3	0.50±0.03	10.06± 3.48	0.14±0.06	3.5
9250	698.9	0.27±0.02	1.30± 1.20	0.05±0.0[illegible]	4.8
9252	667.7	0.16±0.02	-1.92± 0.90	0.07±0.03	[illegible].4
9722	621.3	0.18±0.01	-1.08± 0.73	0.04±0.02	5.2
9727	674.9	0.42±0.02	1.43± 1.41	0.02±0.02	18.0
9754	677.0	5.23±0.19	-5.87± 3.11	0.38±0.13	13.6
20361	650.5	1.85±0.08	-3.34± 2.56	0.27±0.14	6.7
79/6a	557.3	8.09±0.36	-25.72± 5.75	2.53±0.36	3.2
79/6a	701.3	43.54±1.48	-220.24±76.06	7.68±2.52	5.7
(b) Koongarra Area					
PH 27	531.4	61.31±1.87	117.17± 8.18	9.52±0.54	6.4
PH 73	574.8	0.92±0.04	1.28± 0.71	0.17±0.04	5.3
PH 78	649.3	0.36±0.03	-2.01± 1.10	0.05±0.02	10.5
PH94	507.6	0.04±0.01	-0.36± 0.29	0.02±0.02	2.1
KTD1	571.9	0.14±0.01	1.64± 1.17	-0.02±0.02	0.0
KD1	503.3	7.68±0.25	6.45± 1.24	0.72±0.08	10.6
K-Spring	559.3	4.25±0.15	-22.08± 3.21	2.00±0.25	2.1
KPBB	530.6	0.76±0.04	6.44± 1.15	0.39±0.05	1.9
(c) Koongarra samples without filters					
PH 14	364.3	31.49±1.08	11.01± 2.59	3.89±0.40	8.1
PH 49	383.5	275.89±9.75	72.39±26.29	11.69±3.58	23.6
PH49	384.8	280.14±8.74	42.78± 9.35	15.83±1.49	17.7
PH 55	366.0	12.75±0.42	12.80± 1.40	2.65±0.17	4.8
PH 58	365.3	1.58±0.06	1.55± 0.35	0.12±0.03	13.7
LS	484.5	6.17±0.24	99.18±14.64	0.68±0.10	9.1

TABLE 35

ANALYTICAL RESULTS ON FILTERS

Sample No.	Delay (h)	^{224}Ra	^{226}Ra	^{223}Ra	$^{226}Ra/^{223}Ra$
		pCi L^{-1}			
(a) Ranger Area					
79/1	146.1	78.41±2.53	7.58±0.95	6.63±0.40	11.8
82/3	172.8	4.99±0.18	0.69±0.18	0.16±0.04	30.9
OB 29	288.5	3.77±0.14	9.95±1.34	0.34±0.05	11.1
9250	149.8	2.29±0.10	1.01±0.21	0.12±0.02	18.8
9252	216.0	0.60±0.04	0.11±0.07	0.05±0.02	11.2
9722	213.7	0.32±0.02	-0.05±0.05	0.02±0.01	18.1
9727	318.5	4.11±0.16	0.15±0.25	0.30±0.05	13.5
9754	316.5	20.56±0.66	1.96±0.46	0.43±0.06	47.4
20361	337.8	37.56±1.25	25.96±3.81	1.92±0.26	19.6
(b) Koongarra Area					
PH 27	21[illegible].0	96.82±3.10	23.60±2.41	14.89±0.73	6.5
PH 73	165.5	3.22±0.12	0.84±0.14	0.56±0.05	5.7
PH 78	173.5	3.99±0.15	1.88±0.28	0.33±0.04	12.0
PH 94	171.5	0.74±0.06	0.41±0.16	0.06±0.02	11.4
KTD 1	214.5	1.76±0.09	1.14±0.27	0.18±0.04	9.9
KD 1	192.0	43.05±1.32	31.40±1.68	2.54±0.14	17.0
X-Spring	192.5	28.26±1.12	57.30±6.22	3.14±0.33	9.0
YPH 8	164.5	13.16±0.44	16.36±0.88	7.24±0.29	1.8

TABLE 36

ESTIMATES OF FILTER EFFICIENCIES FROM ^{226}Ra ANALYSES OF WATER AND FILTER SAMPLES

Sample No.	Volume % Filtered	Filter Used	^{226}Ra Filter	^{226}Ra Water	Recovery (%)
(a) Ranger Samples					
79/1	50	5	78.4 ±2.5	34.0 ±1.20	92
82/3	62	10	5.0 ±0.2	1.23±0.05	66
OB 29	100	10	3.8 ±0.14	0.50±0.03	76
9250	100	10	2.3 ±0.1	0.27±0.02	85
9252	100	10	0.60±0.04	0.16±0.02	37
9722	150	10	0.32±0.02	0.18±0.01	12
9727	150	15	4.1 ±0.2	0.42±0.02	43
9754	50.5	10	20.6 ±0.7	5.23±0.2	78
20361	250	15	37.6 ±1.3	1.85±0.08	54
(b) Koongarra Samples					
PH 27	100	15	96.8 ±3.1	61.3±1.9	11
PH 73	70	15	3.32±0.1	0.92±0.04	33
PH 78	70	15	3.99±0.15	0.56±0.03	68
PH 94	150	15	0.74±0.06	0.04±0.01	82
KTD 1	150	15	1.76±0.09	0.14±0.01	56
KD 1	100	15	43.1 ±1.3	7.68±0.25	37
X-Spring	100	15	28.3 ±1.1	4.25±0.15	44
XPH 3	150	15	13.2 ±0.4	0.76±0.04	77

APPENDIX A

SOLUTION OF THE URANIUM TRANSPORT EQUATIONS

In Section 8, it was shown that, assuming leaching (or deposition) was a first order process, the uranium transport equations were

Uranium-238:

$$U_8 = U_8(t_o) \exp - (\lambda_8 + \xi)\, t \,, \qquad \text{(A1)}$$

Uranium-235:

$$U_5 = U_5(t_o) \exp - (\lambda_5 + \xi)\, t \,, \qquad \text{(A2)}$$

Uranium-234:

$$-dU_4/dt = (\lambda_4 + R\xi)U_4 - \lambda_8 U_8 \,, \qquad \text{(A3)}$$

Thorium-230:

$$-dI/dt = \lambda_i I - \lambda_4 U_4 \,, \text{ and} \qquad \text{(A4)}$$

Protactinium-231:

$$-dPa/dt = \lambda_p Pa - \lambda_5 U_5 \,, \qquad \text{(A5)}$$

where $\lambda_8 U_8$, $\lambda_5 U_5$, $\lambda_4 U_4$, $\lambda_i I$ and $\lambda_p Pa$ are the activities of ^{238}U, ^{235}U, ^{234}U, ^{230}Th and ^{231}Pa respectively; ξ is the rate of leaching (+ve) or rate of deposition (-ve); R is the $^{234}U/^{238}U$ ratio of the leachate or the depositing material; t is the elapsed time; and $U_8(t_o)$, $U_5(t_o)$ are the levels of ^{238}U and ^{235}U at the initial time t_o. A full list of symbols is given in Appendix C.

Uranium-234

Substituting equation (A1) into (A3),

$$-dU/dt = aU_4 - \lambda_8 U_8(t_o) \exp(-bt) \,, \qquad \text{(A6)}$$

where $a = \lambda_4 + R\xi$, (A7)

and $b = \lambda_8 + \xi$.

From equation (A6), it may be shown that

$$U = U_4(t_o) \exp(-at) + \frac{\lambda_8}{(b-a)} U_8(t_o) (\exp(-at) - \exp(-bt)) \,. \qquad \text{(A9)}$$

The activity ratio,

$$Su = \frac{\lambda_8 U_8}{\lambda_8 U_8} = \lambda_4 U_4 / \lambda_8 U_8(t_o) \exp(-bt) \ . \qquad \text{(A10)}$$

Substituting (A10) into (A9),

$$Su = Su(t_o) \exp (b-a)\ t + \frac{\lambda_4}{(b-a)} (\exp (b-a)t - 1) \ , \qquad \text{(A11)}$$

where $Su(t_o)$ is the activity ratio at the initial time t_o.

Thorium-230

From equations (A4), (A7), (A8) and (A10),

$$-dI/dt = \lambda_i I - \lambda_4 U_4(t_o) \exp (-at) \ +$$

$$+ \frac{\lambda_4 \lambda_8}{(b-a)} U_8(t_o) (\exp (-at) - \exp (-bt)) \ . \qquad \text{(A12)}$$

The solution of (A12), which can be most readily checked by back substitution is

$$I = I_o \exp (-\lambda_i t) + \frac{\lambda_4}{(\lambda_i - a)} U (t_o) (\exp(-at) - \exp(-\lambda_i t)) +$$

$$+ \frac{\lambda_4 \lambda_8 \ U(t_o)}{(b-a)(\lambda_i - a)(\lambda_i \ b)} ((b-a) \exp (-\lambda_i t) +$$

$$+ (\lambda_i - b) \exp (-at) - (\lambda_i - a) \exp (-bt)) \qquad \text{(A13)}$$

The activity ratio,

$$Si = \lambda_i I / \lambda_4 U_4 \ . \qquad \text{(A14)}$$

Substituting (A14) into (A13),

$$Si \times D = Si(t_o) \exp(a - \lambda_i)t + \lambda_i (1 - \exp(a - \lambda_i)t)/(\lambda_i - a)$$

$$+ \lambda_i \lambda_4 ((b - a) \exp((a - \lambda_i)t + \ (a - \lambda_i) \exp -(b - a)t + \lambda_i - b)/$$

$$[(b - a)(a - \lambda_i)(b - \lambda_i) \ S(t_o)] \qquad \text{(A15)}$$

where $D = 1 + \lambda_4 (1 - \exp -(b-a)t)/(b-a) \ Su(t_o)$.

Protactinium-231

From equations (A2) and (A5),

$$-dPa/dt = {}_{p}Pa - \lambda_p Pa - \lambda_5 U_5(t_o) \exp(-ct) , \quad (A16)$$

where $c = \lambda_5 + \xi$. (A17)

From equation (A16) it may be shown that

$$Pa = Pa(t_o) \exp(-\lambda_p t) + \frac{\lambda_5 U_5(t_o)}{c-\lambda_p}(\exp(-\lambda_p t) - \exp(-ct)) . \quad (A18)$$

The activity ratio

$$Sp = \lambda_p Pa/\lambda_5 U_5 , \quad (A19)$$

hence, from (A18) and (A19),

$$Sp = Sp(t_o) \exp(c-\lambda_p)t + \frac{\lambda_p}{(c-\lambda_p)} (\exp(c-\lambda_p)t - 1) . \quad (A20)$$

APPENDIX B

DEFINITIONS AND STANDARDS

Stable Isotopes

Stable isotopes D/H, $^{13}C/^{12}C$, $^{18}O/^{16}O$ are reported in terms of δ-values, which are relative differences of the ratio from a reference material. By definition

$$\delta x = (R_x/R_{std} - 1) \times 1000 \text{ per mille}$$

where R_x is the isotope ratio of the sample, R_{std} is the isotope ratio of the standard.

For D/H and $^{18}O/^{16}O$, standard mean ocean water (SMOW) is the reference. In practice, V-SMOW (Vienna standard mean ocean water), an artificial sample prepared and distributed by the IAEA is used. It has an isotopic composition very close to average seawater.

The $^{13}C/^{12}C$ ratios are referred ultimately to a carbonate standard PDB which is derived from the rostrum of *Belemnitella americana* from the Pee Dee Formation of South Carolina, USA.

Tritium (^3H)

Environmental tritium is measured in terms of tritium units (TU). By definition, one tritium unit is the ratio 1 tritium atom per 10^{18} hydrogen atoms. One TU is approximately 7.2 disintegrations per minute per litre of water (dpm L^{-1}).

Carbon-14

Carbon-14 is measured in terms of the percentage activity of modern carbon (pmc). For laboratory calibrations

$$^{14}C \text{ activity modern carbon} = 0.94\ ^{14}C \text{ activity (NBS oxalic acid in 1950)}$$

An activity of 100 pmc is close to the 'steady-state' activity of tropospheric CO_2 and corresponds to 13.56 dpm g^{-1} of carbon.

APPENDIX C

LIST OF SYMBOLS

a	$\lambda_4 + R\xi$ (equation (12))
A_o, A_f	initial, final solution activity
b	$\lambda_8 + \xi$ (equation 13)
c	$\lambda_5 + \xi$ (equation 14)
D	rate of deposition
E	rate of surface erosion
$F(0)$	uranium flux (Uranium Trend Model - J.N. Rosholt)
h_I, h_{II}, h_{III}	heights above the zones I/II, II/III and III/IV respectively (Section 3.2)
H	depth of weathered host rock
I	^{230}Th
K_d	adsorption coefficient
K_d^r	adsorption coefficient of reference isotope
L	rate of leaching
Pa	^{231}Pa
Pb_4, Pb_6, Pb_7	^{204}Pb, ^{206}Pb, ^{207}Pb
R	$^{234}U/^{238}U$ ratio of groundwater
Ra	^{226}Ra
^6R_a, ^4R_a	level of ^{226}Ra, ^{224}Ra at accessible sites
$^6R_{aq}$, $^4R_{aq}$	level of ^{226}Ra, ^{224}Ra in aqueous solution
R_d	retardation factor
R_{geol}	rate of leaching (or deposition) of radium - allogenic component
^4R_i	level of ^{224}Ra at inaccessible sites
Su, Si, Sp	$^{234}U/^{238}U$, $^{230}Th/^{234}U$, $^{231}Pa/^{235}U$
t	elapsed time
t_o	initial time

t_w	time at which uranium first has access to groundwater
T	annual rate of uranium transport per cubic metre of vertical core
$(^{230}Th/^{234}U)_0$	activity ratio at time t_0, i.e. immediately before the passage of the zone front
U	uranium level
U_4, U_5, U_8	^{234}U, ^{235}U, ^{238}U
$^{234}U(x)$, $^{238}U(x)$	observed level of ^{234}U, ^{238}U in groundwater at a distance x from the deposit
$^{234}U_2$, $^{238}U_2$	level of ^{234}U, ^{238}U in component 2 of the groundwater
$(^{234}U/^{238}U)_0$	activity ratio at time t_0, i.e. immediately before the passage of the zone front
V	groundwater flow velocity
V	solution volume (Section 7.2)
V_c	solute velocity
V_i	interstitial fluid velocity
w	weight of soil
W	rate of advance of the weathering front
λ_4, λ_5, λ_8	decay constants of ^{234}U, ^{235}U, ^{238}U
λ_i	decay constant of ^{230}Th
λ_p	decay constant of ^{231}Pa
λo	decay constant associated with the uranium flux F(0) (Uranium Trend Model, J.N. Rosholt)
υ_5, υ_7	rate of leaching of ^{235}U, ^{238}U in the vicinity of rock fractures
ξ	rate of leaching (+ve) or deposition (-ve)
ξ	ratio υ_5/υ_8 (equation (28))

ξ	$^{234}U(o)/^{238}U(o)$ (equation (46))
π	rate of leaching of Pb in the vicinity of rock fractures
ρ	K_d/K_d^r (equation (18))
ρ_s	density
$\emptyset$	porosity
$\emptyset_a$	recoil parameter, i.e. probability that an α recoil daughter will lodge in an inaccessible site

NRC FORM 335 (2-84) NRCM 1102, 3201, 3202

U.S. NUCLEAR REGULATORY COMMISSION

BIBLIOGRAPHIC DATA SHEET

SEE INSTRUCTIONS ON THE REVERSE

1. REPORT NUMBER (Assigned by TIDC, add Vol. No., if any)
NUREG/CR-3941
AAEC/C40

2. TITLE AND SUBTITLE
Radionuclide Migration Around Uranium Ore Bodies -- Analogue of Radioactive Waste Repositories

3. LEAVE BLANK

4. DATE REPORT COMPLETED
MONTH: June YEAR: 1984

5. AUTHOR(S)
P. L. Airey

6. DATE REPORT ISSUED
MONTH: October YEAR: 1984

7. PERFORMING ORGANIZATION NAME AND MAILING ADDRESS (Include Zip Code)
Australian Atomic Energy Commission
Lucas Heights Research Laboratories
Sutherland, 2232 NWS
AUSTRALIA

8. PROJECT/TASK/WORK UNIT NUMBER

9. FIN OR GRANT NUMBER
B6661

10. SPONSORING ORGANIZATION NAME AND MAILING ADDRESS (Include Zip Code)
Division of Radiation Programs and Earth Sciences
Office of Nuclear Regulatory Research
U.S. Nuclear Regulatory Commission
Washington, DC 20555

11a. TYPE OF REPORT
Technical (Annual)

b. PERIOD COVERED (Inclusive dates)
July 1, 1982 - June 30, 1983

12. SUPPLEMENTARY NOTES

13. ABSTRACT (200 words or less)

A number of uranium ore bodies in the Northern Territory of Australia have been evaluated as geochemical analogues of high-level radioactive waste repositories. The aim of the study is to contribute to the understanding of the scientific basis for the long-term prediction of the transport of radionuclides. Particular attention is being paid to investigations of (i) mechanisms of mobilization and subsequent retardation of uranium series nuclides following the weathering of metamorphic host rocks, (ii) the role of iron minerals in the retardation of uranium and thorium, (iii) the role of groundwater colloids in the transport of radionuclides, (iv) experimental methods for studying the time dependence of adsorption coefficients, and (v) conceptual methods for studying the effect of transport of uranium series nuclides through crystalline host rocks over geological time. The possibility of incorporating certain transuranic and fission product elements into the analogue is discussed.

14. DOCUMENT ANALYSIS - a. KEYWORDS/DESCRIPTORS
nuclear waste, uranium ore bodies, natural analogues of nuclear waste repositories, adsorption, iron hydroxides, groundwater colloids, isotope disequilibria, adsorption kinetics, alpha recoil

b. IDENTIFIERS/OPEN-ENDED TERMS

15. AVAILABILITY STATEMENT
Unlimited

16. SECURITY CLASSIFICATION
(This page) Unclassified
(This report) Unclassified

17. NUMBER OF PAGES

18. PRICE

UNITED STATES
NUCLEAR REGULATORY COMMISSION
WASHINGTON, D.C. 20555

OFFICIAL BUSINESS
PENALTY FOR PRIVATE USE, $300

FOURTH CLASS MAIL
POSTAGE & FEES PAID
USNRC
WASH. D.C.
PERMIT No. G-67

120555078877 1 1AN1RW
US NRC
ADM-DIV OF TIDC
POLICY & PUB MGT BR-PDR NUREG
W-501
WASHINGTON DC 20555